Metropolitan Water Reclamation District of Greater Chicago

RESEARCH AND DEVELOPMENT DEPARTMENT

REPORT NO. 05-12

VERIFICATION OF A CONTINUOUS WATER QUALITY MODEL UNDER UNCERTAIN STORM LOADS IN THE CHICAGO WATERWAY SYSTEM

Prepared By

Institute for Urban Environmental Risk Management
Marquette University, Milwaukee, Wisconsin

AUGUST 2005

Metropolitan Water Reclamation District of Greater Chicago
100 East Erie Street Chicago, Illinois 60611-2803 312-751-5600

VERIFICATION OF A CONTINUOUS WATER QUALITY MODEL UNDER UNCERTAIN STORM LOADS IN THE CHICAGO WATERWAY SYSTEM

Prepared By

Institute for Urban Environmental Risk Management
Marquette University, Milwaukee Wisconsin

Research and Development Department
Richard Lanyon, Director

August 2005

Institute for Urban Environmental Risk Management

Marquette University, Milwaukee WI 53201-1881

TECHNICAL REPORT # 17

VERIFICATION OF A CONTINOUS WATER QUALITY MODEL UNDER UNCERTAIN STORM LOADS IN THE CHICAGO WATERWAY SYSTEM

SUBMITTED TO

The Metropolitan Water Reclamation District of Greater Chicago

Anna NEUGEBAUER, M.S.

Department of Civil and Environmental Engineering

Charles S. MELCHING, Ph.D, P.E.

Department of Civil and Environmental Engineering

Milwaukee, Wisconsin

August 2005

ABSTRACT

In early 2003, the Illinois Environmental Protection Agency (IEPA) initiated an Use Attainability Analysis (UAA) for the Chicago Waterway System (CWS) with Camp, Dresser & McKee (CDM). As a result of the UAA, dissolved oxygen (DO) was found to be a concern for the CWS. DO data from monitoring indicate that water quality processes are complex and vary under a wide range of flows. Therefore, water-quality management problems of interest to the Metropolitan Water Reclamation District of Greater Chicago (MWRDGC) require analysis of unsteady flow conditions. A model capable of simulation of the effects of flow and loading variations in time on water quality in the CWS was developed and tested by the Institute for Urban Environmental Risk Management at Marquette University with usage of the DUFLOW program. This model is to be used to evaluate pollution mitigation alternatives identified in the UAA and to determine the pollution mitigation methods and levels of pollution mitigation needed to achieve DO concentrations greater than 4, 5, and 6 mg/L throughout the study reaches.

Once a model is calibrated its forecasting ability should be validated during verification runs before application to pollution mitigation scenarios. The main purpose of this study is to verify the DUFLOW model of the CWS and test its behavior under uncertain storm loading. Because detailed storm data were used for the CWS water-quality model calibration (07/12/01 – 11/09/01) and such data were not collected for the verification period (05/01/02 – 09/24/02), a new approach to verification was applied to evaluate periods after storms resulting in combined sewer overflows (CSOs). In this approach

event mean concentrations are randomly generated on the basis of observed event mean concentrations for the pump stations, combined sewer overflows points, and tributaries. Multiple simulations of water-quality in the CWS were performed, and the range of simulated DO concentrations is compared to the observed DO concentrations.

The standard verification confirmed the DO prediction ability of the DUFLOW water-quality model. Although the average errors for most locations were greater than 30%, the verification results are similar to the calibration results. The new approach to verification was used to analyze storm load influence on DO concentrations in the CWS. The effect of storm pollutants on water quality can be split into two phases: direct influence and sediment influence. The first phase lasts until the time needed to pass the wave through the downstream boundary, equal to the time needed to drain the system. Substantial impact of storm loading remains in the CWS a few weeks in reaches upstream of the Stickney Water Reclamation Plant (WRP), whereas in reaches downstream of the Stickney WRP the impact remains for a few days. The second phase lasts longer, more than the time between the two consecutive storms. During this phase, DO in the system is affected much less than during the direct influence phase.

TABLE OF CONTENTS

LIST OF FIGURES

LIST OF TABLES

CHAPTER 1: INTRODUCTION

1.1. Problem Definition

Dissolved oxygen (DO) monitoring in the Chicago Waterway System (CWS) conducted by Metropolitan Water Reclamation District of Greater Chicago (MWRDGC) shows that the water quality of the system is not satisfactory. Many studies have been done on the water quality of the CWS in the past, mainly in response to Section 208 of the Federal Water Pollution Control Act Amendments of 1972 (PL 92-500). The 208 Water Quality Management Program done for the Northeastern Illinois Planning Commission (NIPC) was done with the aid of a mathematical water-quality model. Hydrocomp, Inc. (1979a,b) developed the model and then Hey et al. (1980) modified it for NIPC purposes. In the late 1980's and early 1990's the water-quality model QUAL2E (Brown and Barnwell, 1987) was applied to the Chicago Waterway and Upper Illinois River Systems (CDM, 1992) and used for water-quality management purposes. In early 2003, the Illinois Environmental Protection Agency (IEPA) initiated an Use Attainability Analysis (UAA) for the CWS with Camp, Dresser & McKee (CDM). As a result of the UAA, DO was found to be a concern for the CWS. DO data from monitoring indicate that water quality processes are complex and vary under a wide range of flows. Therefore, water-quality management problems of interest to the MWRDGC require analysis of unsteady flow conditions.

A model capable of simulation of the effects of flow and loading variations in time on water quality in the CWS was developed and tested by the Institute for Urban

Environmental Risk Management at Marquette University (Shrestha and Melching, 2003; Alp and Melching, 2004; Alp and Melching, 2005, in preparation). This model is to be used to evaluate pollution mitigation alternatives identified in the UAA and to determine the pollution mitigation methods and levels of pollution mitigation needed to achieve DO concentrations greater than 4, 5, and 6 mg/L throughout the study reaches.

1.2. Objectives of the report

The objective of this report is verification of the model developed by the Institute for Urban Environmental Risk Management at Marquette University. Before a calibrated model is applied to simulate the effects of pollution mitigation alternatives the model's forecasting ability should be validated during verification runs. Verification is a statistically acceptable comparison between model results and a second (independent from the calibration data set) set of field data for another year or at an alternate site (Schnoor, 1996, p. 10). During the verification process, parameters of the calibrated model should be fixed to those determined in calibration. Because detailed storm loading data were used for the CWS model calibration (7/12/01-11/09/01) and such data were not collected for the verification period (05/01/02 – 09/24/02), a new approach of model verification was applied to test periods after storms resulting in combined sewer overflows (CSOs). In this approach event mean concentrations are randomly generated on the basis of observed event mean concentrations for the pump stations, combined sewer overflow points, and tributaries. Multiple simulations of water quality in the CWS were performed, and the range of simulated DO concentrations is compared to the observed DO concentrations.

CHAPTER 2: THE DUFLOW MODEL

2.1. Model Selection

A wide variety of mathematical models describing self-purification of rivers are available. Selection of a proper water-quality management model is an important task, because not every model is adequate for a specific problem. Using too simple or too complex a model may result in unreliable prediction of water quality from the model. Therefore, the selection of a water-quality model should be based on a good balance between three elements: model complexity, uncertainty, and the available amount of data (Manache, 2001).

The water-quality model DUFLOW was selected to simulate flow and water quality in the CWS. The DUFLOW model is considered very useful software for water-quality modeling under unsteady-flow conditions (Manache, 2001). In addition, the program is compatible with Geographical Information Systems (GIS) that facilitate the geographical representation of the model river system and with Microsoft Windows which makes it easy to use. DUFLOW software also allows several options for the simulation of water quality in stream systems and has been successfully applied to the several water-quality problems in European river systems (e.g., Manache and Melching, 2004), as well as to integrated water management problems (Schütze et al., 1999).

2.2. Model Description

DUFLOW is a powerful tool in modeling water quality under one-dimensional, unsteady flow conditions. The model is designed for various types of users and it covers a large range of applications in water quantity and quality management. It can be successfully used for the design of hydraulic structures, flood prevention, operation of irrigation and drainage systems, as well as solving problems relating to algal blooms, contaminated silt, and mitigation of fecal coliforms. In the water-quality part of DUFLOW, there are two pre-defined eutrophication models. However, the user can modify the process descriptions as necessary. This concept makes DUFLOW a very flexible package with which different water-quality models can be developed and tested. All the equations and discussion in the following sections are based on information in DUFLOW (2000).

2.2.1. Hydrodynamics

The hydrodynamic part of the DUFLOW model is based on the one-dimensional partial differential equations that describe unsteady gradually varied flow in open channels (i.e. the de Saint-Venant equations). This mathematical translation of the mass and momentum conservation laws is given by equations 2.1 and 2.2.

$$B\frac{\partial H}{\partial t}+\frac{\partial Q}{\partial x}=0 \tag{2.1}$$

and

$$\frac{\partial Q}{\partial t}+gA\frac{\partial H}{\partial x}+\frac{\partial(\alpha Qv)}{\partial x}+\frac{g|Q|Q}{C^2AR}=b\gamma w^2\cos(\Phi-\phi) \tag{2.2}$$

where:

t = time (s)

x = distance as measured along the channel axis (m)

H = water level with respect to a reference level (m)

v = cross-sectional mean velocity (m/s)

Q = discharge (m^3/s)

R = hydraulic radius (m)

A = cross-sectional flow area (m^2)

b = cross-sectional width (m)

B = cross-sectional storage area (m^2)

g = acceleration due to gravity (m^2/s)

C = coefficient of de Chezy ($m^{1/2}/s$)

w = wind velocity (m/s)

Φ = wind direction, measured clockwise from the north (degrees)

ϕ = direction of channel axis, measured clockwise from the north (degrees)

γ (x) = wind conversion coefficient

α = correction factor for non-uniformity of the velocity distribution in the advection term.

The cross-sectional area of a typical, natural, thus, irregular stream may be divided into two sub-areas: flow area and flood plain area. For streams, a channel may consist of a main channel (area A in equation 2.2) carrying normal discharges and a flood plain, where water is stagnant. The main difference between these two sub-areas is in the Manning's n value, and, therefore, in flow conditions. The total cross-sectional area (area B in equation 2.1) consists of the main channel and flood plain area. Because the

channels in the CWS system are constructed and used for navigational purposes, the majority of the CWS does not have overbank flow (area A is equal to B). The Little Calumet River (south) section is more of a natural river and involves floodplain flows as well as main channel flows (area A may differ from B).

2.2.2.Mass Transport

Pollutant mass transport in DUFLOW is described with an one-dimensional, advection-dispersion equation. This partial differential equation describes the concentration of a constituent in a one-dimensional system as a function of time and space.

$$\frac{\partial(BC)}{\partial t} = -\frac{\partial(QC)}{\partial x} + \frac{\partial}{\partial x}\left(AD\frac{\partial C}{\partial x}\right) + P \qquad (2.3)$$

where:

C = concentration of pollutants (g/m^3)

D = longitudinal dispersion coefficient (m^2/s)

P = reactions and external sources and sinks of the pollutant per unit length of the section (g/m.s)

The term P of equation 2.3 includes all physical, chemical, and biological processes to which a specific pollutant is subject. Equation 2.3 can be rewritten as:

$$\frac{\partial S}{\partial x} + \frac{\partial(BC)}{\partial t} - P = 0 \qquad (2.4)$$

in which S is the transport (quantity of the pollutant passing a cross section per unit of time):

$$S = QC - AD\frac{\partial C}{\partial x} \qquad (2.5)$$

Equation 2.5 describes the transport by advection and dispersion. Equation 2.4 is the mathematical formulation of the mass conservation law, which states that accumulation at a certain location x is equal to the net production rate minus the transport gradient.

2.2.3. Water-Quality Processes

The DUFLOW modeling system allows for various processes affecting water quality to be simulated. There are two water-quality models built-in to the DUFLOW modeling system. One of those named EUTROF2 is more suitable for long-term behavior of systems (DUFLOW, 2000) because it describes the interaction between the water column and sediment bottom layer. For the CWS this interaction is considered an important issue, and, therefore, it was selected as the appropriate unsteady-flow water-quality model for this study. The EUTROF2 water-quality model includes the following state variables: algal biomass species, organic and inorganic phosphorus, organic nitrogen, ammonia nitrogen, nitrate nitrogen, suspended solids, dissolved oxygen, and carbonaceous biochemical oxygen demand.

Algae

Algae is a general term that covers a wide range of microscopic, live floating or suspended aquatic plants containing chlorophyll. In the EUTROF2 model three algae species can be modeled. Algal growth, mortality, and respiration influence the evolution of algal biomass in the way described by equation 2.6:

$$\frac{dA_{W,i}}{dt} = \left[\mu_{\max,i} F_{T,i} F_{N,i} F_{L,i}\right] A_{W,i} - \left[K_{die,i} + K_{res,i}\theta_{ra,i}^{(T-20)} - \frac{v_{sa,i}}{Z}\right] A_{W,i} \quad (2.6)$$

where:

$A_{W,i}$ = algal biomas in the water column for algal species *i*, (mg C/L)

$\mu_{max,i}$ = maximum specific growth rate of algae for algal species *i*, (1/d)

$K_{res,i}$ = algal respiration rate constant for algal species *i*, (1/d)

$\theta_{ra,i}$ = temperature coefficient for respiration for algal species *i*

T = water temperature, (°C)

$K_{die,i}$ = algal die-off rate constant for algal species *i*, (1/d)

$v_{sa,i}$ = settling velocity for algal species *i*, (m/d)

Z = water depth, (m)

Algal growth is considered to be limited by nutrients, light, and temperature (F_N, F_L, F_T). The nutrient limitation factor is described by the Michaelis-Menton equation. This equation indicates that algae need both nutrients (nitrogen and phosphorus) and algae growth is controlled by the most limiting factor.

$$F_{N,i} = \min\left[\frac{DIP_W}{DIP_W + k_{p,i}}, \frac{DIN_W}{DIN_W + k_{n,i}}\right] \quad (2.7)$$

where:

DIP_W =total dissolved inorganic phosphorous concentration in the water column (mgP/L)

DIN_W = total inorganic nitrogen (sum of nitrate and ammonia) concentration in the water column (mg N/L)

$k_{p,i}$ = Monod constant for phosphorous for algal species i, (mg P/L)

$k_{n,i}$ = Monod constant for nitrogen for algal species i, (mg N/L)

The light limitation factor F_L is described by the depth averaged Steele equation:

$$F_{L,i} = \frac{e\,f}{\varepsilon_{tot} Z}\left[\exp(-\frac{I_a}{I_{s,i}}\exp(-\varepsilon_{tot} Z)) - \exp(-\frac{I_a}{I_{s,i}})\right] \tag{2.8}$$

where:

e = Neperian number

f = fraction of daylight during the day

I_a = average light intensity, (W/m^2)

$I_{s,i}$ = optimal light intensity for algal species i, (W/m^2)

The total light extinction coefficient ε_{tot} depends on background extinction of the water, and the concentrations of algae and suspended solids:

$$\varepsilon_{tot} = \varepsilon_0 + \varepsilon_{alg} Chl\text{–}a + \varepsilon_{ss} SS \tag{2.9}$$

where:

ε_0 = background light extinction, (1/m)

ε_{alg} = specific light extinction for chlorophyll, (L/(μg Chl-a·m))

ε_{SS} = specific light extinction for suspended solids, (L/(mg SS·m))

Chl-a = algae concentration, (μg Chl-a/L)

SS = suspended solids concentration, (mg/L)

The algae concentration *Chl - a* mentioned in equation 2.9 is related to the algal biomass *A* of equation 2.6 as follows:

$$Chl\text{-}a = \sum_{i=1}^{3} a_{ChlaC,i} A_{W,i} \tag{2.10}$$

where: $a_{ChlaC,i}$ is the chlorophyll to carbon ratio for algal species *i*.

The temperature limitation factor F_T is given by:

$$F_{Ti} = \frac{T_{cs,i} - T}{T_{cs,i} - T_{os,i}} \exp\left(1 - \frac{T_{cs,i} - T}{T_{cs,i} - T_{os,i}}\right) \tag{2.11}$$

where:

$T_{cs,i}$ = critical temperature species for algal species *i*, (°C)

$T_{os,i}$ = optimal temperature species for algal species *i*, (°C)

The algae concentration in the sediment is given by:

$$\frac{dA_B}{dt} = -K_{daB}\theta_{daB}^{(T-20)} A_B \tag{2.12}$$

where:

A_B = algal biomas in the sediment, (mg C/L)

K_{daB} =anaerobic decay rate constant for algal sediment, (1/d)

θ_{daB} = temperature coefficient for anaerobic decomposition of algal sediment

Organic Phosphorous

Organic phosphorus may be present in the water column either in dissolved or particulate form. During respiration and die-off of the algae, organic and inorganic forms of

phosphorous are released. Mineralization and algal processes govern dynamics of dissolved organic phosphorous concentration in the water column:

$$\frac{dTOP_W}{dt} = -K_{\min}\theta_{\min}^{(T-20)}TOP_W + f_{porg}a_{pc}\sum_{i=1}^{3}\left[\left(K_{die,i} + K_{res,i}\theta_{ra,i}^{(T-20)}\right)A_{wi}\right] \quad (2.13)$$

where:

TOP = total organic phosphorous concentration, (mg P/L)

K_{min} = mineralization rate constant for organic matter, (1/d)

θ_{min} = temperature coefficient for mineralisation

f_{porg} = fraction algal phosphorous released as organic phosphorous

a_{pc}= algal phosphorous to carbon ratio, (mg P/mg C)

The particulate organic form is a subject to settling (see Section 2.2.4 for details). In the sediment bed, organic phosphorous is only released by anaerobic decomposition. The total organic phosphorous in the sediment layer is given by:

$$\frac{dTOP_B}{dt} = -K_{\min B}\theta_{\min B}^{(T-20)}TOP_B + a_{pc}K_{daB}\theta_{daB}^{(T-20)}A_B \quad (2.14)$$

Inorganic Phosphorous

The aerobic and anaerobic mineralization of organic phosphorous in the water column, the release from sediments, and the release during algal respiration and die-off are the main sources and uptake during algal growth is the main sink of inorganic phosphorous in the water column.

$$\frac{dTIP_W}{dt} = K_{\min}\theta_{\min}^{(T-20)}TOP_W - a_{pc}\sum_{i=1}^{3}\left[\mu_{\max,i}F_{T,i}F_{N,i}F_{L,i}A_{W,i}\right] + (1-f_{porg})a_{pc}\sum_{i=1}^{3}\left[\left(K_{die,i}+K_{res,i}\theta_{ra,i}^{(T-20)}\right)A_{W,i}\right] \quad (2.15)$$

where: TIP = total inorganic phosphorous concentration, (mg P/L)

The dissolved fraction of inorganic phosphorous in the water column (W) and in the interstitial water (B) is calculated by:

$$f_{dpW} = \frac{1}{1+K_{pipW}SS_W} \quad (2.16)$$

$$f_{dpB} = \frac{1}{1+K_{pipB}SS_B} \quad (2.17)$$

where:

K_{pip} = partition constant for phosphorous, (1/mg SS)

f_{dp} = fraction dissolved organic phosphorous

SS = suspended solids concentration, (mg/L)

The dissolved fraction of inorganic phosphorous in sediments is calculated by:

$$\frac{dTIP_B}{dt} = K_{\min B}\theta_{\min B}^{(T-20)}TOP_B \quad (2.18)$$

Equations 2.16 and 2.17 imply that it is assumed that equilibrium is reached instantaneously.

Organic Nitrogen

The behavior of organic nitrogen is similar to that of organic phosphorous. Anaerobic mineralization and release during algal loss processes influence organic nitrogen in the water column. In the sediment the anaerobic mineralization of settled algae and organic nitrogen are the controlling processes. The total organic nitrogen concentrations in the water column and sediment layer are given by:

$$\frac{dTON_W}{dt} = -K_{\min W}\theta_{\min W}^{(T-20)}TON_W + f_{norg}a_{nc}\sum_{i=1}^{3}\left[\left(K_{die,i} + K_{res,i}\theta_{ra,i}\right)A_{Wi}\right] \quad (2.19)$$

$$\frac{dTON_B}{dt} = -K_{\min B}\theta_{\min B}^{(T-20)}TON_B + a_{nc}K_{daB}\theta_{daB}^{(T-20)}A_B \quad (2.20)$$

where:

TON = total organic nitrogen, (mg N/L)

f_{norg} = fraction of algal nitrogen released as organic nitrogen, (-)

a_{nc}= nitrogen to carbon ratio, (mg N/mg C)

K_{min} = mineralization rate constant organic matter, (1/d)

Ammonia Nitrogen

As a result of algal respiration and die-off ammonia is released to the water column. Ammonia and nitrate can be used for algal growth. The preference for the source of nitrogen is controlled by the preference factor P_{NH4} calculated by equation 2.21 (if P_{NH4} = 1, nitrogen is taken from ammonia, if P_{NH4} = 0, nitrogen is taken from nitrate).

$$P_{NH4} = NH4_W \frac{NO3_W}{(K_{mN} + NH4_W)(K_{mN} + NO3_w)} + NH4_W \frac{K_{mN}}{(NH4_W + NO3_W)(K_{mN} + NO3_W)} \quad (2.21)$$

where:

K_{mN} = the ammonia preference constant (mg N/L).

$NH4$ = ammonia nitrogen concentration, (mg N/L)

$NO3$ = nitrate nitrogen concentration, (mg N/L)

The nitrification process oxidizes ammonia to nitrite and nitrate forms of nitrogen. The nitrification rate in the water column is controlled by the DO concentration (O2), using a Monod type of equation. The equation of ammonia in the water column is given by:

$$\frac{dNH4_W}{dt} = -K_{nitW}\theta_{nitW}^{(T-20)}\frac{O2_W}{(O2_W + K_{no})}NH4_W + K_{\min W}\theta_{\min}^{(T-20)}TON_W$$
$$-a_{nc}P_{NH4}\sum_{i=1}^{3}\left[\mu_{\max,i}F_{T,i}F_{N,i}F_{L,i}A_{W,i}\right] + a_{nc}\sum_{i=1}^{3}\left(\left[K_{die,i} + K_{res,i}\theta_{ra,i}^{(T-20)}\right)A_{Wi}\right] \quad (2.22)$$

where:

K_{nit} = nitrification rate constant, (1/d)

θ_{nit} = temperature coefficient for nitrification

K_{no} = Monod constant for nitrification, (mg O_2/L)

Hydrolysis of organic nitrogen by bacterial action within sediment adds ammonia to the system. All bottom processes are assumed to be anaerobic, thus, there is no nitrification process in the sediments. The equation describing the sediment ammonia concentration is given by:

$$\frac{dNH4_B}{dt} = K_{\min B}\theta_{\min}^{(T-20)}TON_B \quad (2.23)$$

Nitrate Nitrogen

In the water column nitrate is formed during nitrification. Depending on the ammonia preference factor nitrate can be used as a nitrogen source for algal growth. Denitrification (reduction of nitrate to N_2 under anaerobic conditions) is also included in the EUTROF2 model. The nitrate concentration in the water column is given by:

$$\frac{dNO3_W}{dt} = -K_{denW}\theta_{denW}^{(T-20)}\frac{K_{dno}}{(K_{dno}+O2_W)}NO3_W + K_{nit}\theta_{nit}^{(T-20)}\frac{O2_W}{(O2_W+K_{no})}NH4_W - a_{nc}(1-P_{NH4})\sum_{i=1}^{3}[\mu_{\max i}F_{Ti}F_{Ni}F_{Li}A_{Wi}] \quad (2.24)$$

where:

K_{den} = denitrification rate constant, (1/d)

θ_{den} = temperature coefficient for denitrification

K_{dno} = Monod constant for denitrification, (mg O_2/L)

In the sediment layer, the only process influencing nitrate concentration is denitrification. Nitrate is present in the bottom layer due to the diffusive transport from the overlying water column. Equation 2.25 describes the nitrate concentration in the sediment:

$$\frac{dNO3_B}{dt} = -K_{denB}\theta_{denB}^{(T-20)}NO3_B \quad (2.25)$$

Carbonaceous Biochemical Oxygen Demand

Carbonaceous Biochemical Oxygen Demand (CBOD) is a measure of biodegradable organic material in the water and the oxygen that will be consumed in the process of microbial degradation under aerobic conditions. The CBOD concentration changes are

governed by reduction of the CBOD, settling, denitrification, and algal die-off. The equation used to describe the decay of organic matter is:

$$\frac{dBOD_W}{dt} = -K_{bodW}\theta_{bodW}^{(T-20)}\frac{O2_W}{(O2_W + K_{bodo})}BOD_W + \left[a_{oc}\sum_{i=1}^{3}\left[K_{die,i}A_{Wi}\right] - \frac{5}{4}\frac{32}{14}K_{den}\theta_{den}^{(T-20)}\frac{K_{dno}}{(K_{dno} + O2_W)}NO3_W\right]X_{conv} \quad (2.26)$$

where:

BOD = carbonaceous 5-day biochemical oxygen demand, (mg O_2/L)

K_{bod} = oxidation rate constant for CBOD, (1/d)

θ_{bod} = temperature coefficient for oxidation of CBOD

K_{bodo} = Monod constant for oxidation of CBOD, (mg O_2/L)

a_{oc} = oxygen to carbon ratio, (mg O_2/mg C)

X_{conv} = conversion factor to calculate $CBOD_5$ from ultimate CBOD

$$X_{conv} = 1 - \exp(-5K_{bod}) \quad (2.27)$$

The CBOD that is produced by algal die off and the CBOD consumed by denitrification are ultimate CBOD. Because in practice 5-day CBOD values are used, the conversion factor X_{conv} is applied in equation 2.26. Normally one would expect to see a term describing the reduction in CBOD concentration due to settling in an equation like 2.26, however, in DUFLOW equation 2.26 applies only to the dissolved fraction of CBOD in the water column. The partitioning of dissolved and sediment adsorbed CBOD and the settling of sediment adsorbed CBOD are described in Section 2.2.4.

In the sediment the settled algae and benthic organic matter are subject to anaerobic degradation. In reality the reaction mechanisms involved are very complex. In the EUTROF2 model the redox reactions are not included, but reduction of organic matter is expressed as negative oxygen equivalents that are transported across the sediment water interface. This concept is described by equation 2.28.

$$\frac{dBOD_B}{dt} = [a_{ac} K_{daB} \theta_{daB}^{(T-20)} A_B - \frac{5}{4}\frac{32}{14} K_{denB} \theta_{denB}^{(T-20)} NO3_B] X_{conv} - K_{bodB} \theta_{denB}^{(T-20)} BOD_B \qquad (2.28)$$

Oxygen

The variation of DO concentrations resulting from reaeration, oxidation of CBOD, algal respiration, and nitrification is computed as follows:

$$\begin{aligned} \frac{dO2_W}{dt} &= K_{re} \theta_{re}^{(T-20)} (C_s - O2_W) - K_{bod} \theta_{bod}^{(T-20)} \frac{O2_W}{(O2_w + K_{bodo})} \frac{BOD_W}{X_{conv}} \\ &- \frac{64}{14} K_{nit} \theta_{nit}^{(T-20)} \frac{O2_W}{(O2_W + K_{NO})} NH4_W - \frac{32}{12} \sum_{i=1}^{3} [K_{res,i} \theta_{res,i}^{(T-20)} A_{W,i}] \\ &+ \sum_{i=1}^{3} [\mu_{\max,i} F_{T,i} F_{N,i} F_{L,i} A_{W,i}] \left(\frac{32}{12} + \frac{48}{14} a_{nc} (1 - P_{nh4}) NO3_W \right) \end{aligned} \qquad (2.29)$$

where:

θ_{rea} = temperature coefficient for reaeration

K_{re} = reaeration-rate coefficient, (s^2/m)

$$K_{re} = \frac{k_{mas}}{Z} \qquad (2.30)$$

k_{mas} = mass transfer coefficient for oxygen given by the O'Connor-Dobbins (1958) formula:

$$k_{mas} = kv^{0.5} Z^{-0.5} \qquad (2.31)$$

k =constant in the O'Connor-Dobbins reaeration-rate coefficient formula, originally 3.94, but made a calibration parameter to match the low reaeration common in the CWS,

C_s = oxygen saturation concentration, (mg/L)

$$C_s = 14.5519 - 0.373484T + 0.00501607T^2 \tag{2.32}$$

Equation 2.32 is appropriate for sea level conditions, and a correction for elevation may be made in the DUFLOW code if necessary, but in the case of the CWS such a correction would be small and is not needed. In the sediment layer, the organic carbon and settled algae mineralization process are sinks for oxygen and quickly drive the oxygen concentration within the sediment top layer "negative." The following equation is used to describe the sediment "oxygen concentration":

$$\frac{dO2_B}{dt} = -K_{bodB}\theta_{bodB}^{(T-20)}\frac{BOD_B}{X_{conv}} \tag{2.33}$$

The calculated "negative" concentration is considered to be oxygen equivalence of the reduced intermediate products of the mineralization reaction. It is assumed that the reduced carbon equivalents (expressed as oxygen equivalents) are transported across the sediment interface and are oxidized in the overlying water column.

Suspended solids

The suspended solids concentration in the water column is a result of sedimentation and resuspension processes. Sedimentation and resuspension are assumed to occur simultaneously. The following equation describes the suspended solids concentration in the water column:

$$\frac{dSS_W}{dt} = \left[\frac{v_{SS}}{Z} + \frac{F_{res}}{Z} \right] SS_W \tag{2.34}$$

where:

v_{ss} = settling velocity of suspended solids, (m/d)

F_{res} = suspended solids resuspension flux, (m/d)

2.2.4. Sediment Model

The degradation of organic matter in the sediment can have an important influence on the concentration of oxygen and nutrients in the overlying water column. The sediment model in EUTROF2 describes the interaction between the water column and the sediment layer. The model includes a description of the diffusive exchange flux between the top sediment layer and the water column, the sedimentation flux, the resuspension flux, and the transport between the top and lower sediment layers. For the description of the exchange fluxes a distinction must be made between dissolved constituents (like ammonia, nitrate, and oxygen) and constituents which are associated with the suspended solids (like inorganic and organic phosphorous, organic nitrogen, and CBOD). Inorganic and organic phosphorous, organic nitrogen, and CBOD are also considered to be present in a dissolved form. For a certain constituent X the following forms are distinguished:

$$DX_W = f_{dxw} TX_W \tag{2.35}$$

$$PX_W = (1 - f_{dxw}) \frac{TX_W}{SS_W} \tag{2.36}$$

$$DX_B = f_{dxb} \frac{TX_W}{POR} \tag{2.37}$$

$$PX_B = (1 - f_{dxb}) \frac{TX_B}{SS_B} \tag{2.38}$$

where:

TX_W = the total concentration of constituent X in the water column

TX_B = the total concentration of constituent X in the sediment top layer

DX = represents the dissolved portion of constituent X in mass per volume

PX = represents the particulate portion of constituent X as a fraction of the concentration of suspended sediments

f_{dxw} = dissolved fraction in the water column

f_{dxb} = dissolved fraction in the sediment

POR = porosity of the sediment top layer

The total transport across the interface is equal to the sum of the fluxes. The concentration of the constituent X in the water column is given by:

$$\frac{dX_W}{dt} = \frac{F_{XD} - F_{XS} + F_{XR}}{Z} + PX_W \tag{2.39}$$

The concentration of the constituent X in the sediment top layer is given by:

$$\frac{dX_B}{dt} = \frac{F_{XD} - F_{XS} + F_{XR} + F_{XB}}{HB} + PX_B \tag{2.40}$$

where the fluxes F_{XD}, F_{XS}, F_{XR}, and F_{XB} are described in the following subsections.

The diffusive exchange flux, F_{XD}

The dissolved fraction is a subject to diffuse exchange. The driving force for this mass transfer is the difference between the concentration in the interstitial water (D_{XB}) and the water column (D_{XW}).

$$F_{XD} = \frac{E_{diff}}{HB}(D_{XB} - D_{XW}) \tag{2.41}$$

where:

E_{diff} = diffusive exchange rate constant, (m^2/d)

HB = depth of the sediment top layer, (m)

The sedimentation flux, F_{XS}

The sedimentation flux is dependent on the concentration of the particulate constituent and the inclusion of pore water due to the formation of new sediment by sedimentation. The sedimentation flux is described by:

$$F_{XS} = F_{sed} PX_W + v_S POR\ DX_W \tag{2.42}$$

where:

F_{sed} = sedimentation flux of suspended solids

v_S = benthic sediment settling velocity

The resuspension flux, F_{XR}

The resuspension of particulate X is determined by the particulate X concentration in the sediment and the release of pore water during resuspension:

$$F_{XR} = F_{res} PX_B + v_r POR\ DX_B \tag{2.43}$$

where:

F_{res} = resuspension flux

v_r = benthic sediment resuspension velocity

Transport between top and lower sediment layers, F_{XB}

The sediment model in EUTROF2 assumes the depth of the sediment top layer is constant. Therefore, there is transport between the top and lower sediment layer. If sedimentation occurs sediment is transported from the top layer toward the lower layer. In case of resuspension the sediment top layer is replenished with sediment from the lower layer. The model assumes no diffusion exchange between the two layers. Thus, the concentration in the top layer is only influenced by the quality of the lower layer if resuspension occurs. The following relation describes the transport between top and bottom layers:

$$\begin{aligned} F_{XB} &= -v_{sd} TX_B \qquad if \ v_{sd} > 0 \\ F_{XB} &= -v_{sd} TX_{LB} \qquad if \ v_{sd} < 0 \end{aligned} \tag{2.44}$$

where:

v_{sd} = velocity by which the benthic surface is displaced

TX_{LB} = the total concentration of constituent X in the lower sediment layer

CHAPTER 3: CASE OF STUDY

3.1. Description of Chicago Waterway System

The CWS is a subset of the Chicago River System. It is a network of natural and constructed channels with a total length of 76.3 miles. The Chicago Sanitary and Ship Canal (CSSC), Calumet-Sag Channel, North Shore Channel, lower portion of the North Branch Chicago River, South Branch Chicago River, Chicago River Main Stem, and Little Calumet River (north and south) are constituent parts of the system. The Chicago River System and its tributaries are shown in Figure 3.1.

The CWS is composed of wide and deep channels with average water surface slopes on the order of 0.03 ft/mi. Therefore, the system is characterized by small flow velocities and long residence time. Characteristics of the reaches in the CWS considered in this study are listed in Table 3.1.

The CWS is mainly used for commercial and recreational navigation, and for urban drainage, i.e. draining combined sewer overflows, stormwater runoff, and treated wastewater from the Chicago area. The majority of the flow is treated sewage effluent from 4 water reclamation plants (WRPs) located along the CWS.

Several sources of pollution affect the water quality in the CWS. The UAA done in 2003 determined that DO is a concern at several locations in the system.

Table 3.1 Description of reaches in the Chicago Waterway System modeled in this study.

Reach*	River Mile from Lockport		Length (mi)	Average Width (ft)	Average Depth (ft)
	Beginning	End			
1	50	42.5	7.5	100	8
2	42.5	34.6	7.9	150-200	9 – 21
3	36.1	34.6	1.5	180-400	21
4	34.6	30.7	3.9	150	17
5	30.7	12.6	18.1	150-300	17 – 23
6	12.6	5.2	7.4	160-200	23
7	28.6	12.6	16	300-450	9 – 27
8	35.5	28.6	6.9	300-450	9 – 27
9	35.4	28.6	6.8	**	**

* 1-North Shore Channel; 2-North Branch Chicago River; 3-Chicago River Main Stem; 4-South Branch Chicago River; 5-Chicago Sanitary and Ship Channel (CSSC) to Sag Junction; 6-CSSC from Sag Junction to Romeoville; 7-Calumet-Sag Channel; 8-Little Calumet River (north); 9-Little Calumet River (south).

** Little Calumet River (south) is natural stream, and, thus, the width and depth are highly variable.

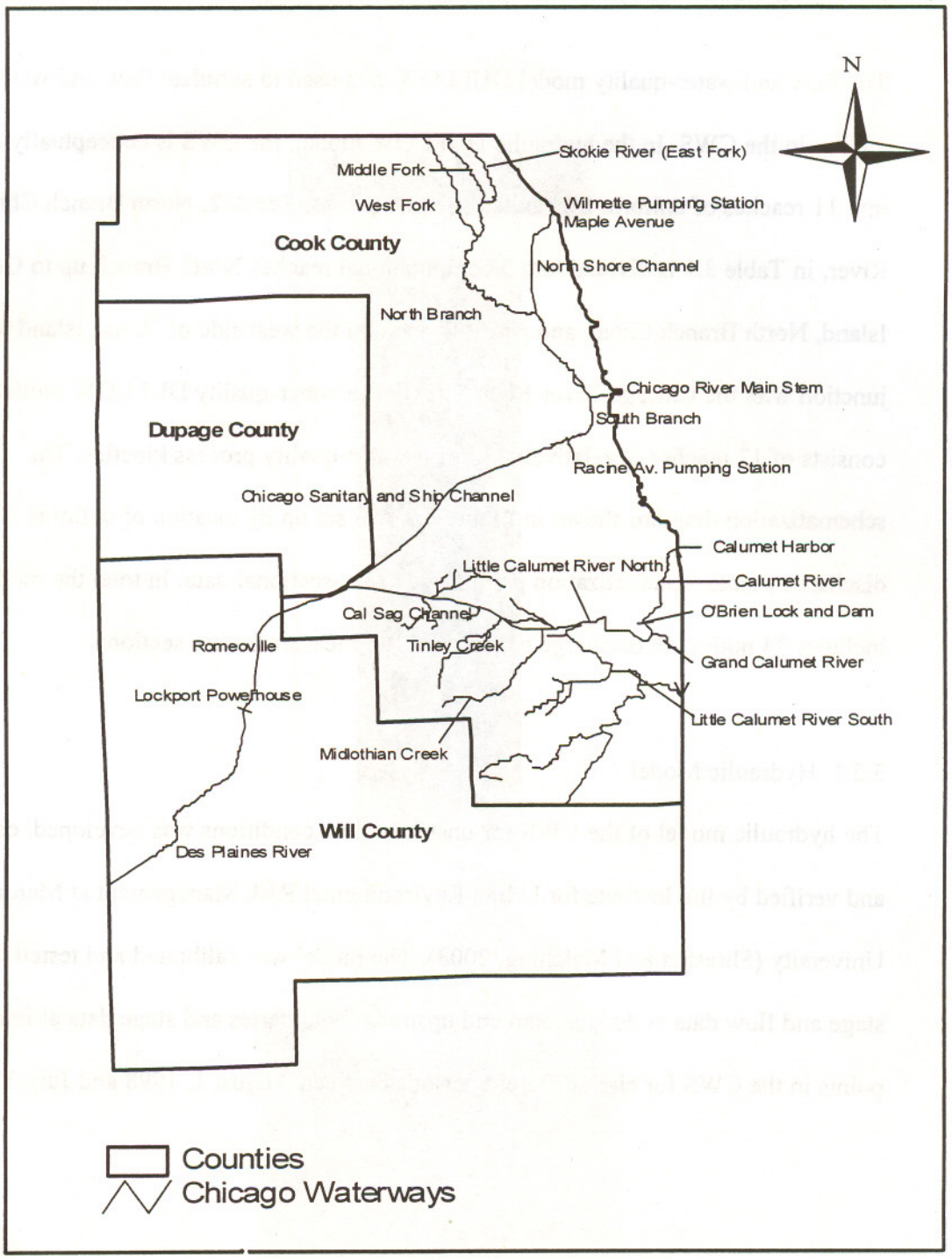

Figure 3.1 The Chicago River System (after Shrestha and Melching, 2003)

3.2. Application of the DUFLOW Model to the Chicago Waterway System

The flow and water-quality model DUFLOW was used to simulate flow and water quality in the CWS. In the hydraulic DUFLOW model, the CWS is conceptually divided into 11 reaches of uniform hydraulic properties (note: Reach 2, North Branch Chicago River, in Table 3.1 is divided into 3 computational reaches North Branch up to Goose Island, North Branch Canal, and North Branch on the west side of Goose Island to the junction with the Chicago River Main Stem). The water-quality DUFLOW model consists of 17 reaches of relatively uniform water-quality process kinetics. The schematization diagram shown in Figure 3.2 was set up by location of defining nodes, discharge points, schematization points, and cross-sectional data. In total the model includes 34 nodes, 46 discharge points, and 193 measured cross sections.

3.2.1. Hydraulic Model

The hydraulic model of the CWS for unsteady-flow conditions was developed, calibrated, and verified by the Institute for Urban Environmental Risk Management at Marquette University (Shrestha and Melching, 2003). The model was calibrated and tested using stage and flow data at downstream and upstream boundaries and stage data at interior points in the CWS for eight different periods between August 1, 1998 and July 31, 1999.

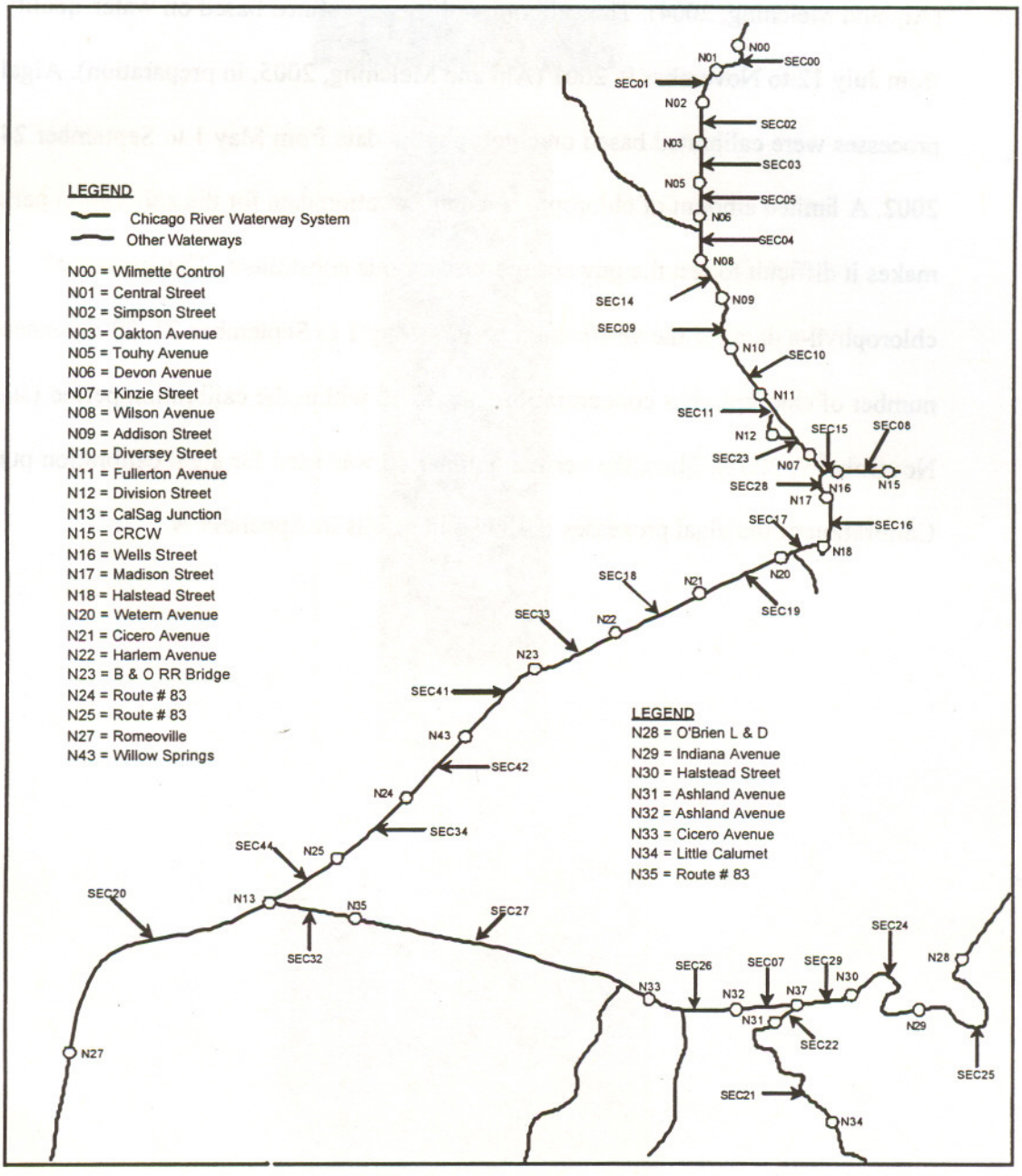

Figure 3.2 Calculation nodes (N) and sections (SEC) for the Chicago Waterway System (after Shrestha and Melching, 2003)

3.2.2. Water Quality Model

The water-quality model initially was calibrated for the period April 1 – May 4, 2002 (Alp and Melching, 2004). The calibration then was refined based on water-quality data from July 12 to November 9, 2001 (Alp and Melching, 2005, in preparation). Algal processes were calibrated based on chlorophyll-a data from May 1 to September 24, 2002. A limited amount of chlorophyll-a concentration data for the calibration period makes it difficult to test the power of model for this constituent. The amount of chlorophyll-a data for the verification period (May 1 to September 24, 2002) exceeds number of chlorophyll-a concentrations measured within the calibration period (July 12 – November 9, 2001). Thus, the verification period was used for algal calibration purposes. Calibration of the algal processes is shown in details in Appendix A.

CHAPTER 4: HYDRAULIC MODEL

4.1. Hydraulic Model Parameters

The system was divided into 11 reaches, similar to those for the UNET (Barkau, 1992) model applied by the U.S. Army Corps of Engineers to the CWS. The river miles bounding the reaches used for the hydraulic model of the CWS are listed in Table 4.1.

Table 4.1 Description of reaches used in the hydraulic model of the Chicago Waterway System

Reach	Waterway	River Mile from Lockport	
		Beginning	End
2	North Shore Channel	50.0	42.5
3	North Branch	42.5	36.8
4	North Branch*	36.8	35.4
5	North Branch*	36.8	35.4
6	North Branch	35.4	34.5
7	Chicago River Main Stem	36.0	34.5
8	South Branch and Chicago Sanitary and Ship Canal (CSSC) to Sag Junction	34.5	12.5
9	Little Calumet River (south)	35.9	28.5
10	Little Calumet River (north)	35.4	28.5
11	Calumet-Sag Canal	28.5	12.5
12	CSSC from Junction to Romeoville	12.5	5.1

*West and east sides of Goose Island, respectively.

Hydraulic model calibration refers to flow resistance parameter adjustment so that model predictions match field data within some acceptable criteria. Flow resistance for hydraulic computations of flow in open channels may be represented either by Manning's n or Chezy's roughness coefficient, C. The DUFLOW model uses Chezy's C. Calibrated values for Chezy's C and equivalent values of Manning's n are listed in Table 4.2.

Table 4.2 DUFLOW calibrated values for Chezy's roughness coefficient C and the equivalent Manning's n values (after Shrestha and Melching, 2003)

Reach	Reach Name	Hydraulic Radius (m)	Chezy's C	Manning's n
2	North Shore Channel	2.37	38	0.030
3	North Branch	3.08	38	0.032
4	Goose Island West	4.86	38	0.034
5	Goose Island East	4.86	38	0.034
6	North Branch	4.86	38	0.034
7	Chicago River Main Stem	5.59	44	0.030
8	South Branch and Chicago Sanitary and Ship Canal (CSSC) to Sag Junction	4.61	60	0.022
9	Little Calumet River (south)	0.93	6	0.165
10	Little Calumet River (north)	2.16	50	0.023
11	Calumet-Sag Canal	2.93	47	0.025
12	CSSC Sag Junction to Romeoville	6.26	41	0.033

4.2. Input Data Used for Verification

The DUFLOW model for the CWS simulates unsteady-state conditions, and, therefore, it requires input data in time series. Time steps vary from 15 minutes to 1-day for hydraulic input. Specification of the data used for the input and their time step are listed in Table 4.3.

Table 4.3 Input data, their source, and time step used in the input to the hydraulic model

Location	Data Source	Type of Input	Time Step
Boundary			
Wilmette Pumping Station	USGS	flow	1 day
Chicago River Controlling Works	USGS	elevation	1 hour
O'Brien Lock and Dam	USGS	elevation	1 hour
Little Calumet River at South Holland	USGS	flow	15 min
Romeoville	USGS	flow/elevation[1]	15 min
Treatment Plants			
North Side Water Reclamation Plant	MWRDGC	flow	1 hour
Stickney Water Reclamation Plant	MWRDGC	flow	1 hour
Lemont Water Reclamation Plant	MWRDGC	flow	1 day
Calumet Water Reclamation Plant	MWRDGC	flow	1 hour
Tributaries			
Tinley Creek	USGS	flow	15 min
Midlothian Creek	USGS	flow	15 min
Grand Calumet River	USGS	flow	1 hour
Stony Creek (East)	Estimation[2]	flow	15 min
Stony Creek (West)	Estimation[2]	flow	15 min
Navajo Creek	Estimation[2]	flow	15 min
Mill Creek	Estimation[2]	flow	15 min
Calumet Sag Watershed	Estimation[2]	flow	15 min
Des Plaines Basin	Estimation[2]	flow	15 min
Calumet Union Ditch	Estimation[2]	flow	15 min
Calumet-Sag End Watershed	Estimation[2]	flow	15 min
CSO and Pump Stations			
North Branch Pump Station	MWRDGC	flow	1 hour
Racine Avenue Pump Station	MWRDGC	flow	1 hour
125th Street Pump Station	MWRDGC	flow	1 hour
28 representative CSO discharges	Estimation[3]	flow	1 hour

1) Flow for period 05/01/02 – 08/11/02, Water-surface elevation for period 08/12/02 – 09/24/02.
2) Based on method developed by Shrestha and Melching (2003).
3) Based on method developed by Alp and Melching (2004).
NOTE: USGS = U.S. Geological Survey, MWRDGC = Metropolitan Water Reclamation District of Greater Chicago, and CSO = Combined sewer overflow.

4.2.1. Boundary Conditions

The CWS has four upstream boundaries at Wilmette Pump Station, Chicago River Controlling Works (CRCW), O'Brien Lock and Dam, and Little Calumet River at South Holland. The downstream boundary is located at Romeoville. As a hydraulic boundary condition for the unsteady-flow model either flow or water-surface elevation versus time data were used. Flow was used as an upstream boundary condition at Maple Avenue in Wilmette (U.S. Geological Survey (USGS) gage #05536101) and South Holland (USGS gage #05536290), whereas water-surface elevation was used as the boundary condition at the Chicago River at Columbus Drive (near CRCW) (USGS gage #05536123), and at the Calumet River at the Thomas J. O'Brien Lock and Dam (USGS gage #05536357).

In the initial calibration of the water-quality model (Alp and Melching, 2004), water-surface elevation versus time was used at Maple Avenue at Wilmette because the water-surface elevation data were substantially more accurate than the available flow data. As reported in Alp and Melching (2004) water-quality simulation was poor on the North Shore Channel upstream from the North Side Water Reclamation Plant, on the Chicago River Main Stem, and on the Little Calumet River (north) upstream from the Calumet Water Reclamation Plant because of differences between measured and simulated flows resulting from the computational need to obtain the proper system-wide water balance. Because improved DO concentrations on the upper North Shore Channel are a key goal of the UAA, a flow boundary was used at Maple Avenue to improve DO simulation on upper North Shore Channel. Water-surface elevation boundaries were retained at

Columbus Drive and O'Brien Lock and Dam to avoid computational problems because of flow imbalances.

As a downstream boundary condition at the USGS gage 05536995 on the Chicago Sanitary and Ship Canal at Romeoville flow was used for the period 05/01/2002 – 08/11/2002 and water-surface elevation was used for the period 08/12/2002 – 09/24/2002 due to a lack of flow data for the beginning of this period (until 08/22/2002).

4.2.2. Measured Inflows to the System

The discharge to the CWS from four treatment plants (North Side, Stickney, Calumet, and Lemont) was measured and provided by MWRDGC. Discharges from pump stations were obtained based on information provided by MWRDGC on pump capacities and time operation schedules. Only a few tributaries to the CWS are gaged by the USGS. Tinley Creek near Palos Park (USGS gage #05536500) and Midlothian Creek at Oak Forest (USGS gage #05536340) are tributary flows to the Calumet-Sag Channel. The USGS gage measurements on the Grand Calumet River at Hohman Avenue at Hammond, Ind. (USGS gage #05536357) are an inflow to the Calumet River. Flow on the North Branch Chicago River is measured just upstream of its confluence with the North Shore Channel at USGS gage #05536105 at Albany Avenue.

4.2.3. Flow Estimation for Ungaged Tributaries

Ungaged tributaries flow into the CWS, therefore, it is necessary to estimate the inflows from them. For this estimation, a procedure developed by Shrestha and Melching (2003)

for the original hydraulic calibration of the model was used. This procedure is based on the assumption that flow in a river channel is proportional to the area drained by this river, and the hydrologic similarity between ungaged watersheds and the Midlothian Creek watershed. Therefore, discharge from ungaged tributaries was estimated based on the ratio between the drainage area of the ungaged stream and Midlothian Creek. The drainage area ratios of ungaged tributaries with Midlothian Creek (at its outlet to the Calumet-Sag Channel, drainage area = 20.0 mi^2) are listed in Table 4.4.

Table 4.4 Calculation of flow in ungaged tributaries and watersheds (after Shrestha and Melching, 2003)

Ungaged Stream	Ratio with Midlothian
Mill Creek West	0.550
Stony Creek West	1.086
Calumet-Sag Watershed East	0.246
Navajo Creek	0.137
Stony Creek East	0.486
Ungaged Des Plaines Watershed	0.703
Calumet Union Ditch	1.168
Calumet-Sag Watershed West	0.991

4.2.4.Overflows from Combined Sewers

In the original hydraulic calibration (Shrestha and Melching, 2003) only 6 locations were used to represent the whole system of nearly 200 CSOs in the modeled CWS drainage area. Since it is practically difficult to introduce all CSO locations in the modeling, 28 representative CSO locations were identified and flow distribution was done on the basis of drainage area for each of these locations (Alp and Melching, 2004). By increasing the number of CSOs from 6 to 28, more appropriate CSO loads are provided. The location

and drainage area for each of the 28 overflow points is as in Alp and Melching (2004). The volume of CSO was determined from the system wide flow balance and water level measurements at Romeoville based on the procedure described in Alp and Melching (2004). The time of overflows from the combined sewer system was assigned based on the North Branch Pump Station operational time.

4.3. Flow Balance

In order to balance the flow, total inflow to the system was compared with total outflow at Romeoville. For the purpose of this balance, it was assumed that the difference in the water balance due to the travel time and change in storage are negligible (Alp and Melching, 2004). The inflow to the CWS is composed of flows from tributaries, water reclamation plants, pumping stations, CSOs, and from Lake Michigan. Not all inflows are gaged and the ungaged flows were estimated by various mathematical and statistical methods described in detail in Shrestha and Melching (2003). In this flow balance CSO discharge was not considered except at the pumping stations. Comparison of total inflow to the CWS and outflow at Romeoville is shown in the Figure 4.1. Table 4.5 presents a balance of average daily inflows and compares it with average daily outflow for the period May 1 to September 24, 2002. Over the whole analyzed period the total inflow listed in Table 4.5 was 7.09% lower than the outflow at Romeoville. This difference results because CSOs were not included in the flow balance, and this difference is used to estimate the CSO discharge as described in Alp and Melching (2004).

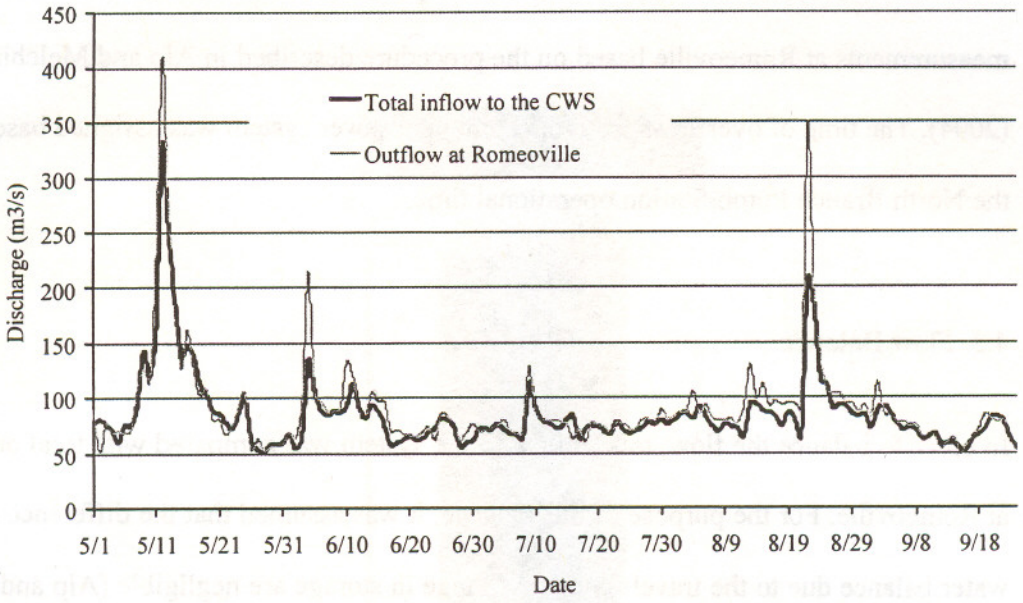

Figure 4.1 Comparison of the summation of all measured or estimated inflows (excepted CSOs) and the measured outflow at Romeoville for May 1 to September 24, 2002

Table 4.5 Balance of average daily flows for the Chicago Waterway System for May 1 to September 24, 2002

Note: Measured inflows are in bold

Flow Balance Component	Flow (m^3/s)
Mill Creek + Stony Creek (W)	0.74
Narajo Creek + Calumet-Sag basin	0.17
Calumet Union Ditch	0.53
Stony Creek (E)	0.22
Calumet-Sag End Watershed	0.45
Lower Des Plaines Basin	0.32
Lemont Water Reclamation Plant	0.10
Calumet Water Reclamation Plant	10.71
Grand Calumet River	0.20
Racine Avenue Pump Station	1.02
125th Street Pump Station	0.06
North Branch Pump Station	0.13
Midlothian Creek	0.45
Chicago River at Columbus Drive	8.27
Calumet River at O'Brien Lock and Dam	5.16
North Shore Channel at Wilmette	2.25
Tinley Creek	0.41
Little Calumet River at South Holland	4.90
North Branch Chicago River at Albany Avenue	4.60
Stickney Water Reclamation Plant	32.70
North Side Water Reclamation Plant	11.16
TOTAL INFLOW	84.55
TOTAL OUTFLOW (Romeoville)	-91.00
Difference	-6.45
% Difference	-7.09

CSO volumes and time periods for the entire CWS are listed in Table 4.6. In Figure 4:1 a substantial discrepancy is shown between measured and estimated inflow to and outflow from the CWS around June 4, 2002. For this period the simulated water levels at Romeoville typically were within 0.1 m of the observed water levels at Romeoville. Indicating there is sufficient water in the system to meet the measured discharge without adding flows from CSOs. This may be a case where the MWRDGC dewatered the canal in anticipation of a major flood that did not result.

Table 4.6 CSO volumes for the Chicago Waterway System for the verification period (May 1 to September 24, 2002)

Event	Start time	End time	CSO volume, (m^3)
1	5/11/02 14:00	5/12/02 23:00	43,214,462
2	5/16/02 15:00	5/16/02 22:00	1,349,309
3	6/11/02 20:00	6/11/02 23:00	3,437,078
4	7/9/02 3:00	7/9/02 6:00	1,182,557
5	8/22/02 4:00	8/23/02 16:00	5,722,272

4.4. Results of Hydraulic Verification

The water-surface elevation data on the CSSC at Western Avenue, Willow Springs, Sag Junction, and Romeoville were used for model calibration and verification (Shrestha and Melching, 2003). Alp and Melching (2004) additionally verified the model at two new stage gages: North Branch Chicago River at Lawrence Avenue and Calumet-Sag Channel at Southwest Highway. In this study, water-surface elevation data on the CSSC at Western Avenue, Willow Springs, and Sag Junction; North Branch Chicago River at Lawrence Avenue; Calumet-Sag Channel at Southwest Highway; and the North Shore Channel at Wilmette were used to verify the model for the whole period of May 1 to

September 24, 2002. Measured water-surface elevation data at Romeoville were compared with simulated values only for the first sub period, May 1 to August 11, 2002, due to a discontinuity in flow data at Romeoville. Graphical comparison of measured and simulated water-surface elevations for the appropriate time periods is presented in Figure 4.2 and statistical comparisons of these water-surface elevations are listed in Tables 4.7 and 4.8.

For verification purposes, measured flow at Romeoville was compared with simulated values for the period of August 12 to September 24, 2002. Average daily measured and simulated flows were compared on the Chicago River at Columbus Drive and the Calumet River at O'Brien Lock and Dam. In addition flow data from a new USGS station on the North Branch Chicago River at Grand Avenue were used for verification purposes. Graphical comparisons of flow are shown in Figure 4.3, and statistical comparisons are presented in Table 4.9.

Table 4.7 Comparison of simulated and measured hourly water-surface elevations relative to the City of Chicago Datum for May 1 to September 24, 2002

Note: wrt= with respect to; Elevation Error = simulated-measured; Abs Error = absolute value of simulated and measured; % Error wrt Depth = (simulated elevation-measured elevation)/measured depth·100; Abs % Error wrt Depth = absolute value of (simulated elevation-measured elevation)/measured depth·100.

Location		Measured Elevation (m)	Simulated Elevation (m)	Simulated Water Depth (m)	Measured Water Depth (m)	Elevation Error (m)	Abs Error	% Error wrt Depth	Abs % Error wrt Depth
Western Avenue	Mean	-0.57	-0.56	6.87	6.86	0.00	0.03	-0.06	0.45
	min.	-0.79	-0.79	6.64	6.64	-0.33	0.00	-4.68	0.00
	max.	1.12	0.90	8.33	8.55	0.43	0.43	5.29	5.29
	STD	0.09	0.09	0.09	0.09	0.04	0.03	0.60	0.40
Willow Springs	Mean	-0.61	-0.59	7.48	7.46	-0.02	0.04	-0.31	0.49
	min.	-1.00	-1.04	7.03	7.07	-0.34	0.00	-4.67	0.00
	max.	-0.28	0.09	8.16	7.79	0.28	0.34	3.62	4.67
	STD	0.05	0.07	0.07	0.05	0.04	0.03	0.55	0.39
Sag Junction	mean	-0.64	-0.60	7.78	7.78	-0.04	0.05	-0.53	0.64
	min.	-1.18	-1.20	7.18	7.20	-0.27	0.00	-3.53	0.00
	max.	-0.41	-0.35	8.03	8.03	0.21	0.27	2.78	3.53
	STD	0.07	0.07	0.07	0.07	0.05	0.04	0.59	0.46
Lawrence Avenue	mean	-0.44	-0.47	3.05	3.07	0.01	0.07	0.44	2.19
	min.	-0.71	-0.65	2.86	2.80	-0.88	0.00	-23.00	0.00
	max.	1.43	1.54	5.06	4.94	0.88	0.88	21.37	23.00
	STD	0.21	0.21	0.21	0.21	0.10	0.08	3.01	2.11
Southwest Highway	mean	-0.57	-0.60	3.36	3.39	0.03	0.05	0.86	1.37
	min.	-0.94	-1.18	2.78	3.02	-0.26	0.00	-7.76	0.00
	max.	0.15	-0.35	3.61	4.11	0.67	0.67	17.39	17.39
	STD	0.08	0.07	0.07	0.08	0.08	0.07	2.14	1.85
Romeoville (May 1 to August 11)	mean	-0.68	-0.69	8.30	8.31	0.01	0.04	0.16	0.55
	min.	-2.35	-2.38	6.61	6.64	-1.21	0.00	-17.63	0.00
	max.	-0.49	-0.39	8.60	8.50	0.49	1.21	6.96	17.63
	STD	0.19	0.22	0.22	0.19	0.07	0.06	0.98	0.82
Wilmette	mean	-0.05	-0.47	3.05	3.47	0.42	0.45	11.97	12.79
	min.	-0.63	-0.65	2.86	2.89	-1.53	0.01	-43.70	0.21
	max.	0.90	1.54	5.06	4.41	0.97	1.53	25.08	43.70
	STD	0.10	0.21	0.21	0.10	0.22	0.15	6.12	4.12

Table 4.8 Percentage of the hourly water-surface elevations for which the error in simulated values compared with measured values relative to the depth of water is less than the specified percentage

	Percentage			
Location	**<±1% of Depth**	**<±2% of Depth**	**<±5% of Depth**	**<±10% of Depth**
Western Avenue	93.46	99.06	99.94	99.97
Willow Springs	91.41	99.31	99.96	99.96
Sag Junction	81.63	98.94	99.97	99.97
Lawrence Avenue	26.14	53.34	96.33	98.65
Southwest Highway	55.44	81.45	96.47	98.55
Romeoville	88.35	97.05	99.35	99.88
Wilmette	0.44	0.84	3.69	21.90

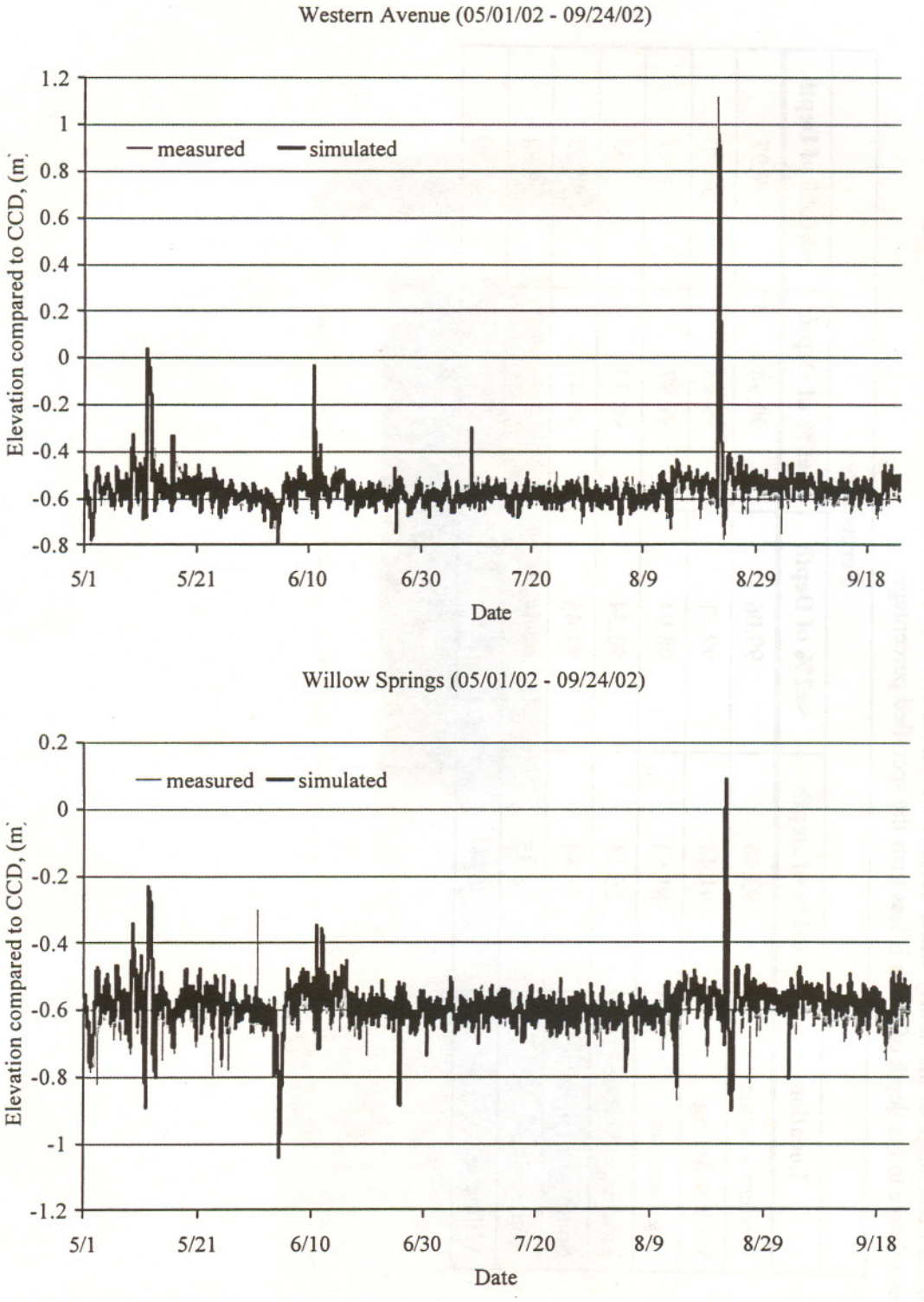

Figure 4.2 Comparison of measured and simulated water-surface elevations relative to the City of Chicago Datum (CCD) at different locations in the Chicago Waterway System

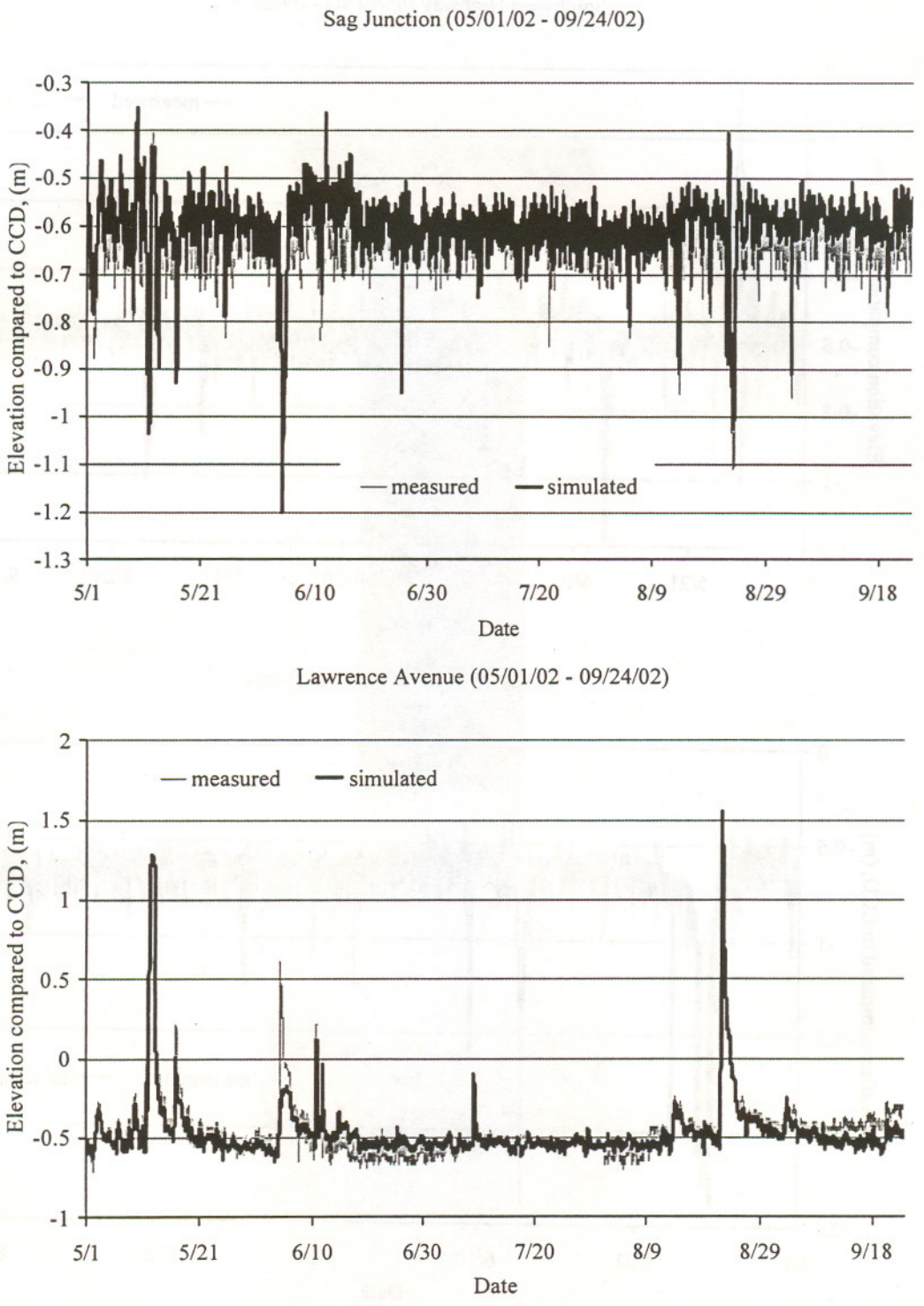

Figure 4.2(cont.) Comparison of measured and simulated water-surface elevations relative to the City of Chicago Datum (CCD) at different locations in the Chicago Waterway System

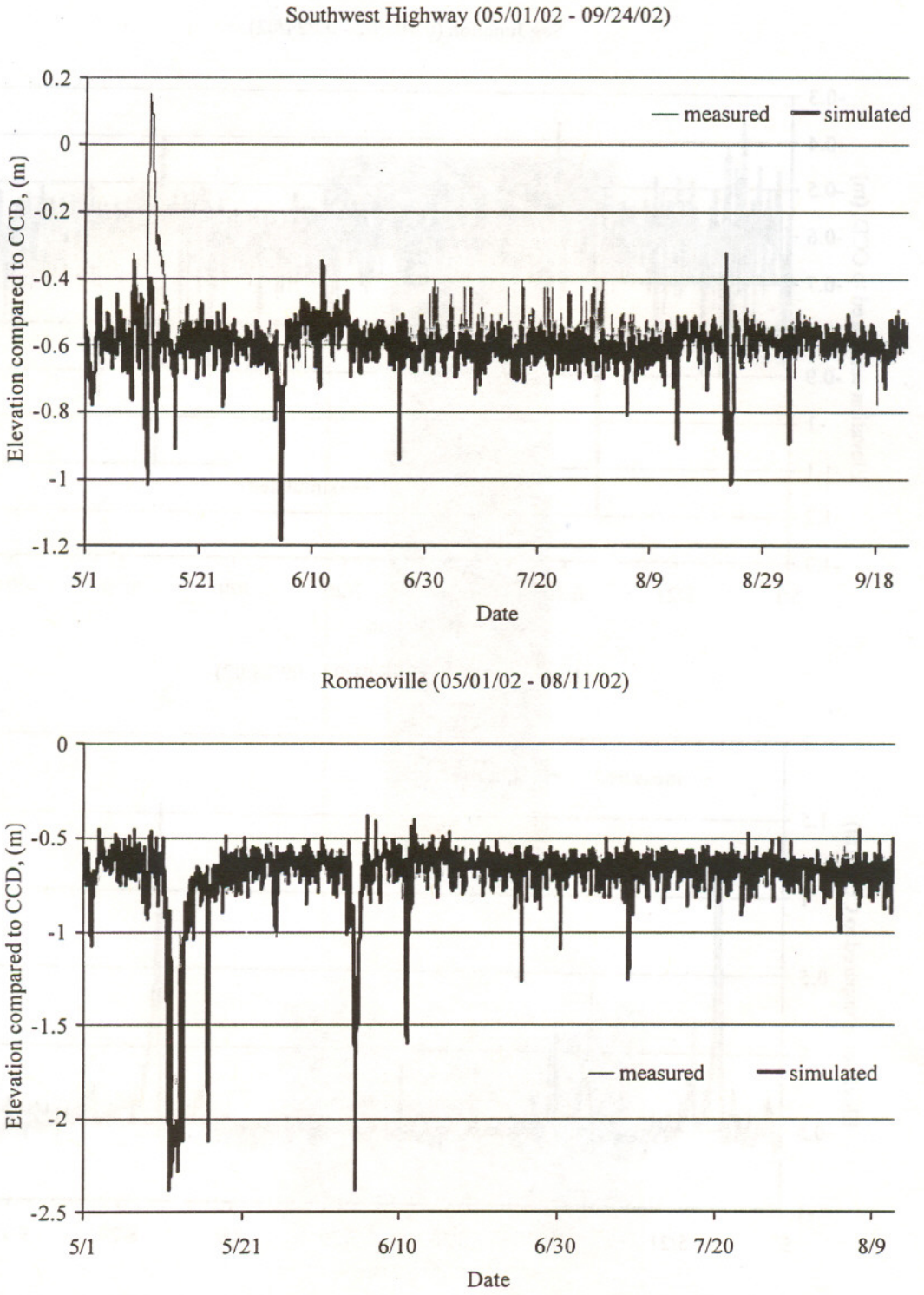

Figure 4.2 (cont.) Comparison of measured and simulated water-surface elevations relative to the City of Chicago Datum (CCD) at different locations in the Chicago Waterway System

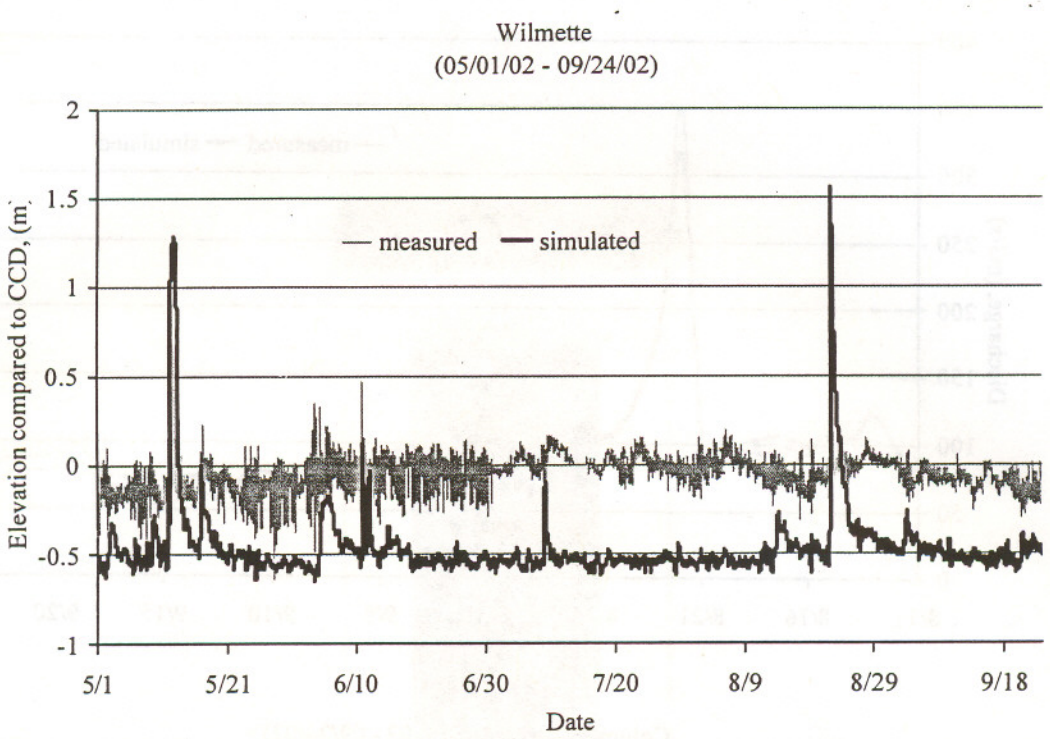

Figure 4.2(cont.) Comparison of measured and simulated water-surface elevations relative to the City of Chicago Datum (CCD) at different locations in the Chicago Waterway System

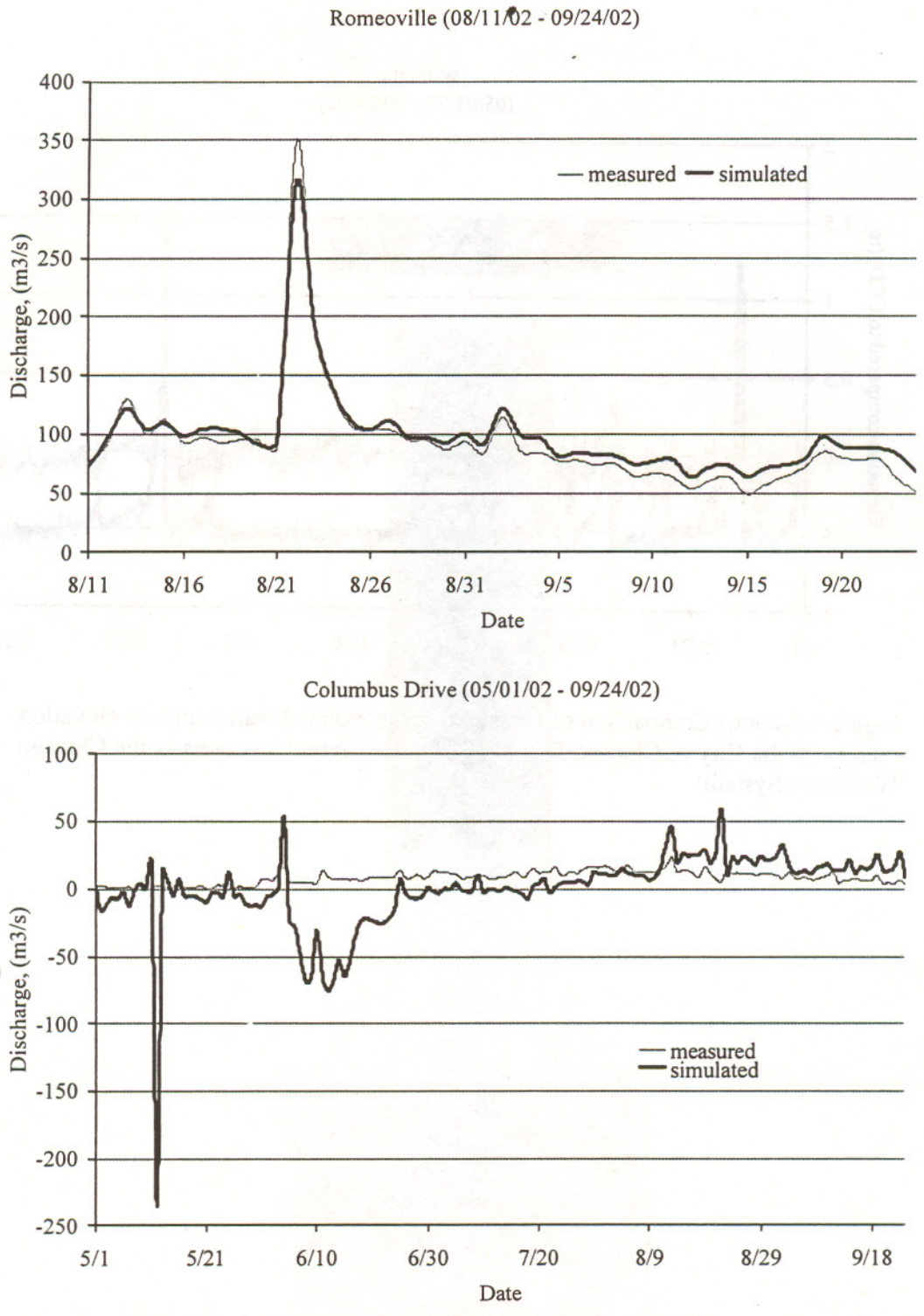

Figure 4.3 Comparison of measured and simulated average daily flows at some locations on Chicago Waterway System

(Note: For Romeoville, the measured flow for August 12-21 is estimated from measurements made at the Lockport Powerhouse and Controlling Works)

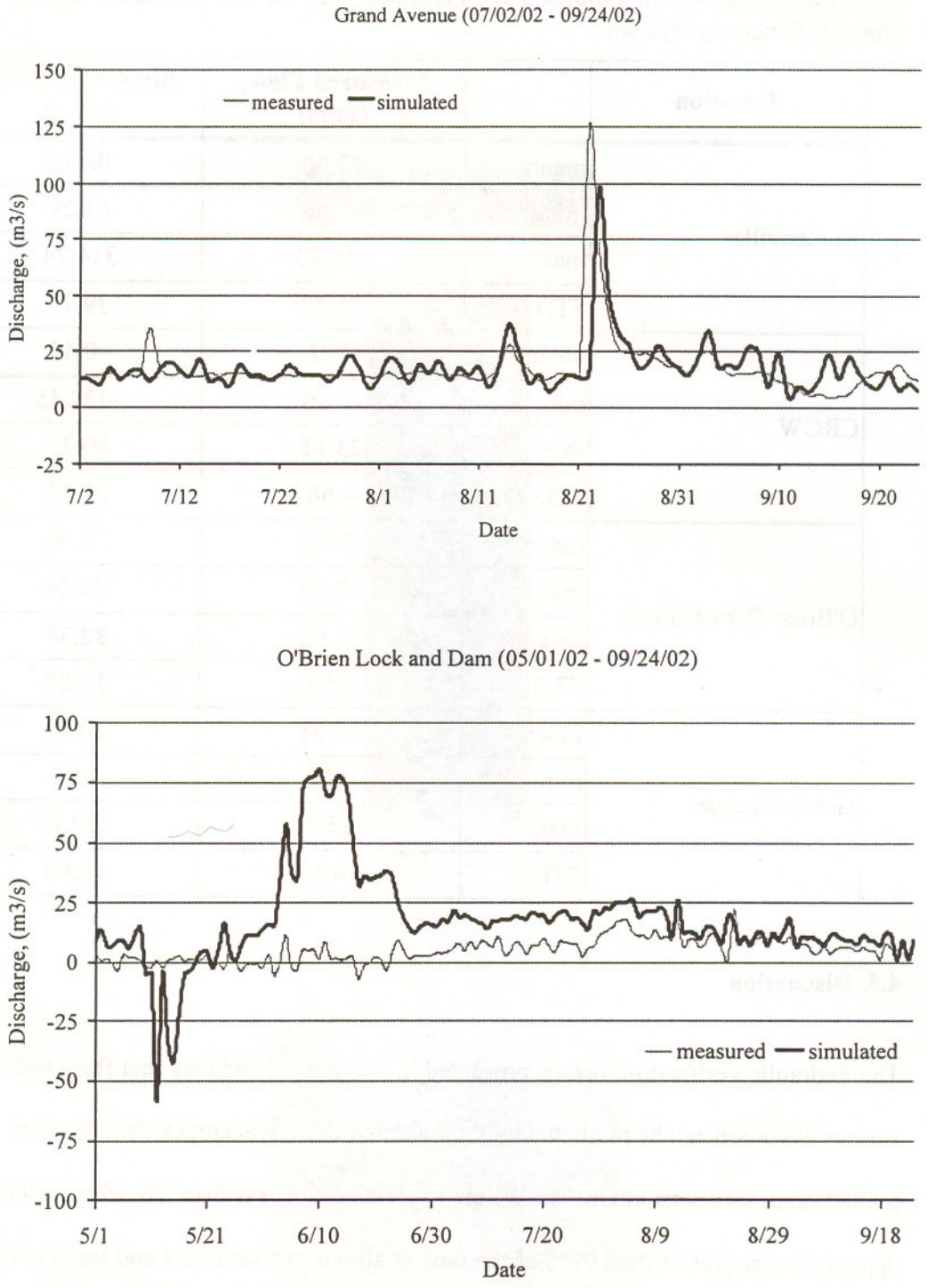

Figure 4.3 (cont.) Comparison of measured and simulated average daily flows at some locations on Chicago Waterway System

Table 4.9 Comparison of simulated and measured daily flow at different locations on the Chicago Waterway System

Location		Measured Flow, (m^3/s)	Simulated Flow, (m^3/s)
Romeoville	mean	92.00	98.42
	min.	48.59	63.29
	max.	348.75	314.74
	STD	46.38	39.75
CRCW	mean	8.27	-0.45
	min.	-0.96	-235.45
	max.	23.11	59.41
	STD	4.68	29.71
O'Brien Dam & Lock	mean	5.16	17.60
	min.	-7.02	-58.90
	max.	21.92	80.34
	STD	4.93	19.84
Grand Avenue	mean	17.58	20.14
	min.	4.71	1.28
	max.	125.46	129.72
	STD	14.40	15.94

4.5. Discussion

The hydraulic verification results presented in Section 4.4 indicate that flow and water-surface elevation can be predicted by the model with high accuracy. Model stage prediction in locations other than Wilmette yields errors less than 2% with respect to the depth of water greater than 97% of the time at all but two locations and less than 5% with respect to depth 96% of the time at these two locations. Good predictability of the model is confirmed by flow results at the Grand Avenue location on the North Branch Chicago River. This gage was not used during calibration and simulated flow shows good

agreement with measured values. Comparison between total measured and simulated flows from July 2 to September 24, 2002 shows that total flow at Grand Avenue is about 0.4% overestimated by the model.

Agreement between measured and simulated flow/stage at the boundary is not as good as in the other locations. For most of the simulation period the general trends of the simulated and measured values are similar. As was discussed in Shrestha and Melching (2003) and Alp and Melching (2004), some deviations result because of the overall flow imbalance shown in Table 4.5, which are more pronounced during wet weather periods. Moreover, the model tends to underestimate flow at Columbus Drive and overestimates flow at O'Brien Lock and Dam and Romeoville. Detailed discussion and interpretation of the phenomena at O'Brien Lock and Dam and Columbus Drive can be found in Shrestha and Melching (2003) and Alp and Melching (2004). However, at the downstream boundary total flow overestimation is less than 7%, which confirms that the DUFLOW model represents well enough the hydraulic processes in the Chicago Waterway System and is useful for water-quality analysis.

CHAPTER 5: WATER-QUALITY MODEL

5.1. Water-quality model parameters

To simulate water quality the CWS was divided into 17 reaches, similar to those used in the QUAL2E study of Camp, Dresser & McKee (1992). The river miles bounding the reaches used for the water-quality model of the CWS are listed in Table 5.1.

Table 5.1 Description of reaches used for water-quality modeling

Note: CSSC = Chicago Sanitary and Ship Canal

Reach	Waterway	River Mile from Lockport	
		Beginning	End
C1	North Shore Channel	50.0	46.0
C2.1	North Shore Channel	46.0	41.6
C2.2	North Branch Chicago River	41.6	37.0
C3	North Branch Chicago River	37.0	35.5
C4	North Branch Chicago River	35.5	34.5
C5	Chicago River Main Stem	34.5	36.0
C6	South Branch Chicago River	34.5	31.0
C7	CSSC	31.0	25.0
C8	CSSC	25.0	17.0
C9	CSSC	17.0	12.5
C10	Calumet River	35.9	35.5
C11	Little Calumet River (North)	35.5	30.5
C12	Little Calumet River (North)	30.5	28.5
C13	Calumet-Sag Channel	28.5	19.0
C14	Calumet-Sag Channel	19.0	12.5
C15	CSSC	12.5	8.0
C16	CSSC	8.0	5.1
C17	Little Calumet River (South)	35.9	28.5

Calibration of the CWS water-quality model led to determination of parameters relating to water-quality processes. These parameters are either constant through the entire system or varied between reaches. Values of calibrated parameters that vary between reaches are given in Table 5.2, and values of calibrated parameters constant through the entire system are given in Table 5.3.

Table 5.2 Calibration parameters varied between reaches used in the DUFLOW water-quality model of the Chicago Waterway System

(D – dispersion coefficient; E_{dif} – diffusive exchange rate coefficient; k – constant of O'Connor-Dobbins equation for estimation of the reaeration-rate coefficient; K_{bod} – oxidation rate constant for CBOD; K_{nit} – nitrification rate constant; μ_{max} – maximum specific growth rate of algae)

Reach	D, (m^2/s)	E_{dif}, (m^2/day)	k, (-)	K_{bod}, (day^{-1})	K_{nit}, (day^{-1})	μ_{max}* (day^{-1})
C1	25	0.02	1.5	0.15	1.2	3
C2.1	15	0.002; 0.03 [1]	3.94	0.1	0.2	5
C2.2	100	0.03	3.94; 0.1 [2]	0.1	1.2	5
C3	100	0.001	3.94	0.01	0.01	5
C4	100	0.001	0.1	0.01	0.01	5
C5	15	0.02	3.94	0.05	0.01	5
C6	15	0	0.1	0.15	1	7
C7	1000	0.002	0.1	0.15	1	7
C8	60	0	0.1	0.01	0.01	7
C9	60	0	0.1	0.01	0.05	5
C10	1000	0.0002	0.1	0.05	0.01	6
C11	1000	0.0002	3.94	0.05	0.01	6
C12	15	0.02	3.94	0.1	0.5	5
C13	15	0	3.94; 0.1 [3]	0.1	0.5	6
C14	10	0	0.1	0.1	0.5	5
C15	50	0	0.1	0.05	0.05	2
C16	50	0	0.1	0.05	0.05	2
C17	15	0.002	3.94	0.035	0.3	5

*Parameters calibrated based on chlorophyll-a concentrations from May 1 to September 24, 2002.
NOTE: Double parameter values indicates that values change in the middle of the section
1) e_{dif} = 0.002 between river miles 46.0 and 42.5; e_{dif} = 0.03 between river miles 42.5 and 41.6
2) k = 3.94 between river miles 41.6 and 39.2; k = 0.1 between river miles 39.2 and 37.0
3) k = 3.94 between river miles 28.5 and 28.1; k = 0.1 between river miles 28.1 and 19.0

Table 5.3 Calibration parameters constant through the entire system used in the DUFLOW water-quality model of the Chicago Waterway System

Parameter		Value	Unit
K_{bodB}	Anaerobic decomposition rate constant for CBOD in the sediment layer	0.05	1/day
K_{bodo}	Oxygen half saturation constant CBOD decay	2	g/m^3
K_{daB}*	Anaerobic decay rate constant for algae in the sediment layer	0.01	1/day
K_{den}	Denitrification rate constant in the water column	0.1	1/day
K_{denB}	Denitrification rate constant in the sediment layer	0.05	1/day
K_{dno}	Monod constant for denitrification	0.5	gO_2/m^3
K_{min}	Mineralization rate for organic matter in the water column	0.1	1/day
K_{minB}	Anearobic mineralization rate constant for organic matter in the sediment layer	0.0004	1/day
K_{mN}*	Ammonia preference constant	0.025	gN/m^3
$k_{n,1}$*	Monod constant for nitrogen in algal growth (species 1)	0.01	gN/m^3
K_{no}	Monod constant for nitrification	0.1	mgO_2/m^3
$k_{p,1}$*	Monod constant for phosphorus in algal growth (species 1)	0.005	gP/m^3
K_{pipB}	Partition coefficient for inorganic phosphorous in the sediment layer	0.0001	m^3/gSS
K_{pipW}	Partition coefficient for inorganic phosphorous in the water column	0.01	m^3/gSS
K_{res}*	Respiration rate constant for algal species 1	0.1	1/day
K_{die}*	Die-off rate constant for algal species 1	0.05	1/day

*Parameters calibrated based on chlorophyll-a concentrations from May 1 to September 24, 2002.

5.2. Water Quality Input Data

In order to consider all water-quality processes relating to the DO concentration in the water column that are included in EUTROF2, input data should consist of concentrations of DO, CBOD, different forms of nitrogen (organic, ammonia, nitrate), organic and inorganic forms of phosphorous, and chlorophyll a. One of the key variables in the water-

quality model is temperature, because it affects reaction kinetics and the DO saturation concentration. Measured in-stream water temperature was introduced to the model at each continuous monitoring location (i.e. the model's nodes) with a one-hour time step. The CWS receives pollutant loads from four water reclamation plants, nearly 200-combined sewer overflow points, direct diversions from Lake Michigan and 11 tributary streams and areas. Additionally, water quality in the system is affected by the DO input load from four Sidestream Elevated Pool Aeration (SEPA) stations and two in-stream aeration stations. In some locations, not all required constituent concentrations or loads are measured. Therefore, some assumptions were made. Assumptions used to determine the various constituents loadings and concentrations from different sources are discussed in the following sections.

5.2.1. SEPA Stations

Within the water-quality study area, there are 4 SEPA stations located on the Calumet-Sag Channel and Little Calumet River (north). At the SEPA stations water is pumped into an elevated pool, from where it flows over cascades back to the stream. Due to increased contact of the water surface with air, the pumped portion of water is aerated. The discharge of aerated water from the SEPA stations is considered as a DO load to the CWS. The oxygen load from the SEPA stations is estimated based on the efficiency of the stations. SEPA station efficiencies ware determined for different numbers of working pumps by Butts et al. (1999 and 2000). These studies were used for oxygen load calculations as is described in detail in Alp and Melching (2004). The oxygen load from the SEPA stations was calculated using equation 5.1:

$$\text{Oxygen Load} = Q_p \cdot a \cdot (C_{SAT} - C_{UPSTREAM}), \text{ g/s} \quad (5.1)$$

where:

Q_p = flow through the SEPA station calculated based on information about the pump operation schedule and pump capacities provided by the MWRDGC, (m^3/s)

a = fraction of saturation achieved as a function of the number of pumps in operation, from Butts et al. (1999)

C_{SAT} = saturation concentration of DO determined from continuous in-stream water temperature data and adjusted to the SEPA station elevation above sea level (based on formula developed by Butts et al. (1999))

$C_{UPSTREAM}$ = DO concentration upstream of the SEPA station determined from monitoring data

A summary of the input loads from the SEPA stations for the verification period is presented in Table 5.4.

5.2.2.In-stream Aeration Stations

Within the water-quality study area, there are 2 diffused aeration stations located on the North Shore Channel (Devon Avenue facility) and the North Branch of the Chicago River (Webster Street facility). The DO transfer efficiency of the Devon Avenue facility was determined in a previous study (Polls et al., 1982). In this study, it was assumed that characteristics of the DO diffusion process for the Devon Avenue facility determined by Polls et al. (1982) are also valid for the Webster Avenue facility (Alp and Melching,

2004). The DO load from the diffused aeration stations is estimated based on the DO transfer efficiency of the stations. The relation between the upstream DO percentage of saturation and downstream dissolved oxygen absorption was determined as a linear relation for different numbers of working blowers. A detailed description of the DO load calculation can be found in Alp and Melching (2004). The oxygen load used as an input to the model was calculated based on a relation described with equation 5.2:

$$\text{Oxygen Load} = \%DO_{INCREASE} \cdot DO_{UPSTREAM} \cdot Q/100, \text{ g/s} \qquad (5.2)$$

where:

Q = discharge at the aeration station, (m^3/s)

$\%DO_{INCREASE}$ = percent DO increase downstream of the aeration station from regression equations between upstream percentage of DO saturation and downstream DO absorption for a given number of working blowers, based on Polls et al. (1982)

$DO_{UPSTREAM}$ = measured DO concentration upstream of the aeration station, (mg/L)

A summary of input loads from the in-stream aeration stations for the verification period is presented in Table 5.4.

Table 5.4 Characteristics of dissolved oxygen load from the sidestream elevated pool and in-stream aeration stations for May 1 – September 24, 2002

DO Load (g/s)						
	Sidestream Elevated Pool Aeration Stations #				**In-stream Aeration Station at**	
	2	**3**	**4**	**5**	**Devon**	**Webster**
mean	5.48	10.49	7.96	8.07	19.19	26.39
max	23.83	23.67	18.16	27.42	90.66	275.49
min	0	0	0	0	0	0
SD	5.24	4.74	4.8	4.87	11.96	25.23

5.2.3. Water Reclamation Plants

There are 4 water reclamation plants (WRPs) discharging to the CWS: North Side WRP, Stickney WRP, Calumet WRP, and Lemont WRP. They have the greatest contribution of loads to the system. Daily measured outfall quality from these facilities is used as an input for the model. Characteristics of effluent quality from these three WRPs are summarized in Table 5.5.

It should be noted that only total phosphorous concentration was measured in effluent from the WRPs. Organic phosphorous was estimated from relations between organic phosphorous, ($P_{ORGANIC}$), and suspended solids (SS) as described by equation 5.3:

$$P_{ORGANIC} = 0.7 \cdot 0.025 \cdot SS \tag{5.3}$$

Inorganic phosphorous was calculated as a difference between total and organic phosphorous (P_{TOTAL} and $P_{ORGANIC}$, respectively):

$$P_{INORGANIC} = P_{TOTAL} - P_{ORGANIC} \tag{5.4}$$

Table 5.5 Characteristics of effluent from water reclamation plants (WRP) for the verification period (May 1 to September 24, 2002)

	DO (mg/L)	$CBOD_5$ (mg/L)	NH_4 (mg/L)	NO_3 (mg/L)	N_{org} (mg/L)	P_{org}* (mg/L)	P_{in}* (mg/L)	SS (mg/L)
North Side WRP								
mean	7.23	5.86	0.53	6.88	1.12	0.08	1.18	4.53
max	7.30	15.00	2.02	8.83	2.10	0.16	2.63	9.00
min	7.10	2.00	0.02	2.78	0.00	0.04	0.01	2.00
STD	0.05	1.97	0.38	1.04	0.28	0.02	0.48	1.31
Stickney WRP								
mean	7.83	4.54	0.41	7.63	1.58	0.08	1.22	4.56
max	9.90	11.00	2.46	11.75	3.59	0.28	3.56	16.00
min	6.30	2.00	0.02	2.30	0.68	0.05	0.00	3.00
STD	0.76	1.82	0.45	1.55	0.46	0.03	0.74	1.93
Calumet WRP								
mean	7.53	3.43	0.11	6.66	1.48	0.07	3.12	4.14
max	9.90	7.00	0.48	16.91	3.88	0.18	5.62	10.00
min	5.80	2.00	0.02	3.81	0.60	0.04	0.88	2.00
STD	1.00	1.09	0.07	1.29	0.42	0.02	1.07	1.39
Lemont WRP								
mean	6.30	5.99	0.22	13.18	1.73	0.11	2.68	6.40
max	7.70	27.00	1.72	17.91	3.66	0.58	3.68	33.00
min	2.80	2.00	0.02	5.10	0.80	0.04	0.71	2.00
STD	0.66	4.72	0.23	2.42	0.52	0.09	0.61	5.28

*Organic and inorganic phosphorous concentrations were calculated based on measured total phosphorous and suspended solids concentrations from equations 5.3 and 5.4.

5.2.4. Tributaries

Pollution loads from 11 tributaries affect water quality in the CWS. Only in three tributaries (Little Calumet River, Grand Calumet River, and North Branch Chicago River), was water quality measured as part of the MWRDGC monthly waterway

sampling program. Like the Little Calumet River basin, all the ungaged tributaries are located in the southern part of the Chicago metropolitan area. Therefore, similarity between the Little Calumet River drainage basin and ungaged tributaries was assumed (Alp and Melching, 2004) resulting in the same input concentrations assigned for all of them. Water-quality input for tributaries consists of two data categories: dry weather long-term average concentrations and wet weather event mean concentrations.

Dry weather concentrations

For dry weather periods, long-term average values were used as a model input. The Little Calumet River at South Holland dry-weather concentrations were calculated using a mass balance approach and data for 2001-2002 from the Little Calumet River at Wentworth Avenue and at Ashland Avenue and Thorn Creek at 170th Street. Average concentrations from 2000 – 2002 period for the North Branch Chicago River at Albany Avenue were assigned as dry-weather concentrations at this location. Concentrations measured between 1990-2002 at the Grand Calumet River at Burnham Avenue were used for the concentrations at the Grand Calumet River at Hohman Avenue. Dry weather concentrations for the tributaries were assumed as listed in Table 5.6.

Table 5.6 Chicago Waterway System tributary dry-weather concentrations (after Alp and Melching, 2004)

DO (mg/L)	$CBOD_5$ (mg/L)	NH_4 (mg/L)	NO_3 (mg/L)	N_{org} (mg/L)	P_{org} (mg/L)	P_{in} (mg/L)	SS (mg/L)
Little Calumet River at South Holland							
5.61	3.15	0.3	3.22	1.42	0.22	0.97	53.05
Grand Calumet River at Hohman Avenue							
*	6.69	2.09	7.64	2.41	0.54	0.22	37.63
North Branch Chicago River at Albany Avenue							
7.54	4.00	0.36	3.41	1.34	0.04	0.81	23.12

*Assigned measured hourly concentrations based on data for the Grand Calumet River at Torrence Avenue.

Data collected by the MWRDGC during the 2002-2004 period show that chlorophyll-a concentration varies from month to month. Therefore, for chlorophyll-a input a monthly time step was used (Alp and Melching, 2004). Chlorophyll-a monthly concentrations for the Little Calumet River and North Branch Chicago River are listed in Table 5.7.

Table 5.7 Monthly mean chlorophyll-a concentrations for tributaries to the Chicago Waterway System

	Chlorophyll-a (µg/L)	
	Little Calumet River at South Holland	North Branch Chicago River at Albany Avenue
May	4.49	22.10
June	8.93	24.50
July	9.63	13.75
August	11.31	11.13
September	4.89	9.63

Wet weather concentrations

For wet-weather periods, event mean concentrations were used as a model input. This simplification is justified by the fact that the total load resulting from the runoff event is more important than the individual concentrations within the event (Novotny and Olem, 1994, p. 484). For the verification period, tributaries were not sampled during storm events. Therefore, for the traditional approach to verification, average values from all available event mean concentration data were used. For the new approach to verification event mean concentrations were randomly generated on the basis of observed event mean concentration data for the Little Calumet River at South Holland and the North Branch Chicago River at Albany Avenue. As was previously mentioned, the Little Calumet River time series was assigned for ungaged tributaries. Event mean concentrations used to derive input for the verification period are listed in Table 5.8.

Table 5.8 Measured event mean concentrations and their statistics for the tributaries to the Chicago Waterway System

	DO (mg/L)	$CBOD_5$ (mg/L)	NH_4 (mg/L)	NO_3 (mg/L)	N_{org} (mg/L)	P_{org}* (mg/L)	P_{in}* (mg/L)	SS (mg/L)
Little Calumet River at South Holland								
07/22-26/01	3.99	1.28	0.30	1.72	1.34	0.20	0.87	78.28
08/02-07/01	4.37	2.03	0.30	0.97	2.08	0.26	1.00	141.67
08/25-29/01	4.82	2.33	0.24	1.48	1.66	0.28	0.79	105.72
09/19-21/01	5.17	3.27	0.16	2.85	1.61	0.26	1.69	107.24
09/23-28/01	5.60	3.00	0.20	3.40	1.76	0.09	1.21	52.00
10/4-11/01	6.28	1.78	0.16	1.82	1.70	0.30	1.00	94.58
10/11-21/01	6.60	3.72	0.08	1.40	1.30	0.23	0.50	80.00
10/23-31/01	6.18	3.38	0.10	1.50	1.52	0.20	0.80	69.43
04/07-09/02	n/a	4.92	0.34	1.74	1.83	n/a	n/a	131.95
04/18-21/02	n/a	3.44	0.28	1.99	1.44	n/a	n/a	55.76
05/01-02/02	n/a	3.00	0.13	2.07	1.29	n/a	n/a	41.17
Average	5.376	2.923	0.208	1.904	1.595	0.226	0.983	87.072
SD	0.949	1.019	0.089	0.686	0.246	0.065	0.352	32.498
North Branch Chicago River at Albany Avenue								
07/22-26/01	4.42	4.18	0.29	1.91	1.73	0.33	0.37	96.19
08/02-06/01	4.83	3.48	0.31	1.55	1.92	0.32	0.33	151.51
08/13/01	4.90	0.00	0.06	1.29	1.25	0.12	0.52	23.00
08/23-28/01	5.41	1.40	0.17	1.23	1.44	0.21	0.25	81.11
08/31-09/2/01	5.99	3.46	0.22	1.37	1.37	0.20	0.09	77.42
09/10/01	5.30	0.00	0.11	2.38	1.14	0.12	0.38	34.00
09/19-10/1/01	6.59	1.72	0.19	1.25	1.35	0.15	0.22	64.61
10/12-22/01	6.85	1.75	0.05	0.86	0.86	0.15	0.17	49.06
10/22-11/5/01	7.10	2.42	0.05	0.79	1.05	0.12	0.16	34.29
04/07-09/02	n/a	6.34	0.20	2.51	1.84	n/a	n/a	65.50
04/18-21/02	n/a	2.18	0.06	2.97	1.22	n/a	n/a	14.94
05/01-02/02	n/a	4.00	0.03	3.08	1.98	n/a	n/a	31.44
AVERAGE	5.710	2.577	0.145	1.766	1.428	0.191	0.277	60.255
SD	0.965	1.824	0.099	0.791	0.361	0.082	0.133	38.322

*Organic and inorganic phosphorous concentrations were calculated based on measured total phosphorous and suspended solids concentrations from equations 5.3 and 5.4.

Note: n/a = not available

5.2.5.Combined Sewer Overflows

There are three CSO pump stations (PS)- North Branch PS, Racine Avenue PS, and 125th Street PS- discharging to the CWS during storm events. In addition to this contribution, there are nearly 200 CSO locations in the system represented by 28 aggregated CSO locations in the model.

CSO discharges usually are not sampled in the CWS. Only a few events in the past were covered with CBOD and SS monitoring at the non-pump station CSOs after the Tunnel and Reservoir Plan (TARP) went on line: Evanston Street, Greenwood Street, and Olmsted Street. The Evanston Street and Olmsted Street CSOs are located in the neighborhood of the North Branch PS, whereas the Greenwood Street CSO is located closer to the Racine Avenue PS. Flow weighted event mean concentrations sampled at these locations are compared with flow weighted event mean concentrations from the pumping stations in Table 5.9.

Table 5.9 Flow weighted event mean concentrations from sampled combined sewer overflow events

	$CBOD_5$ (mg/L)	**SS (mg/L)**
Evanston Street		
4/22/99	40.515	115.136
8/17/97	9.430	37.904
6/1/99	34.453	264.888
12/4/99	33.582	228.515
Olmsted Street		
8/16/97	9.429	27.887
4/23/99	7.451	30.103
6/1/99	16.196	53.013
AVERAGE	21.580	108.207
SD	14.096	99.676
North Branch Pumping Station		
AVERAGE	35.444	101.846
SD	17.412	67.483
Greenwood Street		
4/22/99	47.767	145.333
6/1/99	49.563	233.449
12/4/99	21.373	129.629
AVERAGE	39.568	169.470
SD	15.783	55.961
Racine Pumping Station		
AVERAGE	52.145	499.949
SD	37.112	528.266

Based on a t-test with a 5% significance level statistical similarity was found between $CBOD_5$ and SS concentrations in the North Branch PS discharge and those in the CSOs

at Evanston Street and Olmsted Street. Also, based on a t-test with a 5% significance level statistically similarity was found between pollutant concentrations from the CSO at Greenwood Street and the Racine Avenue PS. Because discharges from CSOs were not sampled in the verification period, May 1 to September 24, 2002, it was assumed based on statistical similarity that pump station discharge quality is representative of neighboring CSO locations. The North Branch PS discharge quality was assigned to North Shore Channel and North Branch CSOs. The Racine Avenue PS discharge quality was assigned to Chicago River Main Stem, South Branch Chicago River, and CSSC CSOs. Water-quality of CSOs discharging to the Calumet-Sag Channel and Little Calumet River were determined using concentrations measured at 125th Street Pumping Station.

For the verification period, none of the pumping stations was sampled. Therefore, for the traditional approach to verification, average values from all available event mean concentration data were used. For the new approach to verification, event mean concentrations were randomly generated on the basis of observed event mean concentrations for the pump stations. Event mean concentrations used to derive input for the verification period are listed in Table 5.10.

Table 5.10 Measured event mean concentrations for combined sewer overflow pumping stations

	DO (mg/L)	$CBOD_5$* (mg/L)	NH_4 (mg/L)	NO_3 (mg/L)	N_{org} (mg/L)	P_{org}*** (mg/L)	P_{in}*** (mg/L)	SS (mg/L)
North Branch Pumping Station								
08/02/01	5.388	27.269	1.812	1.516	5.678	0.382	0.641	92.332
08/09/01	1.925	71.415	3.228	0.656	14.155	2.618	0.078	262.973
09/09/01	4.028	14.851	2.384	0.565	3.441	0.607	0.170	67.006
09/20/01	2.136	20.828	1.765	0.510	5.407	0.834	0.333	83.100
09/23/01	2.407	42.281	5.813	0.265	6.479	1.090	0.645	87.087
10/13/01	1.950	30.221	1.831	0.581	3.816	0.531	0.482	52.226
10/23/01	6.552	42.396	2.201	0.613	5.406	1.146	0.144	107.540
04/7-9/02	n/a	34.290	3.835	0.697	4.430	0.718	0.873	62.500
Average	3.484	35.444	2.859	0.675	6.101	0.991	0.421	101.846
SD	1.875	17.412	1.405	0.364	3.407	0.708	0.286	67.483
Racine Avenue Pumping Station								
07/20/95	n/a	83.867	3.091	n/a	n/a	n/a	n/a	n/a
08/15/95	n/a	35.353	1.843	n/a	n/a	n/a	n/a	n/a
11/10/95	n/a	9.667	0.577	n/a	n/a	n/a	n/a	n/a
07/17/96	n/a	17.260	0.353	0.773	n/a	n/a	n/a	113.431
07/18/97	n/a	59.711	n/a	n/a	n/a	n/a	n/a	887.538
04/22/99	n/a	53.557	n/a	n/a	n/a	n/a	n/a	232.098
06/01/99	n/a	131.579	n/a	n/a	n/a	n/a	n/a	1405.468
12/4/99	n/a	40.315	n/a	n/a	n/a	n/a	n/a	179.159
04/7-9/02	n/a	38.000	n/a	n/a	n/a	n/a	n/a	182.000
Avergae	3.484**	52.145	2.859**	0.675**	6.101**	0.991**	0.421**	499.949
SD	1.875**	37.112	1.405**	0.364**	3.407**	0.708**	0.286**	528.266
125th Street Pumping Station								
11/10/95	n/a	68.023	1.241	n/a	n/a	n/a	n/a	n/a
07/17/96	n/a	27.139	n/a	n/a	n/a	n/a	n/a	99.037
08/16/97	n/a	27.098	n/a	n/a	n/a	n/a	n/a	26.162
04/23/99	n/a	21.000	n/a	n/a	n/a	n/a	n/a	152.952
04/22/99	n/a	26.307	n/a	n/a	n/a	n/a	n/a	77.824
06/01/99	n/a	17.680	n/a	n/a	n/a	n/a	n/a	101.833
08/02/01	4.502	24.441	1.239	1.542	4.318	0.744	1.276	85.959
08/25/01	5.143	12.577	0.876	1.825	3.037	0.473	0.010	68.304
10/13/01	n/a	8.402	0.315	1.733	2.446	0.316	0.142	41.435
04/7-9/02	n/a	24.000	1.550	2.215	4.560	0.245	3.805	30.000
Average	4.822	25.667	1.044	1.829	3.590	0.444	1.308	75.945
SD	0.453	16.186	0.472	0.283	1.014	0.221	1.759	40.429

*$CBOD_5$ was not measured for the Racine Avenue Pumping Station. This concentration was estimated as proportional to the measured BOD_5 concentration. BOD_5 and $CBOD_5$ for the North Branch PS and the 125th Street PS are proportional ($CBOD_5 = 0.707 \cdot BOD_5$).

**Based on the similarity between the North Branch PS and Racine Avenue PS drainage areas, for unavailable Racine Avenue PS event mean concentrations North Branch PS values were assigned.

***Organic and inorganic phosphorous concentrations were calculated based on measured total phosphorous and suspended solids concentrations from equations 5.3 and 5.4.

5.2.6. Boundaries

A location near the Wilmette Pumping Station, the North Shore Channel at Maple Avenue, a location near the Chicago River Controlling Works, the Chicago River at Columbus Drive, and O'Brien Lock and Dam are the three lake front upstream boundaries of the CWS water-quality model. Alp and Melching (2004) noticed that historic data (1990 – 2002) show seasonal variation at the lake front boundaries and monthly variation at O'Brien Lock and Dam (actually 130th Street). In the summer period, the water quality constituent concentrations near the lakefront are dominated by Lake Michigan water due to the discretionary diversion from the lake. Therefore, the inflow at the lake front boundaries should reflect the quality of Lake Michigan water. Thus, the constituent concentrations at Wilmette and Columbus Drive were set equal to the mean measured concentration during periods with discretionary diversion, for the entire verification period (May 1 to September 24, 2002).

Table 5.11 Mean concentrations at the model boundaries

Period	DO (mg/L)	$CBOD_5$ (mg/L)	NH_4 (mg/L)	NO_3 (mg/L)	N_{org} (mg/L)	P_{org} (mg/L)	P_{in} (mg/L)	SS (mg/L)	Chl-a (µm/L)
North Shore Channel at Maple Avenue (Wilmette)									
May-Sep.	*	2.96	0.09	0.21	0.41	0.05	0.04	11.33	1.5
Chicago River at Columbus Drive									
May-Sep.	*	1.63	0.04	0.25	0.38	0.05	0.04	9.80	1.4
O'Brien Lock and Dam (130th Street)									
May	**	5.33	0.25	1.01	0.60	0.03	0.31	12.94	5.60
June	**	1.50	0.14	0.58	0.52	0.00	0.70	10.00	5.90
July	**	2.50	0.08	0.32	0.38	0.03	0.07	8.25	9.70
August	**	4.00	0.09	0.30	0.34	0.01	0.05	11.19	8.30
Sept.	**	3.67	0.09	0.34	0.32	0.01	0.06	9.53	4.90

* Assumed to be equal to saturation DO concentration calculated based on daily lake shore water temperature.

** Continuous hourly DO measurements

5.3. Results of Water Quality Verification

To verify the unsteady-state water-quality model, measured in-stream DO concentrations at 27 locations were compared with simulated concentrations. The locations of the continuous DO monitoring stations and DO statistics at these in-stream stations are listed in Table 5.12. A statistical comparison between daily average simulated and measured DO concentrations for the verification period is listed in Table 5.13. Graphical comparisons of measured and simulated DO concentrations are shown in Figure 5.1.

Table 5.12 Location of the continuous dissolved oxygen monitoring stations of the Metropolitan Water Reclamation District of Greater Chicago in or near the modeled part of the Chicago Waterway System and average daily dissolved oxygen (DO) concentrations measured at these stations between May 1 and September 24, 2002

DO Sampling Station	Waterway	River Mile from Lockport	Average DO (mg/L)	
			Dry Weather	Wet Weather
Linden Street	North Shore Channel	49.8	7.38	2.51
Simpson Street	North Shore Channel	48.5	5.86	1.50
Main Street	North Shore Channel	46.7	5.44	2.34
Addison Street	North Branch Chicago River	40.4	6.06	6.57
Fullerton Avenue	North Branch Chicago River	38.5	4.64	5.44
Division Street	North Branch Chicago River	36.4	5.53	5.92
Kinzie Street	North Branch Chicago River	34.8	4.90	5.43
Chicago River Controlling Works	Chicago River Main Stem	36.1	8.13	8.53
Michigan Avenue	Chicago River Main Stem	35.4	8.39	8.45
Clark Street	Chicago River Main Stem	34.9	7.97	7.56
Jackson Boulevard	South Branch Chicago River	34.0	5.10	5.02
Cicero Avenue	Chicago Sanitary and Ship Canal	26.2	4.25	4.15
Baltimore and Ohio Railroad	Chicago Sanitary and Ship Canal	21.3	5.11	5.31
Route #83	Chicago Sanitary and Ship Canal	13.1	3.88	4.56
River Mile 302.6*	Chicago Sanitary and Ship Canal	11.6	4.68	5.25
Romeoville	Chicago Sanitary and Ship Canal	5.1	4.12	4.59
130th Street**	Calumet River	36.0	7.57	7.89
Conrail Railroad	Little Calumet River (north)	34.4	6.82	6.63
Central and Wisconsin Railroad	Little Calumet River (north)	31.6	6.57	7.41
Ashland Avenue	Little Calumet River (south)	29.3	4.74	5.57
Division Street	Calumet-Sag Channel	27.6	5.47	5.40
Kedzie Avenue	Calumet-Sag Channel	26.1	6.27	6.19
Cicero Avenue	Calumet-Sag Channel	24.0	5.86	5.59
Harlem Avenue	Calumet-Sag Channel	20.5	6.18	5.82
Southwest Highway	Calumet-Sag Channel	19.7	6.19	5.85
104th Avenue	Calumet-Sag Channel	16.3	6.17	5.77
Route #83	Calumet-Sag Channel	13.3	5.82	5.48

* River mile relative to the mouth of the Illinois River at Grafton.

** 130th Street is taken as representative of O'Brien Lock and Dam

NOTE: Dry-weather periods were distinguished from wet-weather periods based on discharges at Romeoville. Flows greater than 100 m^3/s which were not short-term flow fluctuations, were considered wet-weather periods.

Table 5.13 Comparison of daily average simulated and measured dissolved oxygen concentrations in mg/L in the Chicago Waterway System for May 1 to September 24, 2002

	Average measured	Average simulated	Error	Absolute Error	% Error	% Abs Error
Linden Street	6.78	6.71	0.82	1.75	12.98	40.03
Simpson Street	5.00	5.42	0.03	1.66	38.14	76.81
Main Street	4.86	4.88	-0.02	1.61	59.47	89.09
Addison Street	6.14	6.53	0.39	0.75	7.32	12.70
Fullerton Avenue	4.78	5.59	0.81	1.11	21.17	26.48
Division Street	5.60	5.78	0.18	0.88	4.61	16.46
Kinzie Street	4.99	5.50	0.52	0.85	12.65	19.08
Chicago River Controlling Works	8.20	7.00	-1.19	2.34	-10.54	27.63
Michigan Avenue	8.40	6.24	-2.16	2.83	-21.75	32.07
Clark Street	7.90	5.81	-2.09	2.62	-23.35	31.83
Jackson Boulevard	5.08	5.12	-0.01	1.16	-0.09	23.39
Cicero Avenue	4.23	4.10	-0.02	1.45	21.72	52.77
Baltimore and Ohio Railroad	5.14	4.76	-0.38	0.87	-6.87	17.06
Route #83	3.96	4.40	0.30	0.84	11.51	25.00
River Mile 302.6*	4.78	5.11	0.49	1.24	19.95	33.99
Romeoville	4.20	4.76	0.56	1.09	19.63	30.39
O'Brien Lock and Dam (130th Street)	7.63	7.39	-0.22	0.35	-2.58	4.45
Conrail	6.79	7.40	0.59	1.05	12.81	18.29
Central and Wisconsin Railroad	6.70	7.41	0.50	1.43	19.09	30.37
Division Street**	5.46	6.58	1.13	1.45	25.21	30.12
Ashland Avenue	4.89	6.57	1.68	2.10	49.53	54.17
Kedzie Avenue	6.26	6.78	0.45	1.04	9.14	17.57
Cicero Avenue**	5.81	6.56	0.75	1.45	17.51	27.91
Harlem Avenue	6.12	4.99	-1.12	1.48	-16.36	23.27
Southwest Highway	6.13	6.47	0.30	1.55	8.75	26.58
104th Avenue	6.11	6.25	0.13	1.62	5.70	27.22
Route #83**	5.76	6.00	0.25	1.87	13.79	37.29

* River mile relative to the mouth of the Illinois River at Grafton. River mile 11.6 relative to Lockport

** Locations on the Calumet-Sag Channel

THIS PAGE INTENTIONALLY LEFT BLANK

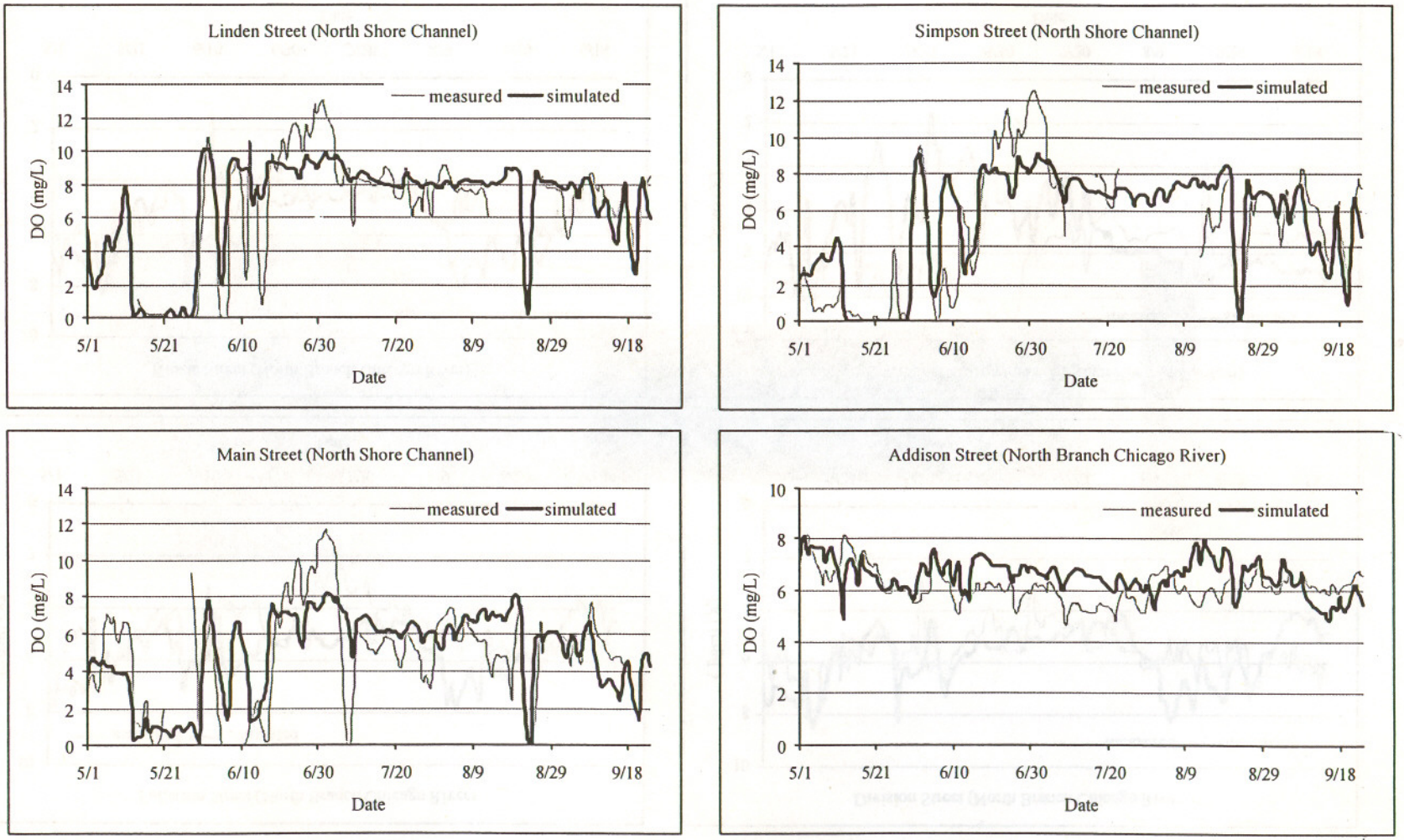

Figure 5.1 Comparison of measured and simulated daily mean dissolved oxygen (DO) concentrations at different locations on the Chicago Waterway System for the verification period (May 1 to September 24, 2002).

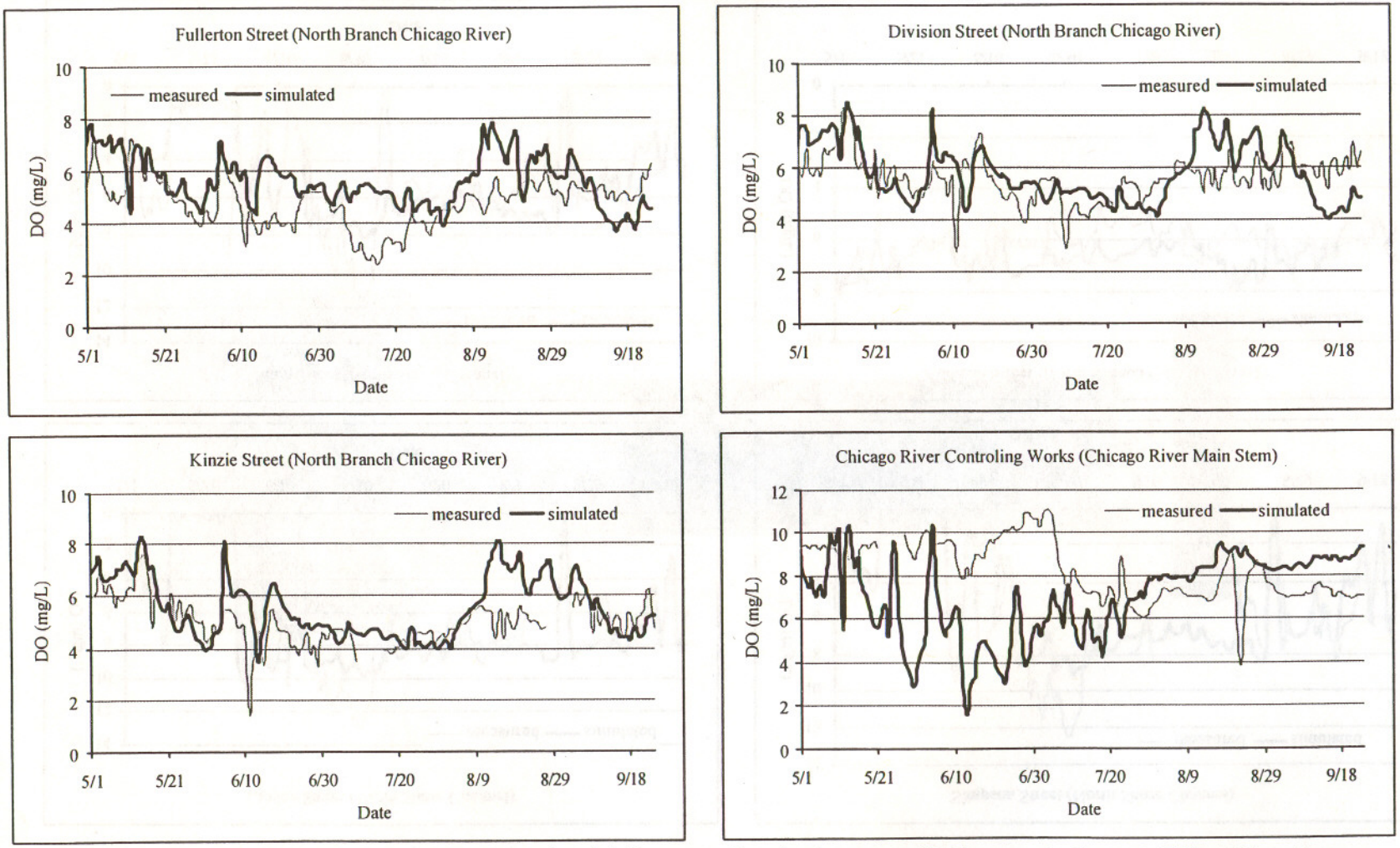

Figure 5.1(cont.) Comparison of measured and simulated daily mean dissolved oxygen (DO) concentrations at different locations on the Chicago Waterway System for the verification period (May 1 to September 24, 2002)

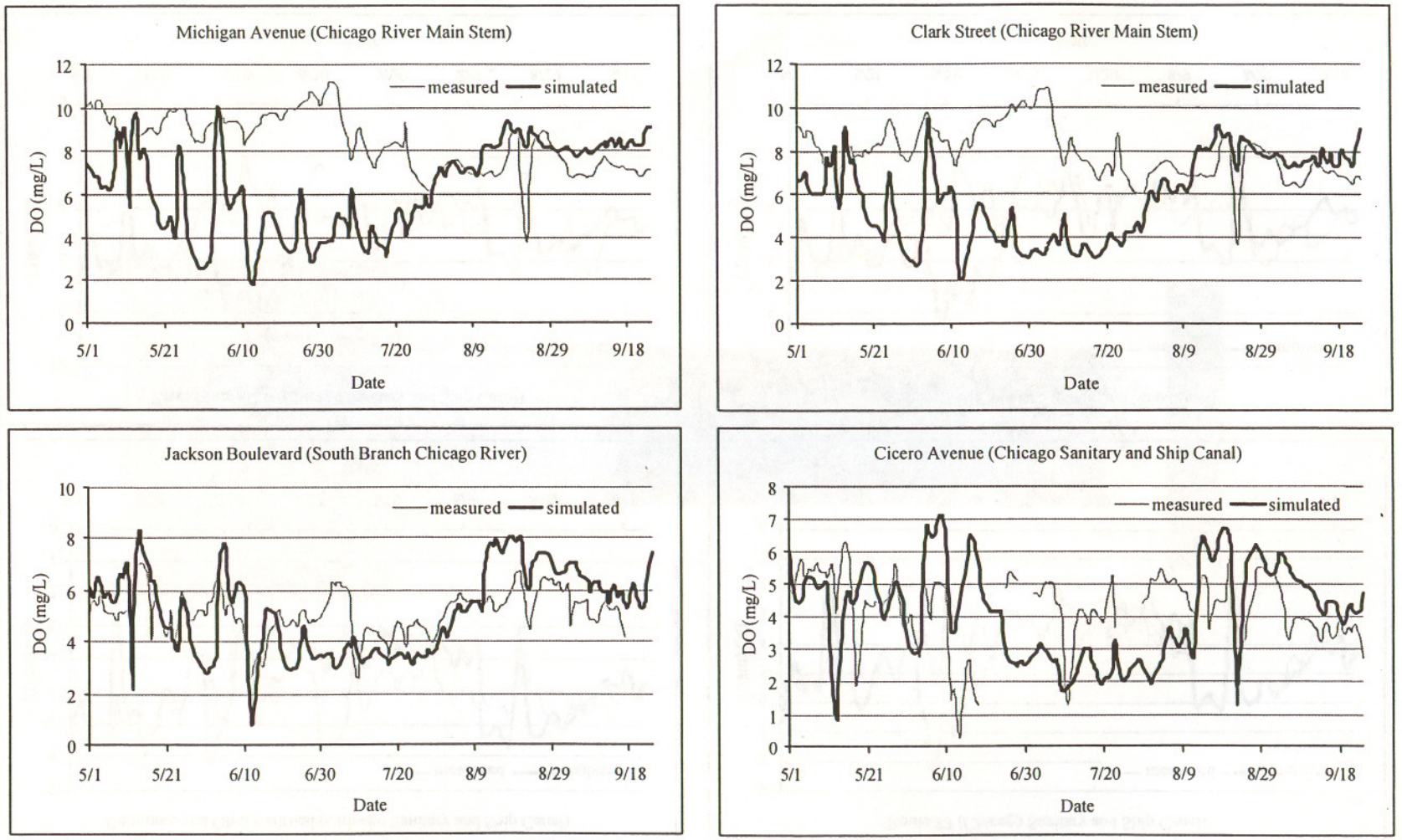

Figure 5.1(cont.) Comparison of measured and simulated daily mean dissolved oxygen (DO) concentrations at different locations on the Chicago Waterway System for the verification period (May 1 to September 24, 2002)

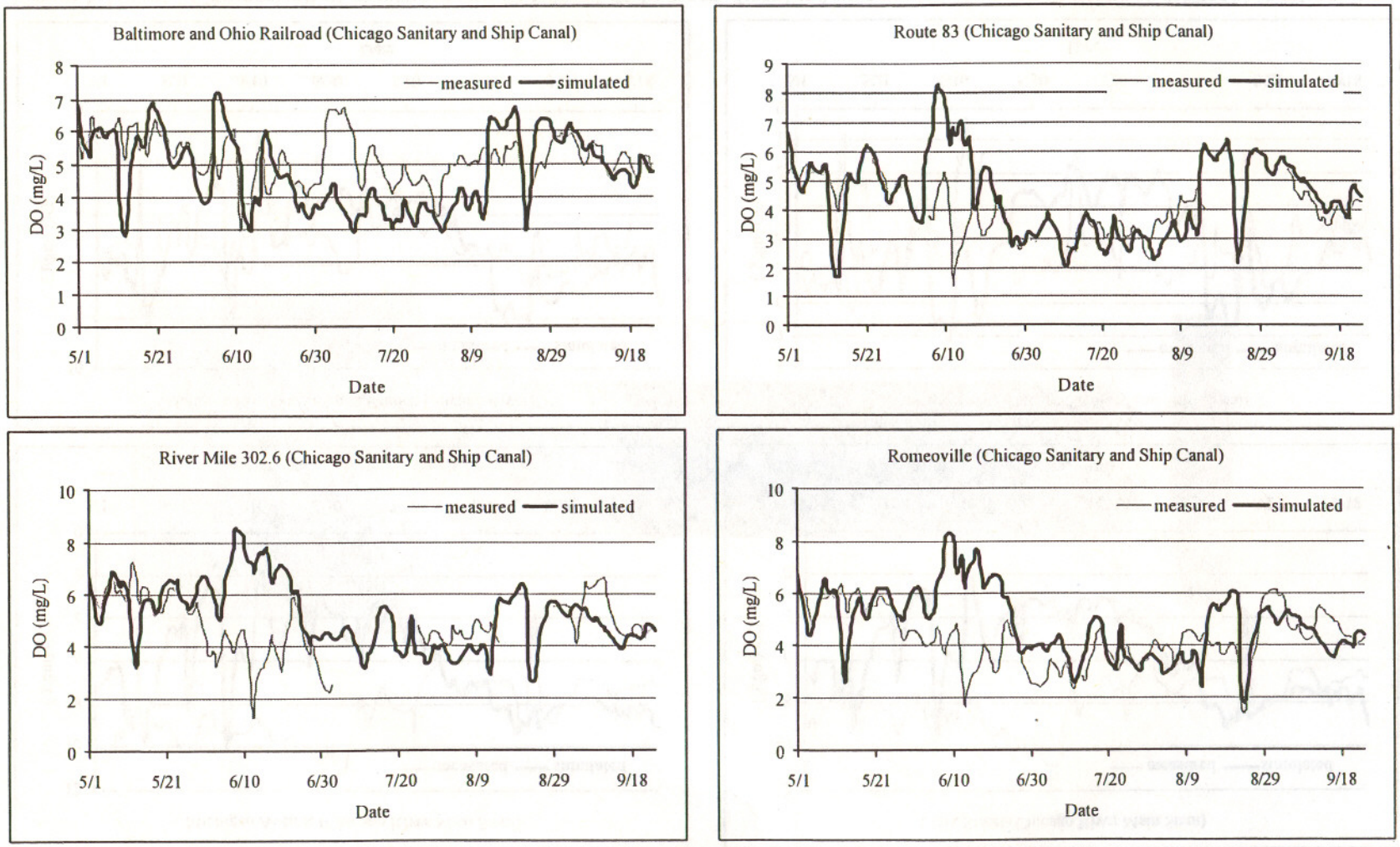

Figure 5.1(cont.) Comparison of measured and simulated daily mean dissolved oxygen (DO) concentrations at different locations on the Chicago Waterway System for the verification period (May 1 to September 24, 2002)

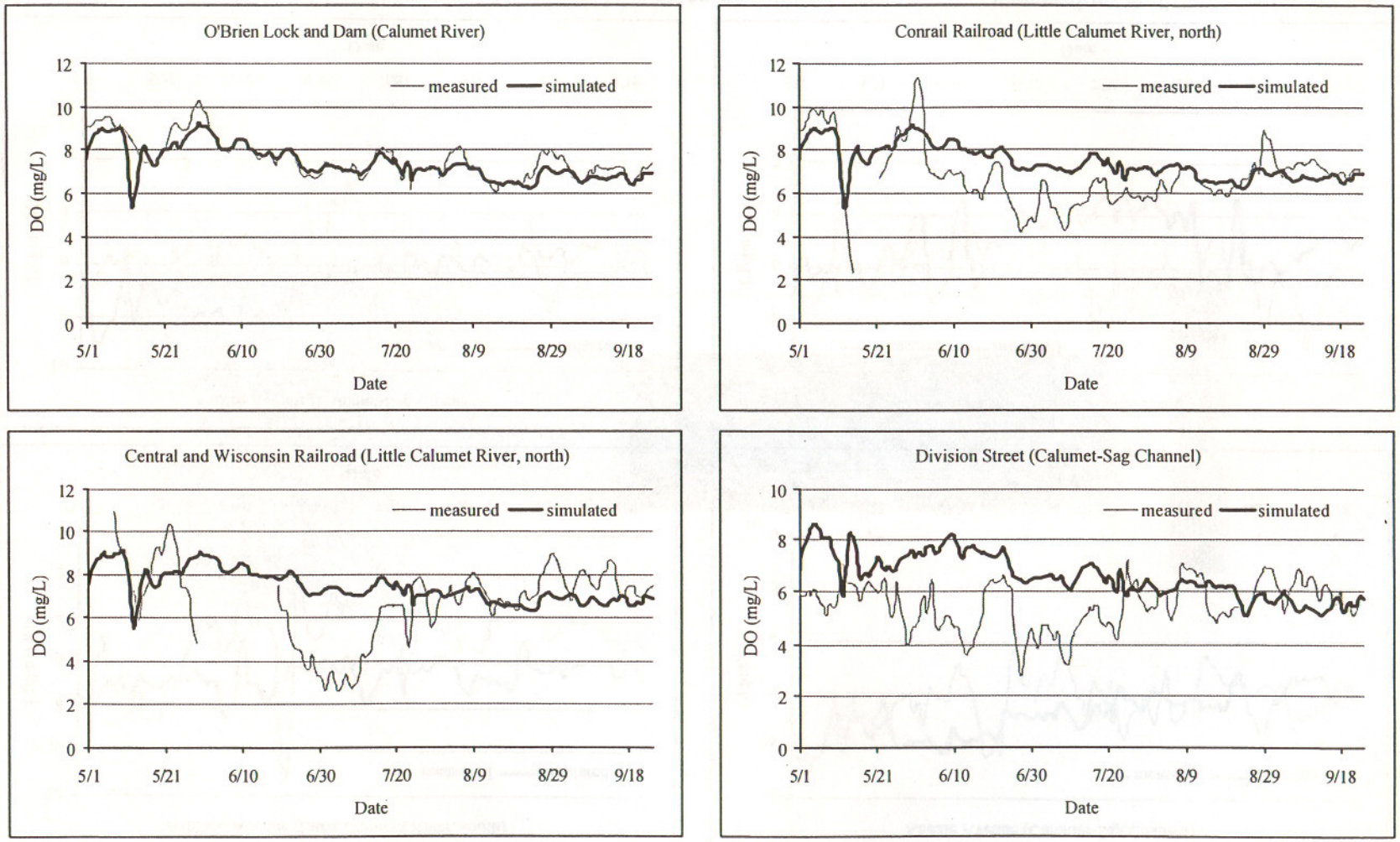

Figure 5.1(cont.) Comparison of measured and simulated daily mean dissolved oxygen (DO) concentrations at different locations on the Chicago Waterway System for the verification period (May 1 to September 24, 2002)

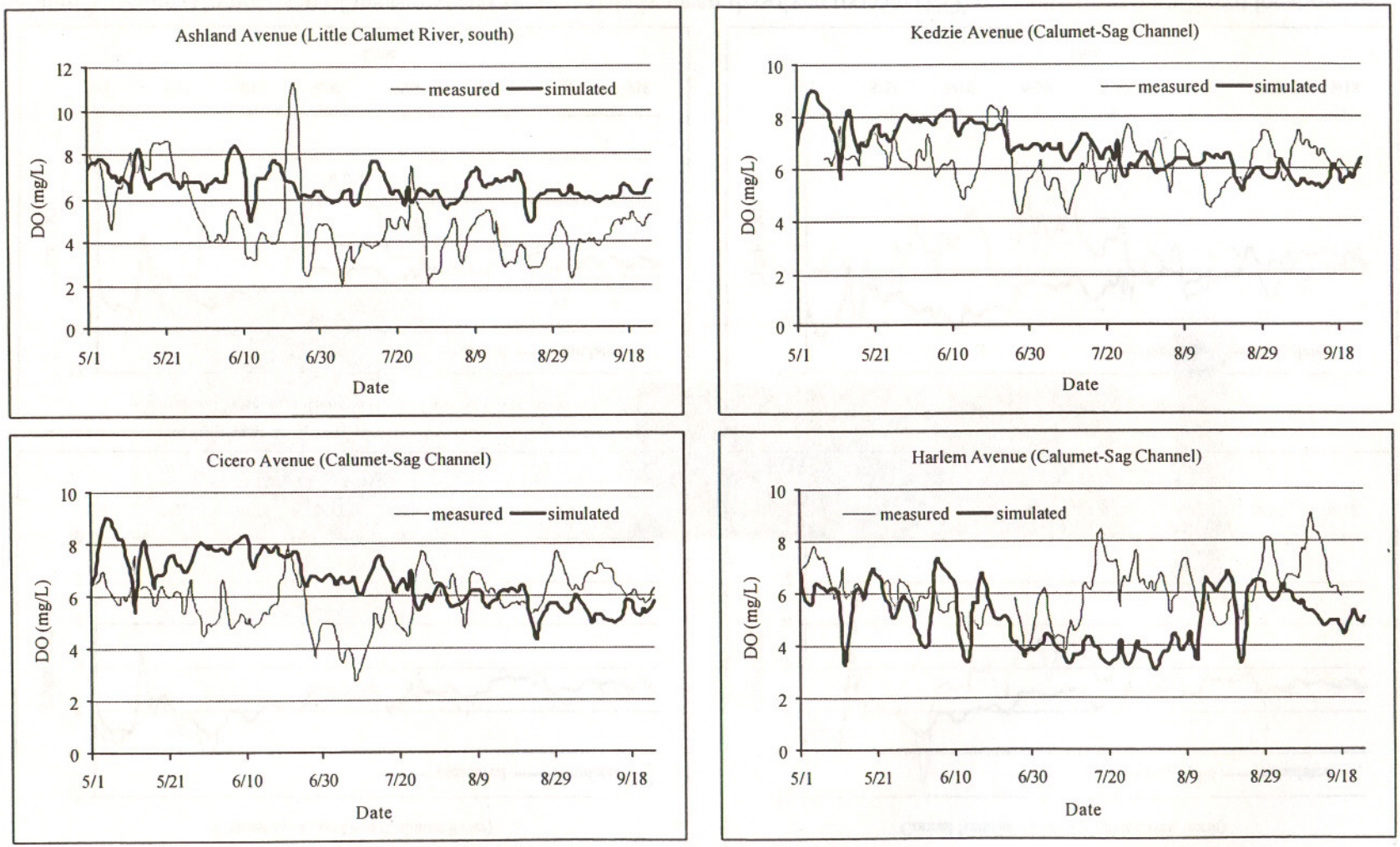

Figure 5.1(cont.) Comparison of measured and simulated daily mean dissolved oxygen (DO) concentrations at different locations on the Chicago Waterway System for the verification period (May 1 to September 24, 2002)

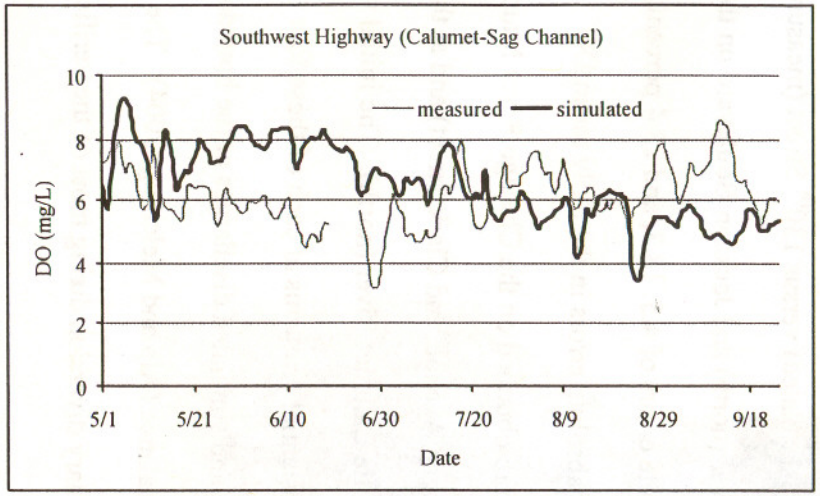

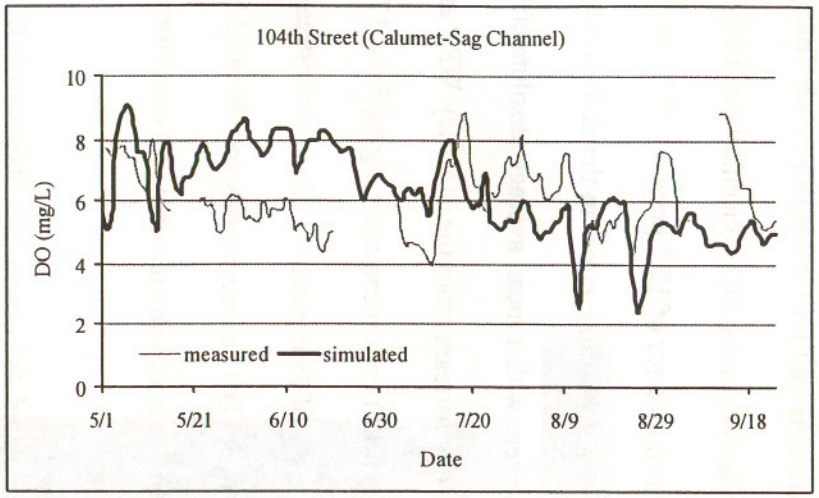

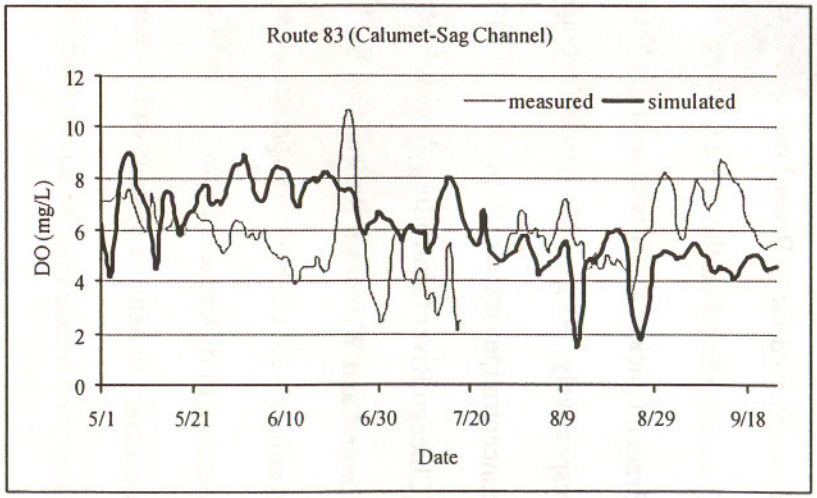

Figure 5.1(cont.) Comparison of measured and simulated daily mean dissolved oxygen (DO) concentrations at different locations on the Chicago Waterway System for the verification period (May 1 to September 24, 2002)

The best results for the verification period are obtained for the North Branch Chicago River where the average absolute errors in the daily mean DO concentrations range from 12.7 to 26.5 percent with a mean average absolute error of 18.7 percent. Results for the Calumet-Sag Channel also are good with average absolute errors in the daily mean DO concentrations ranging from 17.6 to 37.3 percent with a mean average absolute error of 27.1 percent. Finally, results for the CSSC downstream from the Stickney WRP are good with average absolute errors in the daily mean DO concentrations ranging from 17.1 to 34.0 percent with a mean average absolute error of 26.6 percent. Thus, downstream from the 3 major WRPs good estimates of daily mean DO concentrations are obtained because of the strong relation between WRP effluent loads and downstream DO concentrations.

Good agreement between measured and simulated daily mean DO concentrations also were obtained for O'Brien Lock and Dam (simulated) versus 130th Street (measured) and Conrail Railroad on the Little Calumet River (north) and Jackson Boulevard on the South Branch Chicago River with average absolute errors of 4.5, 18.3, and 23.4 percent, respectively. Reasonable results (average absolute errors in the daily mean DO concentrations around 30 percent) even were obtained on the Chicago River Main Stem (Chicago River Controlling Works, Michigan Avenue, and Clark Street) and at the Central and Wisconsin Railroad on the Little Calumet River (north). The initial water quality model calibration experienced substantial problems at each of these four locations because of differences between measured and simulated discharges at the boundaries necessary to achieve system-wide water balance (Alp and Melching, 2004). The improved results may be due to discretionary diversion during most of the verification

period (May 1 to September 24, 2002) as opposed to no discretionary diversion during the preliminary calibration period (April 1 to May 4, 2002).

The worst agreement of the model in terms of average absolute error in the daily mean DO concentrations is at three locations on the upper North Shore Channel (Linden Street, Simpson Street, and Main Street) where errors range from 40.0 to 89.1 percent. In part these poor results are a function of the fact that very low DO concentrations are most common on the upper North Shore Channel. Thus, relatively small absolute differences can result in large percentage errors. Also, detailed explanation and justification of poor agreement between the model and the real system on the upper North Shore Channel are presented in Alp and Melching (2004). Switching from a stage versus time (used by Alp and Melching, 2004) to a flow versus time boundary condition at Wilmette improved the DO simulation, but flow is very difficult to measure at Wilmette and so hydraulic uncertainties still adversely affect the DO simulation. The average errors at Simpson Street and Main Street are 0.03 and 0.02 mg/L, respectively, and the average absolute errors of 1.66 and 1.61 mg/L, respectively, are similar to those at other locations where 25-30 percent accuracy was indicated. Finally, Figure 5.1 shows that the simulated DO concentration matched several of the large DO sags at Simpson Street and Main Street quite well. These results indicate that the model can provide useful information when evaluating flow augmentation for the upper North Shore Channel for the UAA.

Poor results (average absolute error in daily mean DO concentrations of 52.8 percent) also were obtained at Cicero Avenue on the CSSC. In part these poor results are a

function of the fact that low DO concentrations are common at this location. These low DO concentrations can be the result of the complex hydraulic behavior in the vicinity of Cicero Avenue. The discharge from the Stickney WRP effectively acts as a hydraulic dam for the flows passing Cicero Avenue. The resulting hydraulic complexities and flow interactions with the South Fork South Branch Chicago River (Bubbly Creek) make DO simulation at Cicero Avenue difficult. Nevertheless, the average error at Cicero Avenue is -0.02 mg/L, and the average absolute error of 1.45 mg/L is similar to those at other locations where 25-30 percent accuracy was indicated. Finally, Figure 5.1 shows that the simulated DO concentration matched several of the large DO sags at Cicero Avenue well, and in general the simulated sags tended to be larger than the observed sags. These results indicate that the model probably will provide conservative results when evaluating mitigation alternatives for the UAA in the vicinity of Cicero Avenue, which, outside of the upper North Shore Channel, is the most likely place for low DO concentrations and a key location for the UAA.

Poor results (average absolute error in daily mean DO concentrations of 54.2 percent) also were obtained at Ashland Avenue on the Little Calumet River (south). Because it is not downstream of or affected by the WRPs of the MWRDGC and, thus, not a focus of the UAA, detailed hydraulic and water-quality calibration were not done for the Little Calumet River (south) at Ashland Avenue.

As was mentioned before, for the verification period no detailed storm loading data were available for the pumping stations, CSO discharges, and tributaries. For model

verification purposes, average values derived as a mean from historic measured data were applied. Statistical comparison between the model output and the real system response to storm loadings can be implied from a separate analysis for wet and dry weather periods (Table 5.14). Dry-weather periods were distinguished from wet-weather periods based on discharges at Romeoville. Flows greater than 100 m^3/s which were not short-term flow fluctuations were considered wet-weather periods. On average at 11 locations marked in bold in Table 5.14, the prediction ability of the model during dry weather is better than for wet weather periods. For the remaining 16 out of 27 locations, there is either no difference between wet-weather and dry-weather periods in model prediction accuracy or model fit is better for after-storm periods. This means that the water-quality model is driven more by loads from water reclamation plants than loads from pumping stations and CSO outflows.

Table 5.14 Comparison of daily average simulated and measured dissolved oxygen concentrations for dry weather and wet weather periods for the Chicago Waterway System.

Location	Error	Abs Error	% Error	% Abs Error	Error	Abs Error	% Error	% Abs Error
	WET-WEATHER PERIOD				DRY-WEATHER PERIOD			
Linden Street	1.67	2.06	31.62	127.74	0.69	1.70	10.60	28.86
Simpson Street	1.16	1.91	115.82	187.45	-0.20	1.60	22.09	53.96
Main Street	-0.51	1.65	4.35	70.14	0.06	1.60	68.92	92.33
Addison Street	0.06	0.77	2.88	12.33	0.46	0.75	8.23	12.78
Fullerton Avenue	0.64	1.03	17.40	23.28	0.85	1.12	21.95	27.14
Division Street	0.81	0.98	18.38	20.75	0.05	0.85	1.78	15.58
Kinzie Street	1.13	1.14	31.91	32.12	0.39	0.78	8.49	16.26
Chicago River Controlling Works	-0.64	1.96	-2.97	26.29	-1.31	2.42	-12.17	27.92
Michigan Avenue	-1.27	2.20	-10.86	28.51	-2.34	2.96	-23.99	32.80
Clark Street	-0.88	1.75	-8.44	25.12	-2.33	2.80	-26.41	33.21
Jackson Boulevard	0.86	1.33	18.63	29.84	-0.20	1.12	-4.16	21.99
Cicero Avenue	-0.04	1.56	13.59	46.58	-0.01	1.42	23.62	54.22
Baltimore and Ohio Railroad	-0.24	1.11	-1.08	21.64	-0.41	0.82	-8.06	16.12
Route #83	0.33	1.68	28.91	58.76	0.30	0.72	9.15	20.43
River Mile 302.6*	0.63	1.59	34.44	48.95	0.47	1.18	17.06	30.99
Romeoville	0.44	1.20	17.60	30.68	0.58	1.07	20.04	30.33
130th Street	-0.37	0.51	-4.51	6.30	-0.19	0.32	-2.16	4.05
Conrail Railroad	0.85	1.23	23.52	28.29	0.54	1.03	11.04	16.64
Central and Wisconsin Railroad	-0.05	1.15	8.30	22.79	0.60	1.48	21.11	31.78
Division Street**	1.54	1.64	32.95	34.48	1.04	1.41	23.63	29.23
Ashland Avenue	1.03	1.75	34.23	43.14	1.82	2.17	52.67	56.43
Kedzie Avenue	0.87	1.12	15.22	18.82	0.36	1.02	7.83	17.30
Cicero Avenue**	1.25	1.61	27.07	32.73	0.65	1.42	15.55	26.92
Harlem Avenue	-0.49	0.88	-8.51	15.25	-1.26	1.62	-18.15	25.09
Southwest Highway	0.91	1.54	16.54	26.42	0.17	1.55	7.07	26.62
104th Avenue	0.81	1.55	15.17	27.53	-0.01	1.64	3.75	27.16
Route #83**	0.88	1.37	18.18	26.87	0.12	1.98	12.85	39.52

*River mile relative to the mouth of the Illinois River at Grafton. River mile 11.6 relative to Lockport

** Locations on the Calumet-Sag Channel

Comparison between the DUFLOW model prediction ability for the verification (May 1 to September 24, 2002) and calibration (July 12 to November 9, 2001) periods is presented in Table 5.15, and it indicates that the prediction ability of the DUFLOW model is comparable for these two different periods. For both verification and calibration periods, the model underestimates DO concentrations relative to measured concentrations at two locations, Baltimore and Ohio Railroad and O'Brien Dam and Lock, whereas the model overestimates measured DO concentrations at Main Street, Fullerton Avenue, Kinzie Street, Cicero Avenue (CSSC), Route #83 (CSSC), River Mile 302.6, Romeoville, Ashland Avenue, Division Street, and Route #83 (Calumet-Sag Channel). At the other locations, the model gives underestimated DO concentrations for the calibration period whereas verification results yield positive error, and vice versa. In this final case, better fit for the calibration period would cause worse verification results.

It can be concluded that, in general, the DUFLOW model represents water-quality processes in the Chicago Waterway System well enough to be a useful tool for solving water-quality planning and management problems of interest to the MWRDGC.

Table 5.15 Comparison between calibration (July 12 to November 9, 2001) and verification (May 1 to September 24, 2002) results for the DUFLOW model of the Chicago Waterway System

Location	Error		%Error		Abs Error		%Abs Error	
	Verification	Calibration	Verification	Calibration	Verification	Calibration	Verification	Calibration
Linden Street	0.82	-1.69	12.98	-39.55	1.75	1.73	40.03	41.07
Simpson Street	0.03	-0.60	38.14	-37.69	1.66	1.40	76.81	142.98
Main Street	-0.02	0.27	59.47	93.39	1.61	1.06	89.09	118.22
Addison Street	0.39	-0.40	7.32	-5.90	0.75	0.58	12.70	9.38
Fullerton Avenue	0.81	0.07	21.17	15.88	1.11	0.74	26.48	28.81
Division Street	0.18	-0.27	4.61	-4.18	0.88	1.02	16.46	18.15
Kinzie Street	0.52	0.10	12.65	2.20	0.85	0.90	19.08	17.34
Chicago River Controlling Works	-1.19	0.82	-10.54	13.35	2.34	1.13	27.63	17.28
Michigan Avenue	-2.16	-0.05	-21.75	-0.05	2.83	1.08	32.07	13.90
Clark Street	-2.09	-0.18	-23.35	0.63	2.62	1.33	31.83	20.79
Jackson Boulevard	-0.01	0.46	-0.09	9.54	1.16	1.23	23.39	24.36
Cicero Avenue	-0.02	0.51	21.72	15.25	1.45	1.09	52.77	30.21
Baltimore and Ohio Railroad	-0.38	-0.15	-6.87	-2.99	0.87	0.82	17.06	15.62
Route #83	0.30	0.38	11.51	35.84	0.84	1.21	25.00	52.81
River Mile 302.6*	0.49	0.32	19.95	24.55	1.24	1.03	33.99	38.12
Romeoville	0.56	0.32	19.63	10.46	1.09	0.94	30.39	25.14
130th Street	-0.22	-0.33	-2.58	-4.90	0.35	0.42	4.45	6.22
Conrail Railroad	0.59	-0.42	12.81	-4.20	1.05	0.71	18.29	10.44
Central and Wisconsin Railroad	0.50	-1.18	19.09	-13.68	1.43	1.25	30.37	14.92
Ashland Avenue	1.13	0.24	25.21	6.90	1.45	0.66	30.12	14.16
Division Street**	1.68	1.68	49.53	43.03	2.10	1.68	54.17	43.09
Kedzie Avenue	0.45	-0.12	9.14	-0.46	1.04	0.62	17.57	10.85
Cicero Avenue**	0.75	-0.19	17.51	-1.50	1.45	0.68	27.91	12.07
Harlem Avenue	-1.12	0.11	-16.36	3.67	1.48	0.95	23.27	17.57
Southwest Highway	0.30	-0.13	8.75	-1.29	1.55	0.78	26.58	14.16
104th Avenue	0.13	-0.28	5.70	-1.53	1.62	1.05	27.22	19.82
Route #83**	0.25	0.02	13.79	1.66	1.87	0.87	37.29	16.60

* River mile relative to the mouth of the Illinois River at Grafton. River mile 11.6 relative to Lockport

** Locations on the Calumet-Sag Channel

CHAPTER 6: WATER-QUALITY MODEL VERIFICATION UNDER UNCERTAIN LOAD

6.1. Uncertainties in Modeling

Mathematical models are simplifications of the real chemical, biological, and physical processes within a system. As a simplified approximation of the real system, environmental models contain errors. The following 4 types of error propagate through models to affect output certainty:

- Model error: related to incorrect formulation of the model due to the use of arbitrary assumptions such as those used to determine important variables and processes, formulate the processes and resolve variability in space and time.
- Errors in the state variables: related to temporal or spatial randomness of natural processes.
- Parameter error: related to natural variability and measurement errors.
- Errors in the input data used to drive the model: related to measurements errors, inconsistency and nonhomogenity of data, and data handling and transcription errors. In most studies these errors are transferred to the parameters of the model as bias in the parameters (Troutman, 1983).

In this study, storm-loading data for the verification period are not available. The verification presented in Section 5.3, was done with the mean values of the event mean concentration assigned for the unknown storm concentration input. The verification confirmed, in general, sufficient agreement between measured and simulated DO

concentrations. However, the assigned event mean concentration values do not necessarily correspond with real event mean concentrations for each storm. Therefore, it is important to know how sensitive the DUFLOW water-quality model is to its storm load input and whether the verification results change substantially if different event mean concentrations are used. To determine how the model output responds to changes in storm-loadings, a Monte Carlo analysis, more precisely the Latin Hypercube Sampling approach, was used to evaluate the output sensitivity.

6.2. Monte Carlo Analysis

Monte Carlo analysis is a global type of sensitivity analysis in which a model under investigation is considered as a black box and the whole range of the input variables is examined. Therefore, this approach is a very powerful, efficient, and conceptually simple technique, especially when the investigated model is complex and its input parameters range over several orders of magnitude (Saltelli et al., 1995). Monte Carlo analysis assumes that uncertainties in the model input variables can be described by specific probability distributions, which reflect the probability of the values that the inputs can take. Random numbers are generated from a known or suspected distribution and the investigated model is executed with these sampled values. Statistical analysis of the multiple simulation outputs reflects the combined uncertainty of all parameter errors.

Monte Carlo simulation requires the following steps:

- Specification of ranges and probability distributions for every uncertain parameter
- Generation of a sample from these distributions

- Execution of the model with the different sets of sampled input variables

6.2.1. Specification of Probability Distribution

The correct choice and parameterization of a probability distribution is the most important step, because it determines the uncertainty in the model output and the relative importance of the individual input variables that contribute to this uncertainty. Iman and Helton (1988) reported that the sensitivity analysis results generally depend more on the selected ranges (mean, variance, etc.) than on the specific distribution. However, correct description of the input distribution is important in the case when the estimation of distributions of the output is of interest. The selection of the probability density function (distribution) can be done based on literature results, expert judgment, or by using statistical techniques applied to samples collected in the field. Typical distributions of parameters are normal, lognormal, uniform, triangular, etc. In case no or limited measured data are available, the distribution should be selected based on expert judgment or information in the literature. If only a range of possible values is known, a uniform or log-uniform distribution is most applicable. If the central value of an uncertain input variable, such as mean, median, or mode can be estimated, one can use distributions with a maximum probability such as a normal, log-normal, triangular, and others (Manache, 2001). For all parameters in the environment in the case of a lack of information on how the parameter varies, the lognormal distribution should be assumed (Schnoor, 1996, p. 266).

Variables under consideration may be correlated. In such a case, it is necessary to incorporate an appropriate correlation structure into the sample. This is very often a difficult task because the selected variable distributions have to be consistent with the imposed correlation (Manache, 2001).

6.2.2. Generation of Random Numbers

Values of the input variables are randomly generated from an assigned distribution. The most common sampling techniques are random sampling (also called Monte Carlo sampling) and Latin Hypercube sampling (LHS). In random sampling, random values for each variable are generated from the distribution specified. In this method, points from different regions of the sample space occur in direct relationship to the probability of occurrence and each sample value is selected independently from all other sample values. As a result a large sample size is required in the random sampling technique. The size of the sample varies with model complexity. Melching (1994) reported that 1,000 simulations were needed to obtain convergence in the output standard deviation when studying the propagation of parameter uncertainty through a Streeter-Phelps model of critical DO concentration. Brown and Barnwell (1987) reported that for the QUAL2E multiple constituent (DO, nitrogen cycle, algae, etc.), steady-state, surface water-quality model 2,000 simulations are required to obtain accurate estimates of the output standard deviation.

The LHS method is a variant on Monte Carlo simulation that allows a better coverage of the sample space for a smaller sample size. In this technique, the range of each of the

input uncertain variables is divided into N intervals each with a probability of 1/N. Random values of each basic variable are generated for each of the ranges, covering the entire range of probability. Randomly generated basic variable values are then randomly arranged to form N sets of randomly generated variables. Using LHS, allows reducing the large sample size required for Monte Carlo simulation into a much smaller sample, e.g., equal to 4/3 times the number of uncertain variables (Iman and Helton, 1985).

Although, Beck (1985) reported, "when computing power is available, there can be no strong argument against the use of Monte Carlo simulation," for complex models with many input variables the use of the random sampling method is expensive and time consuming. LHS is a good alternative method providing reliable results without high computational requirements (Iman and Helton, 1988). Thus, LHS was applied in this study.

6.3. Input for the Random Number Generator

Within the DUFLOW model of the CWS, storm loads from pumping stations, CSOs, and tributaries were not measured for the verification period, and, thus, are considered uncertain. For the application of the LHS procedure, for each loading a probability distribution specified by the mean and standard deviation should be defined. The mean and standard deviation were calculated based on available measured data for each source (Tables 5.8 and 5.10). Statistical analysis showed no relation between discharge volume and event mean concentration at pumping stations discharging to the CWS. There were not enough sampled events to define a probability distribution. Therefore, the assumption

of a log-normal probability distribution was made based on results of Novotny's (2004) studies that showed that for many pollutants, event mean concentrations in runoff, follow the log-normal probability distribution. The mean value, standard deviation, and variance used for the LHS of the input event mean concentration for tributaries and pump stations (which then are applied to nearby CSOs as described in Section 5.2.5) are listed in Table 6.1.

A number of computer packages containing routines for Monte Carlo simulation and its modification, LHS are available. In this study, the UNCSAM program developed by the Dutch Institute for Public Health and the Environment (Janssen et al., 1992) was used to generate the 50 sets of the random event mean concentrations for pumping stations, CSOs, and tributaries for the DUFLOW model input. For 50 Latin Hypercube samples, each sample concentration subrange encloses a probability range of 0.02. With the assumption of a lognormal distribution with a mean of 52.145 mg/L and standard deviation of 37.112 mg/L for CBOD at the Racine Avenue Pumping Station the maximum subrange enclosing the probability from 0.98 to 1.00 corresponds to concentration range of ! 12.2 mg/L to infinity. Whereas the minimum subrange enclosing the probability from 0.00 to 0.02 corresponds to a concentration range of 0.0 to 20.7 mg/L. One value in each of these ranges will be generated as well as from each other probability subrange and each pump station and tributary for all constituents. These random values are then randomly arranged into 50 sets of input concentrations to evaluate the range of DO concentrations resulting from these ranges of storm loadings.

For all storm events within the verification period the same event mean concentration of each constituent was assigned rather than generating different concentrations for each event due to limitations on the maximum of number of samples in the UNCSAM program. For example, for LHS run 1 CBOD concentrations of 102.6, 15.3, and 13.8 mg/L were generated for the Racine Avenue, North Branch, and 125th Street Pumping Stations (and related CSOs), respectively, these concentrations were used for all overflow periods during the verification period in this run, and then for LHS run 2 new CBOD concentrations (11.0, 64.0, and 27.9 mg/L, respectively) from other probability ranges were used. This concept applies for all other constituents.

Table 6.1 The mean values, standard deviations, and variances used for the Latin Hypercube sampling of the event mean concentrations in mg/L for tributaries and pumping stations discharging to the Chicago Waterway System

	Constituent	Mean	Standard Deviation	Variance
North Branch Pumping Station	DO	3.484	1.875	3.516
	$CBOD_5$	35.444	17.412	303.166
	NH4	2.859	1.405	1.975
	NO3	0.675	0.364	0.133
	Norg	6.101	3.407	11.607
	Porg	0.991	0.708	0.502
	Pin	0.421	0.286	0.286
	SS	101.846	67.483	4554.021
Racine Avenue Pumping Station	DO	3.484	1.875	3.516
	$CBOD_5$	52.145	37.112	1377.322
	NH4	2.859	1.405	1.975
	NO3	0.675	0.364	0.133
	Norg	6.101	3.407	11.607
	Porg	0.991	0.708	0.502
	Pin	0.421	0.286	0.286
	SS	499.949	528.266	279065.336
125th Street Pumping Station	DO	4.822	0.453	0.205
	$CBOD_5$	25.667	16.186	261.994
	NH4	1.044	0.472	0.223
	NO3	1.829	0.283	0.080
	Norg	3.590	1.014	1.029
	Porg	0.444	0.221	0.049
	Pin	1.308	1.759	3.094
	SS	75.945	40.429	1634.484
North Branch Chicago River at Albany Avenue	DO	5.710	0.965	0.932
	$CBOD_5$	2.577	1.824	3.327
	NH4	0.145	0.100	0.010
	NO3	1.766	0.791	0.625
	Norg	1.428	0.362	0.131
	Porg	0.191	0.084	0.007
	Pin	0.277	0.134	0.018
	SS	60.255	38.322	1468.610
Little Calumet River at South Holland	DO	5.376	0.949	0.901
	$CBOD_5$	2.923	1.019	1.039
	NH4	0.208	0.089	0.008
	NO3	1.904	0.686	0.471
	Norg	1.595	0.245	0.060
	Porg	0.226	0.063	0.004
	Pin	0.983	0.352	0.124
	SS	87.072	32.498	1056.143

6.4. Results

To analyze the influence of storm loadings on DO concentrations in the CWS, the water-quality model was run 50 times, each time with a different set of constituent concentrations for every storm load source. As a result, the randomly generated storm pollutant loads established minimum and maximum bounds on the simulated DO concentration. Measured in-stream DO concentrations at 27 locations listed in Table 5.12 were compared with established bounds (e.g., Figure 6.1). Ideally, during dry-weather periods or more precisely during periods when the storm loading effect on water-quality parameters is negligible, the simulated DO concentrations should be similar to the observed one, and during wet-weather periods the measured DO concentrations should pass through the bounds. The results for all 27 locations of this new approach to verification are presented in the Appendix B. The percentage of measured DO passing through the bounds at the 27 DO monitoring locations is listed in Table 6.2. At no location did 50 percent of the measured values pass through the DO concentration bounds generated by LHS, and at 18 of 27 locations less than 20 percent of the measured DO concentrations passed through the DO concentration bounds. Thus, the basic modeling errors involved in simulating DO concentrations in the CWS have a larger influence on the difference between measured and simulated DO concentrations than does the uncertainty in the CSO loads. This result is in agreement with the discussion of Table 5.14 in Section 5.3. Therefore, the standard verification described in Section 5.3 is adequate to evaluate the usefulness of the model.

6.5.Effect of Storm Load on DO Concentration

Standard deviations of hourly DO concentration computed from the 50 simulated values under different storm loadings are greater for wet-weather periods than for dry-weather periods. For after-storm periods the value of the standard deviation decreases and approaches zero when the effect of storm load on DO concentration at a location in the CWS has become negligible. To determine how long storm loadings affect the DO concentrations in the CWS for each location the standard deviation (SD) variation was plotted against time together with flow (e.g., Figure 6.2). At Romeoville the CWS responds to storm-pollution for more than 2 weeks in some cases after the end of the event. Right after the discharge of storm water to the CWS (event day), simulated DO concentrations are sensitive to pollution loads. Therefore, the space between minimum and maximum DO concentration bounds becomes wider (e.g., Figure 6.1). During after-storm periods, the range of possible DO concentrations narrows as the variability between maximum and minimum DO concentration lines decreases. At the point where the standard deviation approaches zero storm pollution does not affect water quality in the system at that location anymore.

There are two main types of sinks of DO in the DUFLOW model those in the water column and those from the sediments. Oxidation of CBOD, algal respiration, and nitrification are oxygen-consuming processes within the water column. The sediment sink involves diffusion of oxygen between the water body and the sediment layer and resuspension of oxygen consuming substances as described in Section 2.2.4. The transformation of constituents in the sediment bed layer is described in Section 2.2.3.

Therefore, the period of storm loading effect on water quality in any system can be divided into two sub-periods: intense oxygen consumption in the water layer (1) and background oxygen consumption related to interaction between the water body and sediments (2). Since intensities of the self-purification processes within the water layer are much higher than rates of oxygen-consuming processes between the sediments and the overlying water, the effect of the sediments on water quality lasts longer. On average, the first sub-period lasts about a week (on Figure 6.2 sub-period 1) and is approximately equal to time needed to drain the system. This confirms the assumption for analysis of dry-weather and wet-weather verification results, that the wet-weather period can be considered when flow at Romeoville is greater than 100 m^3/s. The influence of storm

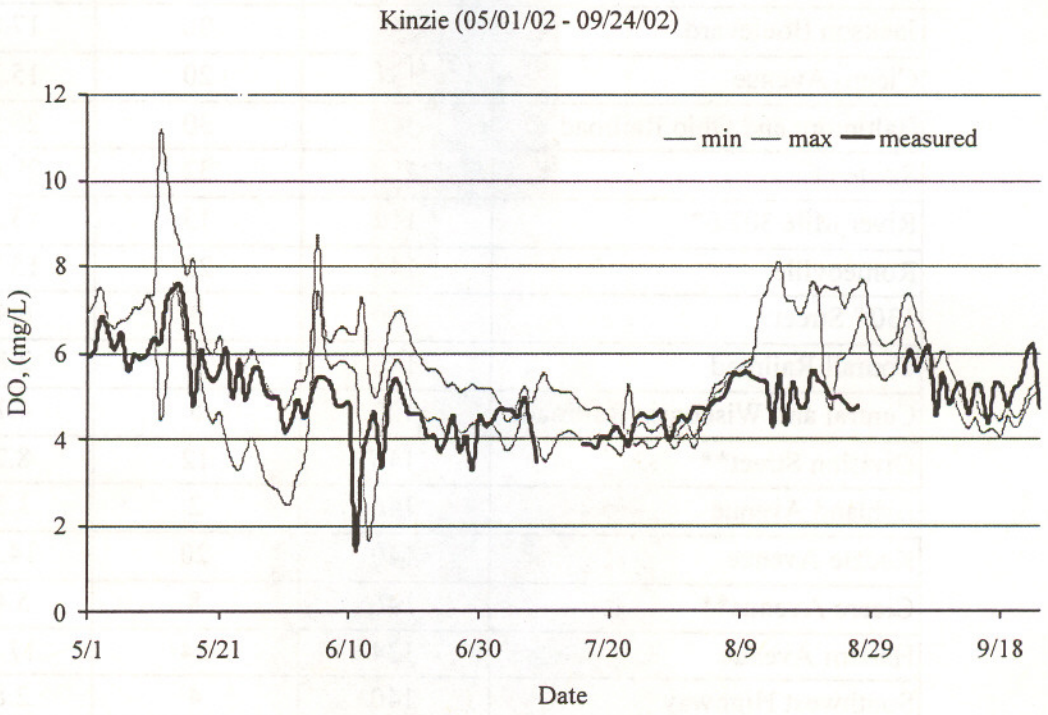

Figure 6.1 Range of simulated dissolved oxygen (DO) concentrations at Kinzie Street on the North Branch Chicago River obtained by Latin Hypercube sampling of storm event mean concentrations compared with the measured DO concentration

Table 6.2 Percentage of measured daily mean dissolved oxygen (DO) concentrations passing through the range of simulated daily mean DO concentrations obtained from Latin Hypercube sampling of storm event mean concentrations at 27 locations for May 1 to September 24, 2002

Location	Number of Days	Number within Bounds	% within Bounds
Linden Street	121	29	23.97
Simpson Street	120	53	44.17
Main Street	134	47	35.08
Addison Street	146	30	20.55
Fullerton Avenue	146	41	28.08
Division Street	146	44	30.14
Kinzie Street	134	39	29.10
Chicago River Controlling Works	140	2	1.43
Michigan Avenue	146	5	3.43
Clark Street	146	4	2.74
Jackson Boulevard	146	26	17.81
Cicero Avenue	131	20	15.27
Baltimore and Ohio Railroad	146	30	20.55
Route #83	108	32	29.63
River Mile 302.6*	112	15	13.39
Romeoville	146	23	15.75
130th Street	140	9	6.43
Conrail Railroad	140	4	2.86
Central and Wisconsin Railroad	120	5	4.17
Division Street**	146	12	8.22
Ashland Avenue	146	2	1.37
Kedzie Avenue	140	20	14.29
Cicero Avenue**	146	8	5.48
Harlem Avenue	134	24	17.91
Southwest Highway	140	4	2.86
104th Avenue	123	5	4.07
Route #83**	140	10	7.14

* River mile relative to the mouth of the Illinois River at Grafton. River mile 11.6 relative to Lockport

** Locations on the Calumet-Sag Channel

loading on DO consumption due to water-sediment reactions is longer than the time distance between two consecutive storm events, and, therefore, it is difficult to estimate based on the analyzed results.

The primary storm load effect on DO occurs mainly in the first sub-period, when the standard deviation of DO concentrations is greater than 0.1 mg/L. Therefore, for practical consideration, it is assumed based on engineering judgment that there is no storm load effect on DO in the system when the standard deviation is less than 0.1 mg/L. Durations of each storm effect at 24 monitored locations are listed in Table 6.3. Results for the stations on the upper North Shore Channel (i.e. Linden Street, Simpson Street, and Main Street) are not included in Table 6.3 because during low flow periods the residence time in the channel is so long that the effects of nearly all storms overlap.

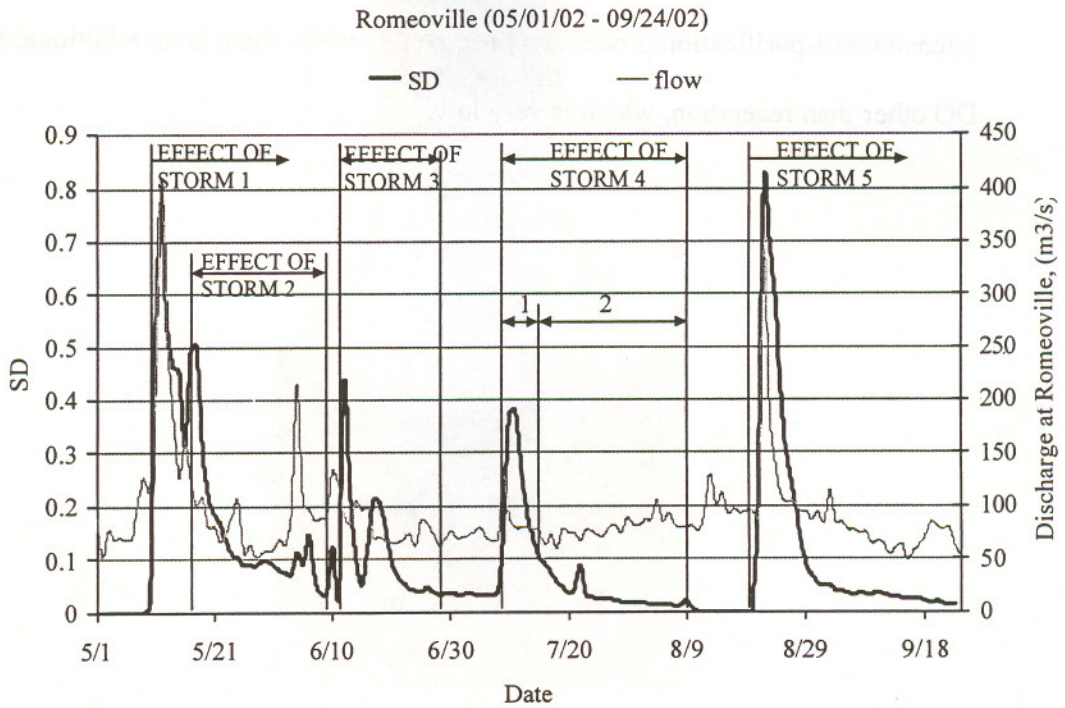

Figure 6.2 Duration of storm effect on dissolved oxygen (DO) concentration at Romeoville for May 1 to September 24, 2002

Substantial impact of storm loading on DO concentration in the CWS on average lasts one day to a few weeks depending on the location in the CWS. In general, the storm load effect remains in the system longer in the North Shore Channel, North Branch Chicago River, South Branch Chicago River, and in CSSC, than in the Little Calumet River and Calumet-Sag Channel. Moreover, for locations upstream from the Stickney WRP, the storm effect lasts even longer than for the rest of the CSSC. The explanation for this can be found in the hydraulic characteristics and behavior of the system. Effluent from the Stickney WRP dominates the hydraulics of the system. Due to small slopes and velocities, the Stickney WRP discharge flows in two directions: upstream from the plant and downstream towards Romeoville, causing in this way a "hydraulic dam" for upstream flow. In these sections water becomes practically stagnant. In such cases, the residence time of storm loads upstream from the plant are greater than downstream, and intensive self-purification processes consume DO while there is no additional source of DO other than reaeration, which is very low.

Table 6.3 Duration of storm effect on dissolved oxygen (DO) concentration in days in the Chicago Waterway System for 3 storms within the verification period (May 1 to September 24, 2002)

Location	STORM 3 (6/11/02)	STORM 4 (7/9/02)	STORM 5 (8/22/02)
Addison Street	17	2	11
Fullerton Avenue	24	10	23
Division Street	>28	15	24
Kinzie Street	>28	16	21
Chicago River Controlling Works	28	9	n/d
Michigan Avenue	>28	15	1
Clark Street	>28	17	1
Jackson Boulevard	>28	17	7
Cicero Avenue	11	9	8
Baltimore and Ohio Railroad	10	8	7
Route #83	12	9	7
River Mile 302.6*	9	6	8
Romeoville	10	7	8
O'Brien Lock and Dam	n/d	n/d	3
Conrail	n/d	n/d	3
Central and Wisconsin Railroad	n/d	n/d	3
Division Street**	1	1	7
Ashland Avenue	3	2	20
Kedzie Street	1	2	8
Cicero Avenue**	1	3	8
Harlem Avenue	8	8	6
Southwest Highway	2	3	9
104th Avenue	2	3	10
Route #83**	2	4	10

* River mile relative to the mouth of the Illinois River at Grafton. River mile 11.6 relative to Lockport
** Locations on the Calumet-Sag Channel.
NOTE: At some locations, the after-storm period standard deviation is not greater than 0.1. This is denoted as n/d (= not detected).
In the cases of the first two storms (5/11/02 and 5/16/02 storms) the duration of the storm effect exceeded the time between the two consecutive storms. Thus, the duration of the storm effect could not be properly evaluated.

CHAPTER 7: CONCLUSIONS

An unsteady hydraulic and water-quality model for the Chicago Waterway System (CWS) developed by the Institute for Urban Environment Risk Management at Marquette University, has been verified for the period of May 1 to September 24, 2002.

The hydraulic DUFLOW model was calibrated based on flow and stage data for 8 different periods between August 1, 1998, and July 31, 1999. The verification showed that the model simulates quite well the hydrologic and hydraulic behavior of the system. In this study, measured water surface elevation data were compared with simulated values at 7 locations: Western Avenue, Willow Springs, Sag Junction, North Branch Chicago River at Lawrence Avenue, Calumet-Sag Channel at Southwest Highway, Wilmette, and Romeoville. The power of the model to correctly predict flow was tested at gages previously used for calibration and verification: Romeoville, Chicago River Controlling Works, and O'Brien Dam and Lock. In addition flow data from a new station USGS on the North Branch Chicago River at Grand Avenue, were used for verification purposes. Comparison between measured and simulated flow at this location confirmed the hydraulic accuracy of the DUFLOW model.

The water-quality model calibrated for the July 12 – November 9, 2001 period, has been verified with the data collected between May 1 and September 24, 2002. Because for the verification period, no detailed storm loading data are available, two approaches to verification were done. In the first, the traditional verification, for unknown event mean concentrations from pumping stations, CSOs, and tributaries, averages from historic

measurements were used. Although in most compared locations on average absolute errors were greater than 30%, the model verification results were similar to the calibration results. Therefore, the water-quality DUFLOW model can be considered satisfactory for dissolved oxygen simulation on the CWS. The DUFLOW model of the CWS is able to simulate water quality under unsteady flow conditions, and can be used to assist water-quality management and planning decision-making.

The second approach applied to model verification was used to test the model prediction for after-storm periods. In this approach event mean concentrations were randomly generated on the basis of observed flow weighted event mean concentrations for the pump stations and tributaries. Fifty simulations of the water quality in the CWS were executed. As a result, ranges of possible DO concentrations were established for 27 DO monitoring locations. Ideally, during dry-weather periods, simulated DO concentrations should be close to measured values and for wet-weather the simulated DO concentrations should pass through the DO bounds established by multiple simulations. For no locations in the system, did more than 50% of measured DO concentrations pass within the DO bounds established by multiple simulations. Thus, the basic modeling errors involved in simulating DO concentrations in the CWS have a larger influence on the difference between measured and simulated DO concentrations than does the uncertainty in the CSO loads. Therefore, the standard verification described in Section 5.3 is adequate to evaluate the usefulness of the model.

Variability of DO concentrations determined from the new approach to verification was used to determine the duration of the storm load effect on DO in the CWS. The effect of storm pollutants on water quality in the system can be split into two phases: direct influence and sediment influence. The first phase lasts until the time needed to pass the wave through the downstream boundary, equal to the time needed to drain the system. The second phase lasts longer, but during it DO in the system is affected much less than during the first phase. It was assumed, that storm load affects DO in the system as long as standard deviation from DO concentrations at the given time-step is less than 0.1 mg/L. After-storm period durations were determined for each of 3 storms at 24 locations. On average, DO is affected for more than 10 days after CSO events in the North Branch Chicago River, Chicago River Main Stem, and South Branch Chicago River. In the Chicago Sanitary and Ship Canal the effect lasts on average 10 days after CSO events, in the Little Calumet River and Calumet-Sag Channel the effect lasts less than 7 days.

REFERENCES

Alp, E. and Melching, C.S. (2004) Preliminary Calibration of a Model for simulation of Water-Quality During Unsteady Flow in the Chicago Waterway System and Application to Proposed Changes to Navigation Make-Up Diversion Procedures. *Technical Report 13.* Institute of Urban Environmental Risk management, Marquette University, Milwaukee, WI, and *Department of Research and Development Report No. 04-14.* Metropolitan Water Reclamation District of Greater Chicago, Chicago, IL.

Barkau, R.L. (1992) *UNET, One-dimensional Unsteady Flow Through a Full Network of Open Channels*. Computer Program, St. Louis, MO.

Beck, M.B. (1985) Water quality management: A review of the development and application of mathematical models. *Lecture Notes in Engineering 11*. C. A. Brebia and S. A. Orszag, eds. Springer-Verlag, New York.

Brown, L.C., and Barnwell, T.O., Jr. (1987) The enhanced stream water quality models QUAL2E and QUAL2E-UNCAS: documentation and user manual. *Report EPA/600/3-87/007*. U.S. Environmental Protection Agency, Athens, GA.

Butts, T.A., Shackleford, D.B., and Bergerhouse, T.R. (1999) Evaluation of Reaeration Efficiencies of Sidestream Elevated Pool Aeration (SEPA) Stations. *Illinois State Water Survey Contract Report 653*. Champaign, IL.

Butts, T.A., Shackleford, D.B., and Bergerhouse, T.R. (2000) Sidestream Elevated Pool Aeration (SEPA) Stations: Effect on Instream Dissolved Oxygen. *Illinois State Water Survey Contract Report 2000-02*. Champaign, IL.

Camp, Dresser, & McKee (CDM). (1992) *Water Quality Modeling for the Greater Chicago Waterway and Upper Illinois River Systems. Main Report*. Chicago, IL.

DUFLOW. (2000) *DUFLOW for Windows V3.3: Duflow Modelling Studio: User's Guide, Reference Guide DUFLOW, and Reference Guide RAM.* STOWA eds. Utrecht, The Netherlands.

Hey, D.L., Dreher, D.W., and Trybus, T.W. (1980) *NIPC Chicago Waterways Model: Verification/Recalibration.* Northeastern Illinois Planning Commision Technical Report. Chicago, IL.

Hydrocomp, Inc. (1979a) *Chicago Sanitary and Ship Canal Hydrologic Calibration.* Report to the Northeastern Illinois Planning Commision, Areawide Clean Water Planning Water Quality Evaluation.

Hydrocomp, Inc. (1979b) *Chicago River, Sanitary and Ship Canal, Calumet Sag Channel Basin.* Report to the Northeastern Illinois Planning Commision, Areawide Clean Water Planning Water Quality Evaluation.

Iman, R.L. and Helton, J.C. (1985) A comparison of uncertainty and sensitivity analysis techniques for computer models. Report NUREGICR-3904, SAND 84-1461, Sandia National Labortaries, Albuquerque, New Mexico.

Iman, R.L. and Helton, J.C. (1988) An investigation of uncertainty and sensitivity analysis techniques for computer models. *Risk Analysis*, **8**(1), 71-90.

Janssen, P.H.M., Heuberger, P.S.C., and Sanders, R. (1992) *UNCSAM 1.1: a software package for sensitivity and uncertainty analysis.* Report No. 959101004. National Institute of Public Health and Environmental Protection, Bilthoven, The Netherlands.

Manache, G. (2001) *Sensitivity of a Continuous Water-Quality Simulation Model to Uncertain Model-Input Parameters*. Vrije Universiteit Brussel-Hydrologie Report, **38**, Brussels, Belgium.

Manache, G. and Melching, C.S. (2004) Sensitivity Analysis of a Water-Quality Model Using Latin Hypercube Sampling. *Journal of Water Resources Planning and Management*, **130**(3), 232-242.

Melching, C.S. (1994) Sensitivity of Monte Carlo Simulation to the probability distribution of the Input Parameters. *Water resources planning in a changing world, Proc. of the IHP-UNESCO Symp.*, Karlsruhe, Germany, p.II.81-II.91.

Novotny, V., and Olem, H. (1994) *Water Quality: Prevention, Identification, and Management of Diffuse Pollution.* Van Nostrand Reinhold, New York.

Novotny, V. (2004) Simplified Databased Total Maximum Daily Loads, or the World is Log-Normal. *Journal of Environmental Engineering*, **130**(6), 674-683.

O'Connor, D.J. and Dobbins, W.E. (1958) Mechanism of reaeration in natural streams. *Transactions, ASCE,* **123**, 641-666.

Polls, I., Washington, B., and Lue-Hing, C. (1982) Improvements in Dissolved Oxygen Levels by Artificial In-Stream Aeration in Chicago Waterways, Metropolitan Sanitary District of Greater Chicago, *Department of Research and Development Report No. 82-16.* Chicago, IL.

Saltelli, A., Andres, T.H., and Homa, T. (1995) Sensitivity analysis of model output; performance of the iterated fractional factorial design method. *Computational Statistics and Data Analysis*, **20**, 387-407.

Schnoor, J.L. (1996) *Environmental Modeling. Fate and Transport of Pollutants in Water, Air, and Soil, Environmental Science and Technology.* A Wiley-Interscience Publication, New York.

Schütze, M., Butler, D., and Beck, M.B. (1999) *Synopsis – A tool for the development and simulation of real-time control strategies for the urban wastewater system*. Joliffe, I. B., and Ball, J.E., eds., Processing of the Eight International Conference on Urban Storm Drainage. Sydney, 1847-1854.

Shrestha, R.L. and Melching, C.S. (2003) Hydraulic Calibration of an Unsteady Flow Model for the Chicago Waterway System, *Technical Report 14*. Institute of Urban Environmental Risk Management, Marquette University, Milwaukee, WI, and Metropolitan Water Reclamation District of Greater Chicago, *Department of Research and Development Report No. 03-18*. Chicago, IL.

Troutman, B.M. (1983) Runoff prediction errors and bias in parameter estimation induced by spatial variability of precipitation. *Water Resources Research*, **19**(3), 791-810.

APPENDIX A

Algal processes calibration

In the DUFLOW model three species of algae can be simulated. The algae species containing chlorophyll-a were of interest to this study. Algal maximum growth rate, die-off rate, and respiration rate were the subject of algal processes calibration. As shown in the water-quality model description, algal growth is limited by the availability of nutrients, light, and temperature. Thus, as a part of the calibration procedure, it is necessary to determine the values of parameters in the equations describing these limitations (equations 2.7, 2.8, and 2.11).

The calibration of the model was performed using trial and error adjustment of selected model input parameters until a reasonable fit between the measured and the simulated chlorophyll-a concentrations was obtained. Simulated values were compared with measurements at 8 locations on the North Shore Channel, Chicago River Main Stem, South Branch Chicago River, Chicago Sanitary and Ship Canal, Little Calumet River, and Calumet-Sag Channel. Values of the parameters related to algal activity after the DUFLOW chlorophyll-a model calibration, are given in Table A.1. Calibrated chlorophyll-a results are shown in Figure A.1.

Table A.1 The DUFLOW chlorophyll-a parameters

Parameter		Unit	Default*	Value
a_{ChlaC}	Chlorophyll-a to carbon ratio	µgChl-a/mgC	30	30
e_0	Background light extinction	1/m	1.0	0.627
e_{alg}	Specific light extinction for algae as chlorophyll-a	µgChl-a/(L·m)	0.016	0.021
e_{SS}	Specific light extinction for suspended solids	mgSS/(L·m)	0.05	0.025
$I_{s,1}$	Optimal light intensity for algal specie 1	W/m^2	40	30
K_{daB}	Anaerobic decay rate constant for algae sediment	1/day	0.01	0.01
K_{die}	Die-off rate constant for algal species 1	1/day	0.1	0.1
K_{mN}	Ammonia preference constant	mgN/m^3	0.025	0.025
$k_{n,1}$	Monod constant for nitrogen for algal growth (species 1)	mgN/m^3	0.01	0.01
$k_{p,1}$	Monod constant for phosphorus for algal growth (species 1)	mgP/m^3	0.005	0.005
K_{res}	Algal respiration rate constant	1/day	0.05	0.05
$?_{ra,1}$	Temperature coefficient for algal respiration	-	1.04	1.04
$?_{daB}$	Temperature coefficient for anaerobic decomposition in the sediment layer	-	1.08	1.04
T_{cs}	Critical temperature for algal species 1	°C	35	28
T_{os}	Optimal temperature for algal species 1	°C	20	18
$\mu_{max,i}$	Maximum specific growth rate algae	1/day	1.2	2-7**
$v_{sa,1}$	Settling velocity for algal species 1	m/day	0.005	0.001

* Default values after DUFLOW, 2000.

** Varies between reaches as shown in Table 5.2..

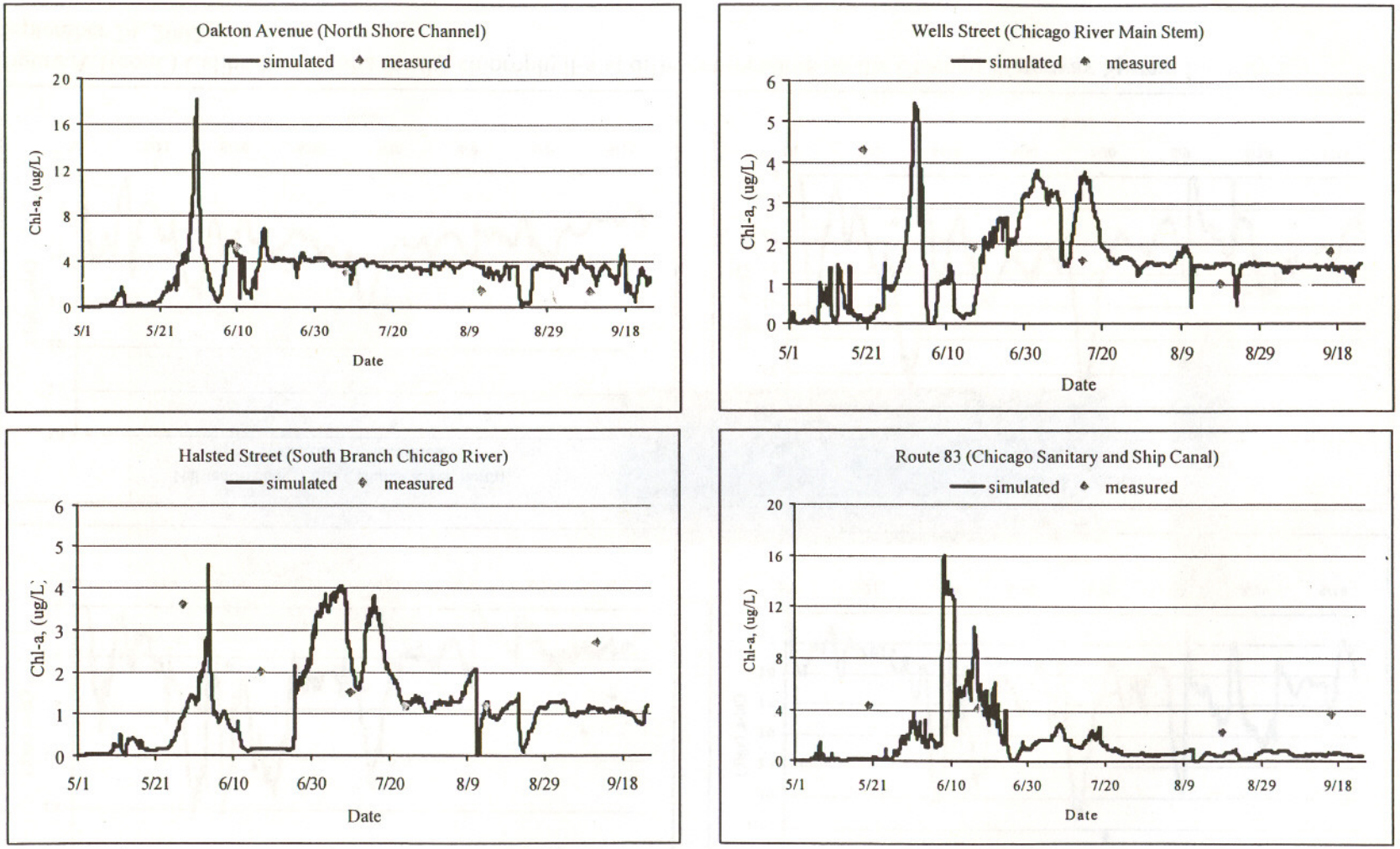

Figure A.1 Calibration results for the chlorophyll-a at different locations on the Chicago Waterway System for May 1 – September 24, 2002

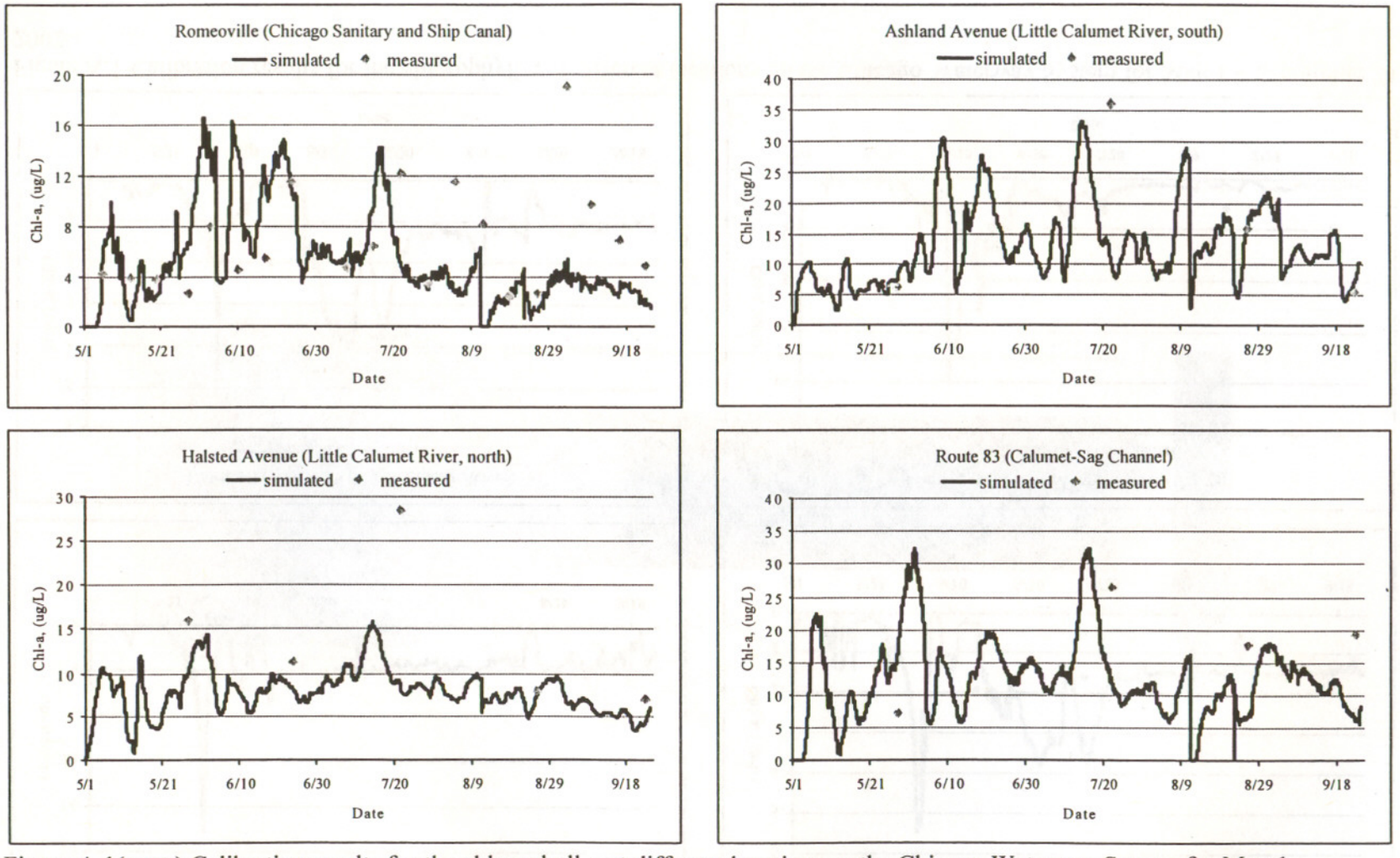

Figure A.1(cont.) Calibration results for the chlorophyll-a at different locations on the Chicago Waterway System for May 1 – September 24, 2002

APPENDIX B

Range of possible dissolved oxygen (DO) concentrations at different locations on the Chicago Waterway System and its standard deviation (SD), established by execution of the new (Latin Hypercube sampling) approach to verification

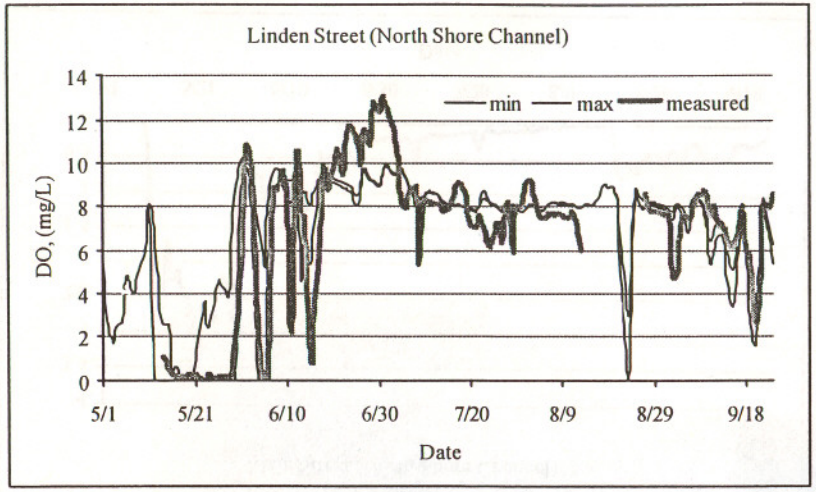
Linden Street (North Shore Channel)
min
max
measured
DO, (mg/L)
0
2
4
6
8
10
12
14
5/1
5/21
6/10
6/30
7/20
8/9
8/29
9/18
Date

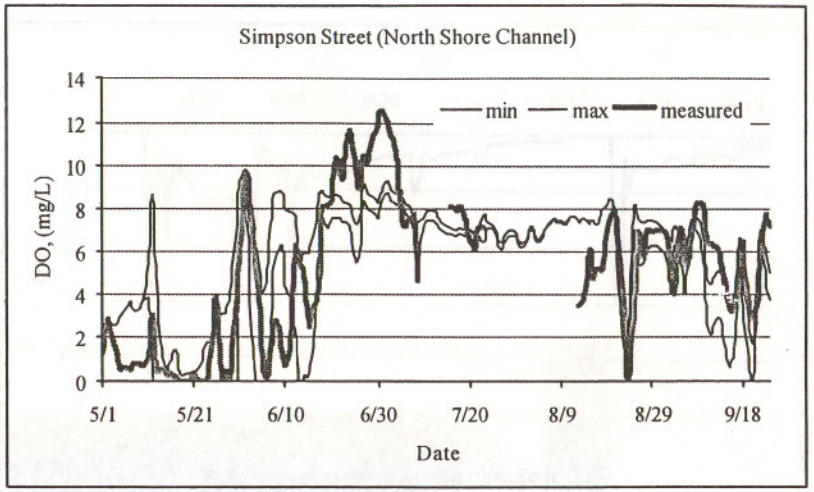
Simpson Street (North Shore Channel)
min
max
measured
DO, (mg/L)
0
2
4
6
8
10
12
14
5/1
5/21
6/10
6/30
7/20
8/9
8/29
9/18
Date

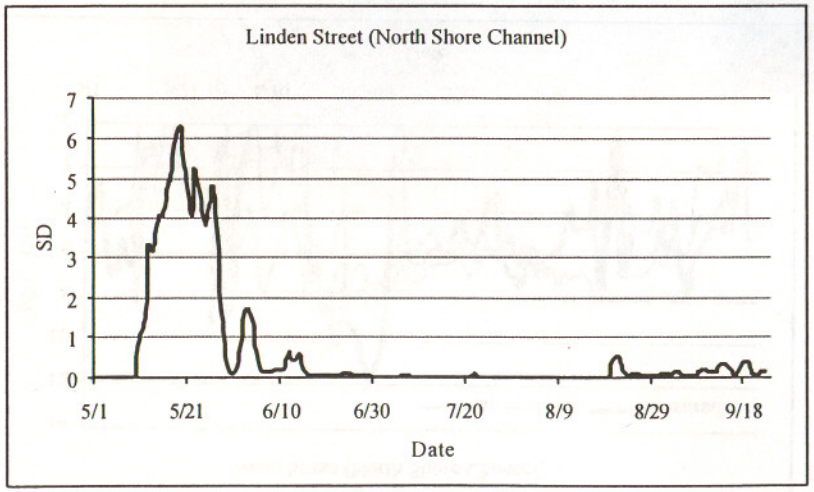
Linden Street (North Shore Channel)
SD
0
1
2
3
4
5
6
7
5/1
5/21
6/10
6/30
7/20
8/9
8/29
9/18
Date

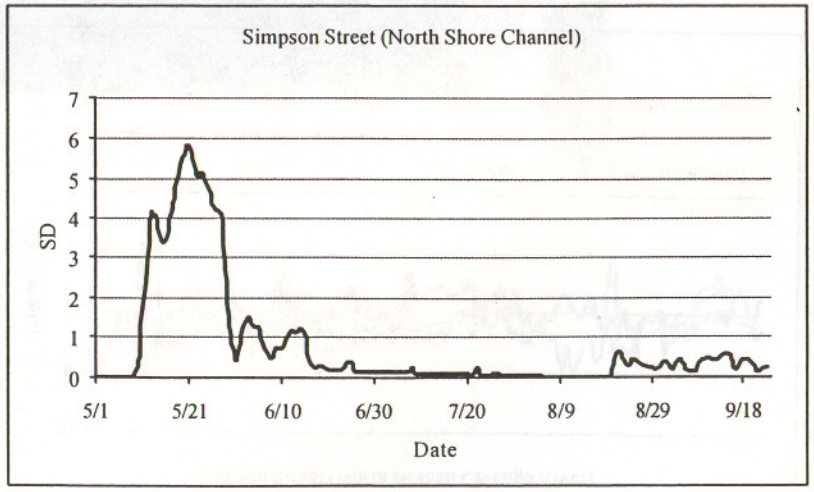
Simpson Street (North Shore Channel)
SD
0
1
2
3
4
5
6
7
5/1
5/21
6/10
6/30
7/20
8/9
8/29
9/18
Date

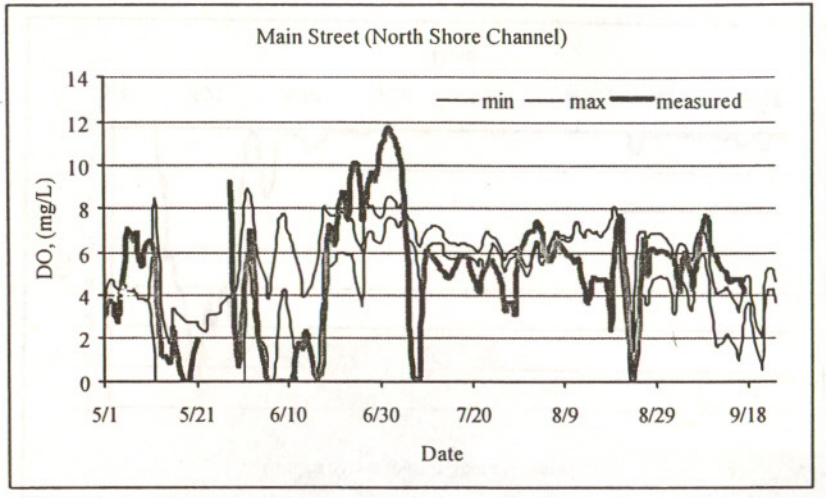
Main Street (North Shore Channel)
min
max
measured
DO, (mg/L)
14
12
10
8
6
4
2
0
5/1
5/21
6/10
6/30
7/20
8/9
8/29
9/18
Date

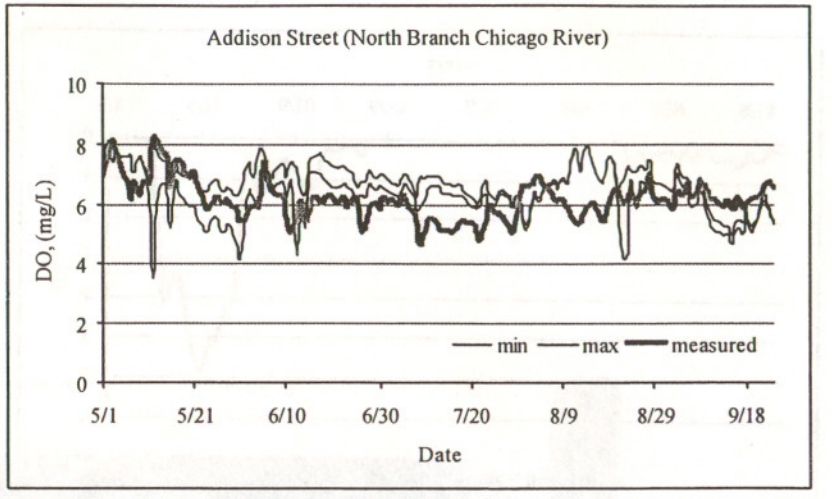
Addison Street (North Branch Chicago River)
DO, (mg/L)
10
8
6
4
2
0
min
max
measured
5/1
5/21
6/10
6/30
7/20
8/9
8/29
9/18
Date

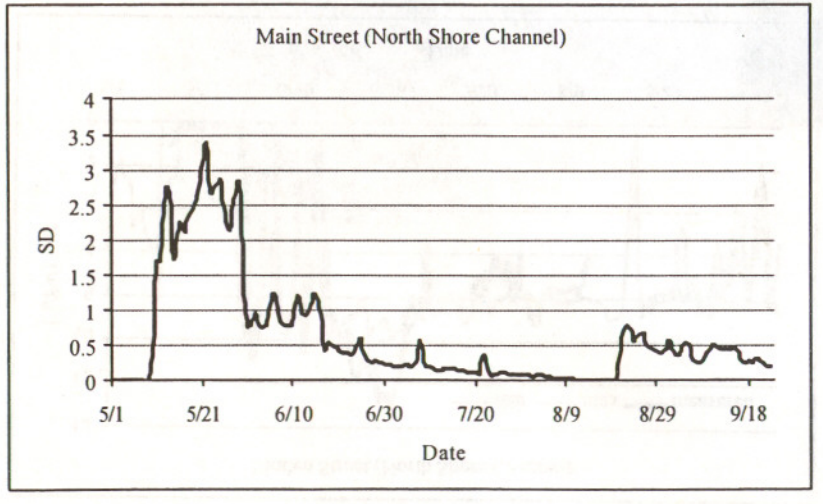
Main Street (North Shore Channel)
SD
4
3.5
3
2.5
2
1.5
1
0.5
0
5/1
5/21
6/10
6/30
7/20
8/9
8/29
9/18
Date

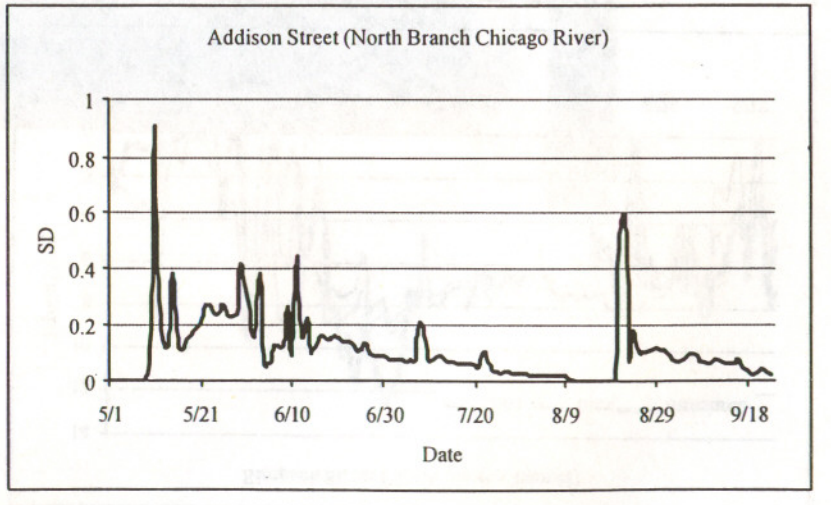
Addison Street (North Branch Chicago River)
SD
1
0.8
0.6
0.4
0.2
0
5/1
5/21
6/10
6/30
7/20
8/9
8/29
9/18
Date

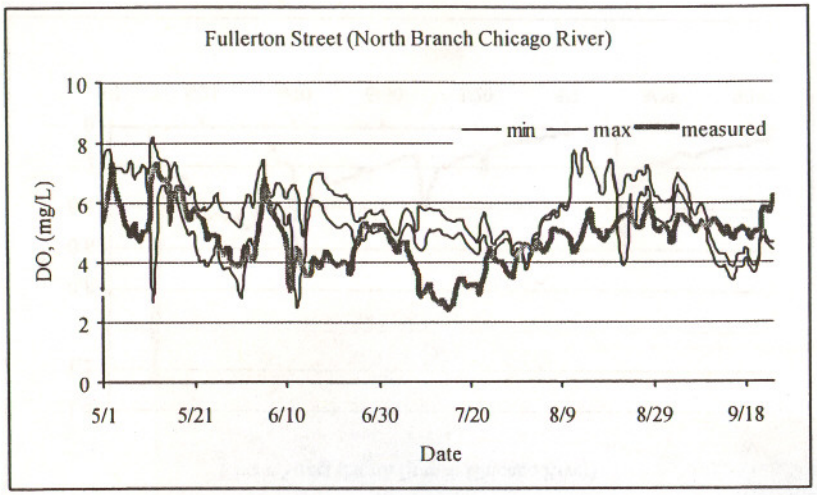
Fullerton Street (North Branch Chicago River)
DO, (mg/L)
min
max
measured
10
8
6
4
2
0
5/1
5/21
6/10
6/30
7/20
8/9
8/29
9/18
Date

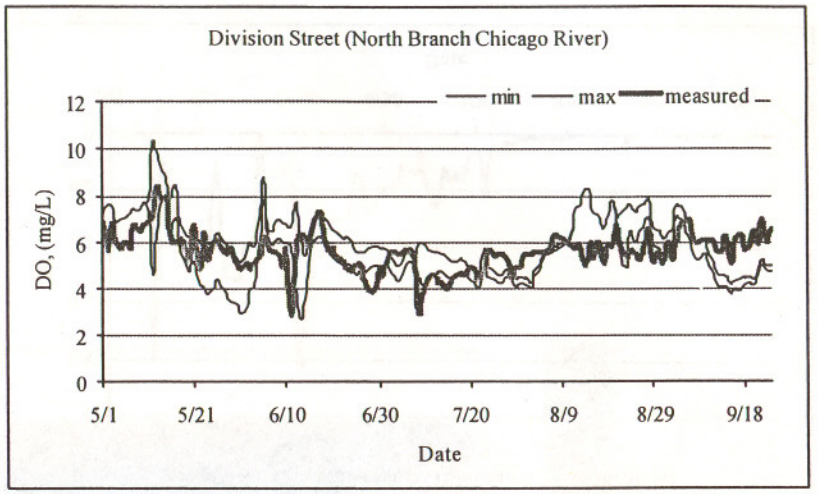
Division Street (North Branch Chicago River)
DO, (mg/L)
min
max
measured
12
10
8
6
4
2
0
5/1
5/21
6/10
6/30
7/20
8/9
8/29
9/18
Date

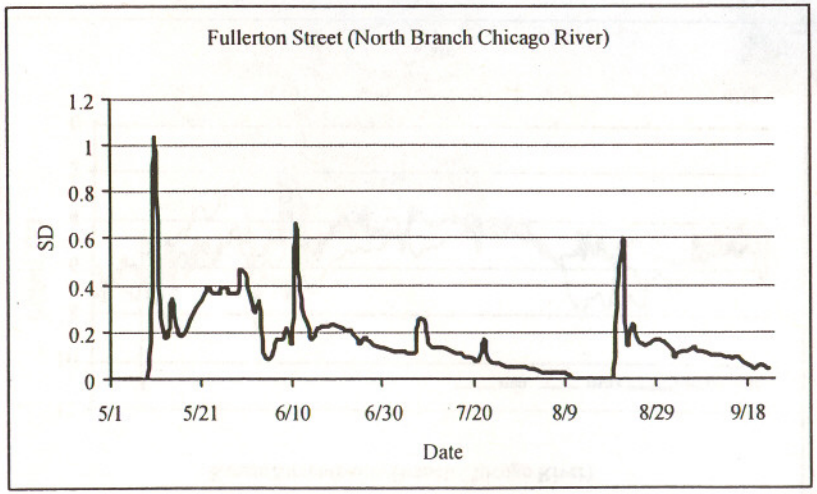
Fullerton Street (North Branch Chicago River)
SD
1.2
1
0.8
0.6
0.4
0.2
0
5/1
5/21
6/10
6/30
7/20
8/9
8/29
9/18
Date

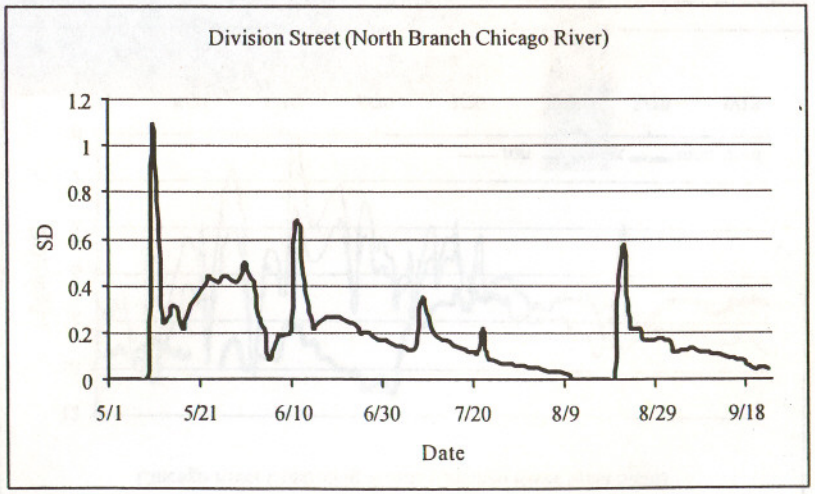
Division Street (North Branch Chicago River)
SD
1.2
1
0.8
0.6
0.4
0.2
0
5/1
5/21
6/10
6/30
7/20
8/9
8/29
9/18
Date

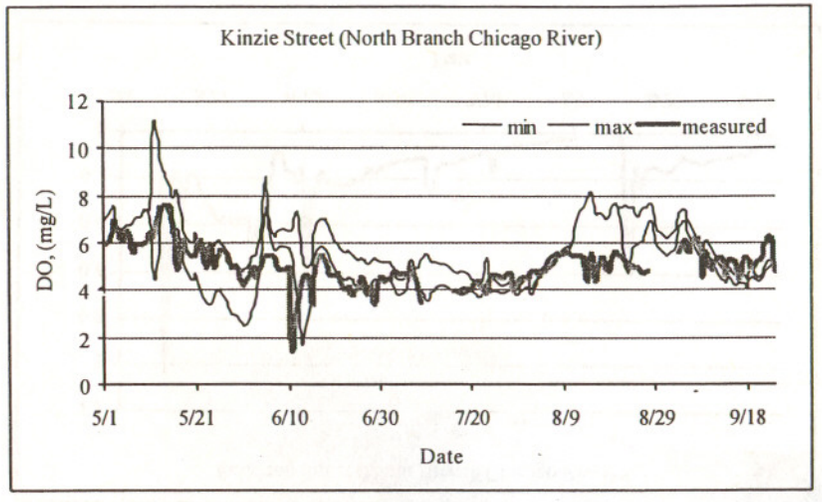
Kinzie Street (North Branch Chicago River)
DO, (mg/L)
12
10
8
6
4
2
0
min
max
measured
5/1
5/21
6/10
6/30
7/20
8/9
8/29
9/18
Date

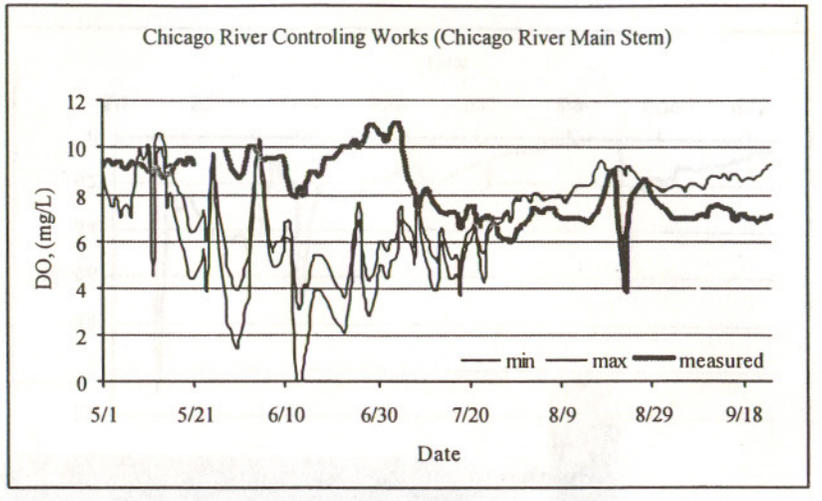
Chicago River Controling Works (Chicago River Main Stem)
DO, (mg/L)
12
10
8
6
4
2
0
min
max
measured
5/1
5/21
6/10
6/30
7/20
8/9
8/29
9/18
Date

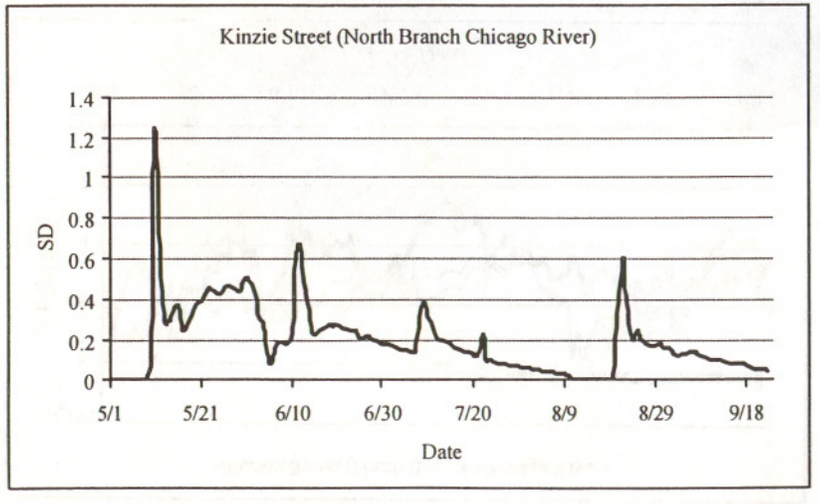
Kinzie Street (North Branch Chicago River)
SD
1.4
1.2
1
0.8
0.6
0.4
0.2
0
5/1
5/21
6/10
6/30
7/20
8/9
8/29
9/18
Date

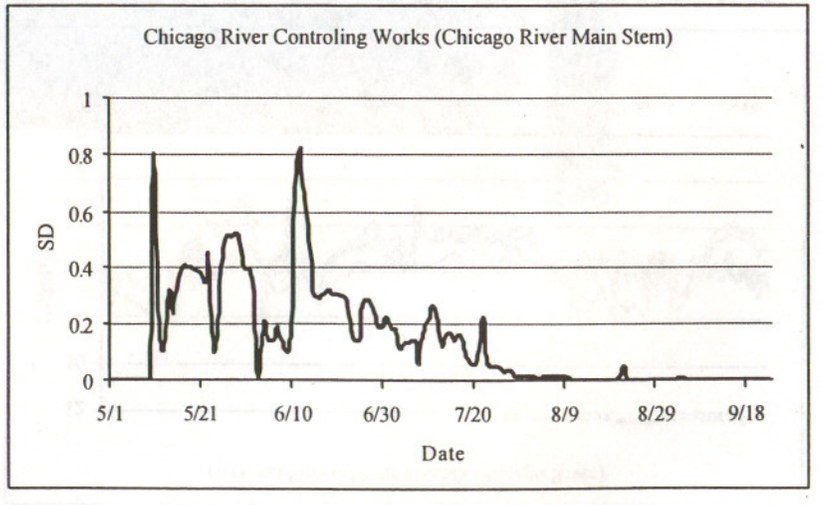
Chicago River Controling Works (Chicago River Main Stem)
SD
1
0.8
0.6
0.4
0.2
0
5/1
5/21
6/10
6/30
7/20
8/9
8/29
9/18
Date

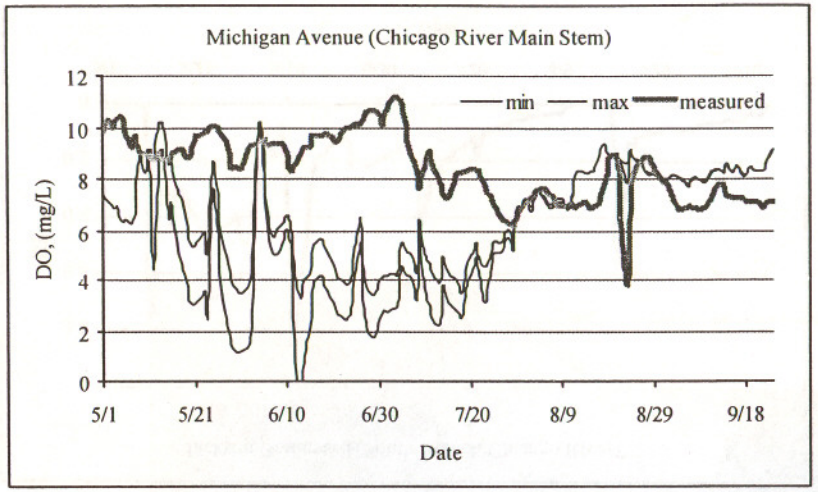
Michigan Avenue (Chicago River Main Stem)
DO, (mg/L)
12
10
8
6
4
2
0
min
max
measured
5/1
5/21
6/10
6/30
7/20
8/9
8/29
9/18
Date

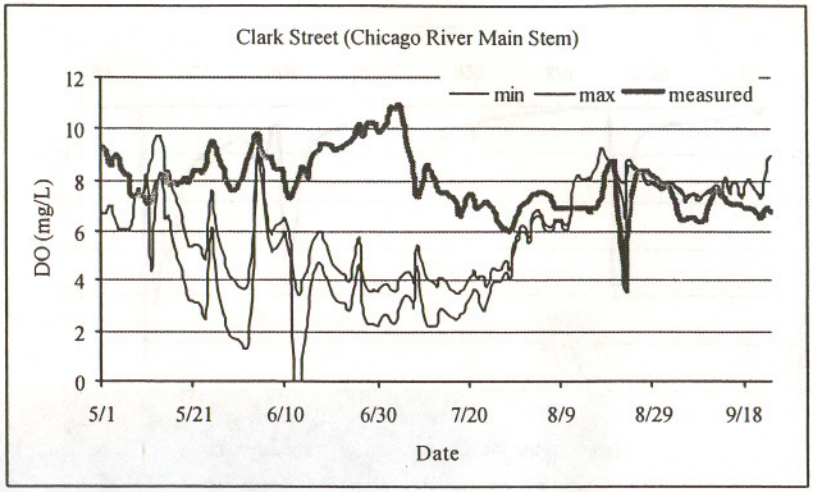
Clark Street (Chicago River Main Stem)
DO (mg/L)
12
10
8
6
4
2
0
min
max
measured
5/1
5/21
6/10
6/30
7/20
8/9
8/29
9/18
Date

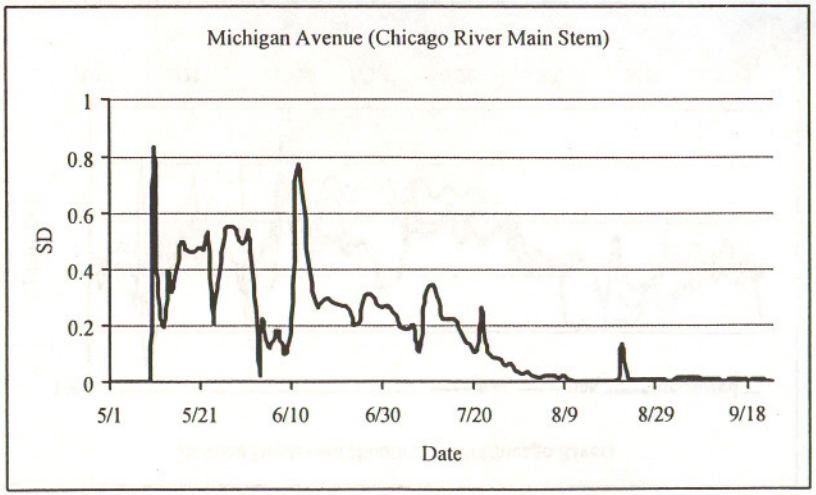
Michigan Avenue (Chicago River Main Stem)
SD
1
0.8
0.6
0.4
0.2
0
5/1
5/21
6/10
6/30
7/20
8/9
8/29
9/18
Date

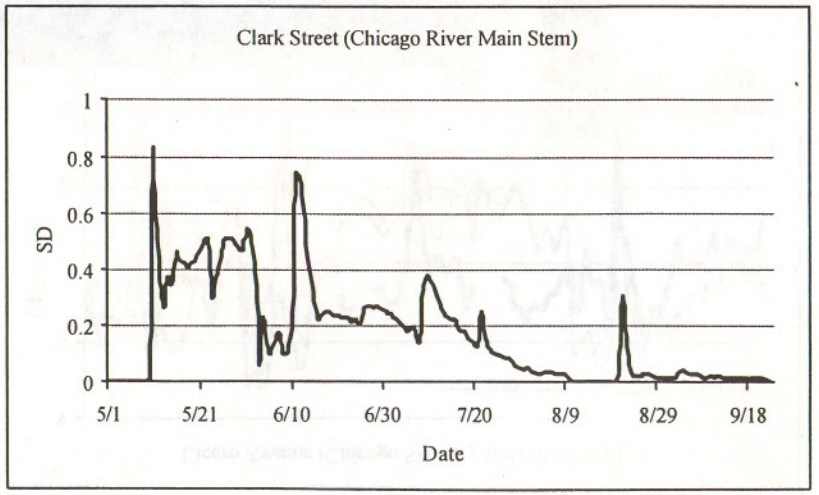
Clark Street (Chicago River Main Stem)
SD
1
0.8
0.6
0.4
0.2
0
5/1
5/21
6/10
6/30
7/20
8/9
8/29
9/18
Date

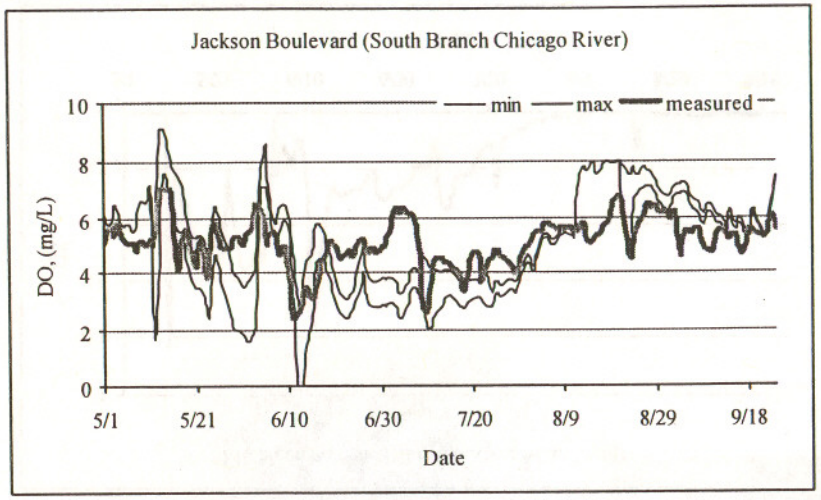
Jackson Boulevard (South Branch Chicago River)
min
max
measured
DO, (mg/L)
10
8
6
4
2
0
5/1
5/21
6/10
6/30
7/20
8/9
8/29
9/18
Date

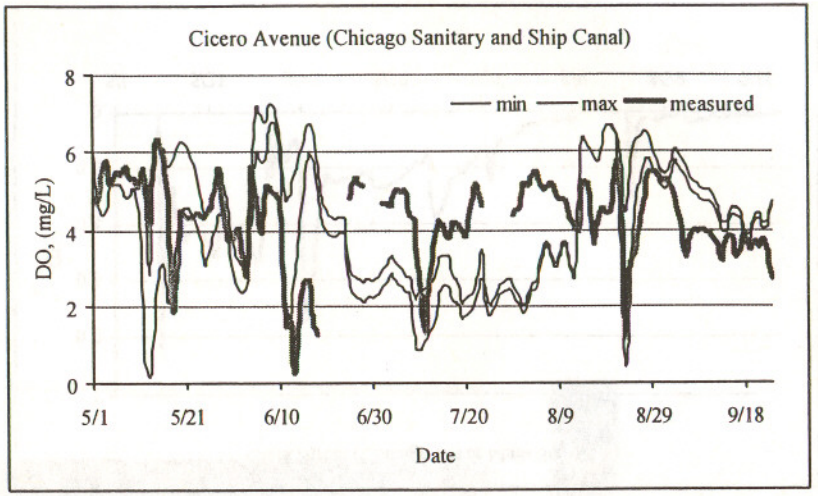
Cicero Avenue (Chicago Sanitary and Ship Canal)
min
max
measured
DO, (mg/L)
8
6
4
2
0
5/1
5/21
6/10
6/30
7/20
8/9
8/29
9/18
Date

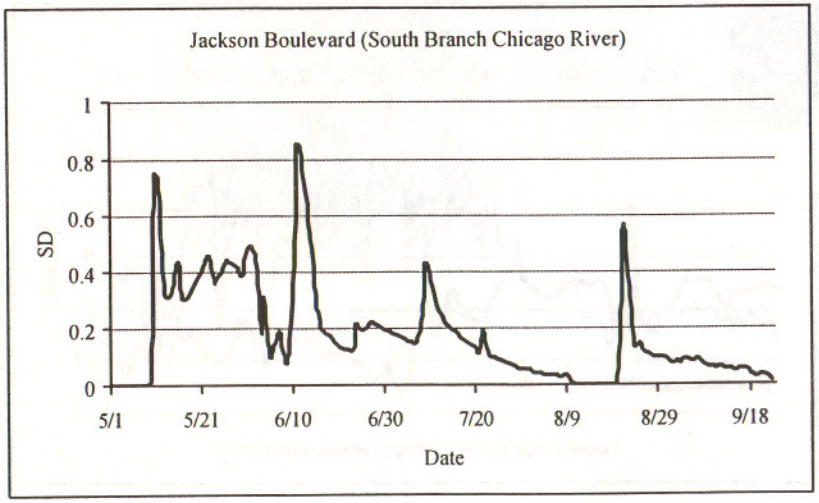
Jackson Boulevard (South Branch Chicago River)
SD
1
0.8
0.6
0.4
0.2
0
5/1
5/21
6/10
6/30
7/20
8/9
8/29
9/18
Date

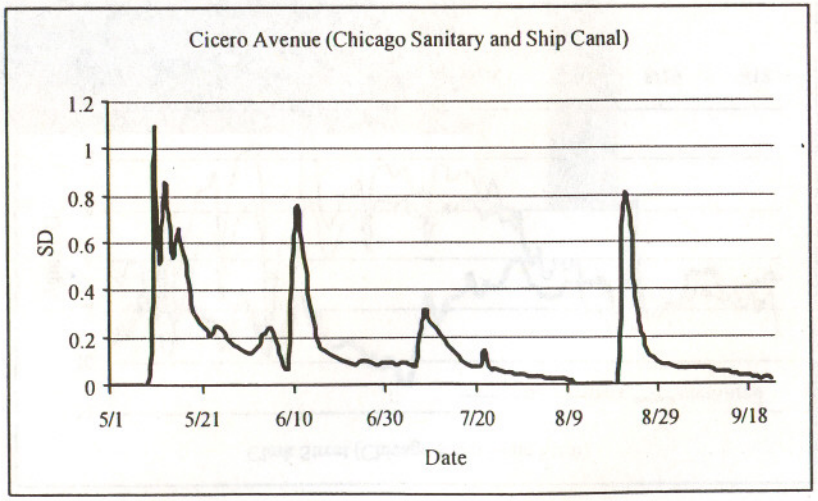
Cicero Avenue (Chicago Sanitary and Ship Canal)
SD
1.2
1
0.8
0.6
0.4
0.2
0
5/1
5/21
6/10
6/30
7/20
8/9
8/29
9/18
Date

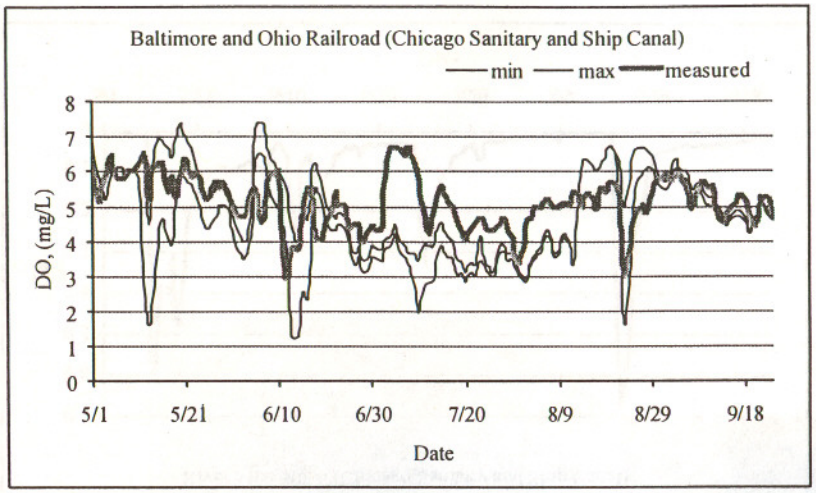
Baltimore and Ohio Railroad (Chicago Sanitary and Ship Canal)
min
max
measured
DO, (mg/L)
0
1
2
3
4
5
6
7
8
5/1
5/21
6/10
6/30
7/20
8/9
8/29
9/18
Date

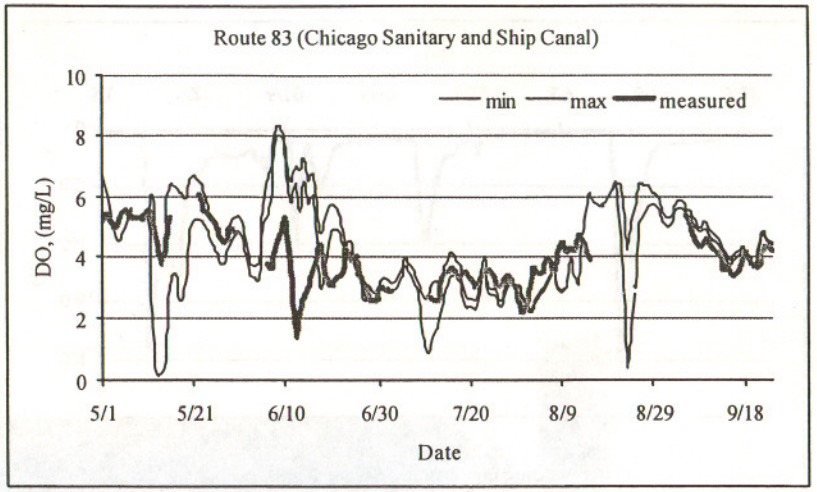
Route 83 (Chicago Sanitary and Ship Canal)
min
max
measured
DO, (mg/L)
0
2
4
6
8
10
5/1
5/21
6/10
6/30
7/20
8/9
8/29
9/18
Date

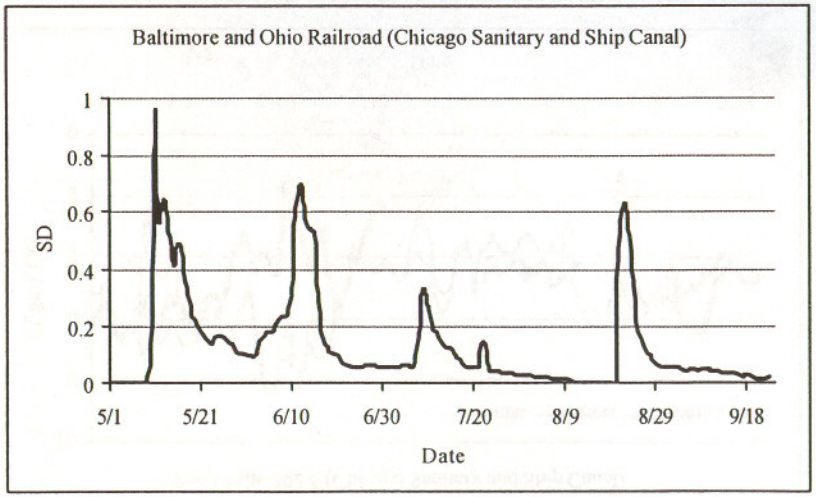
Baltimore and Ohio Railroad (Chicago Sanitary and Ship Canal)
SD
0
0.2
0.4
0.6
0.8
1
5/1
5/21
6/10
6/30
7/20
8/9
8/29
9/18
Date

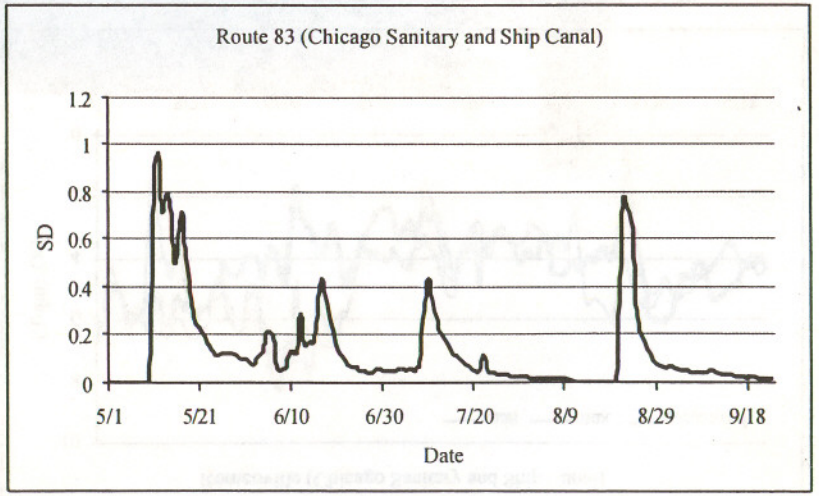
Route 83 (Chicago Sanitary and Ship Canal)
SD
0
0.2
0.4
0.6
0.8
1
1.2
5/1
5/21
6/10
6/30
7/20
8/9
8/29
9/18
Date

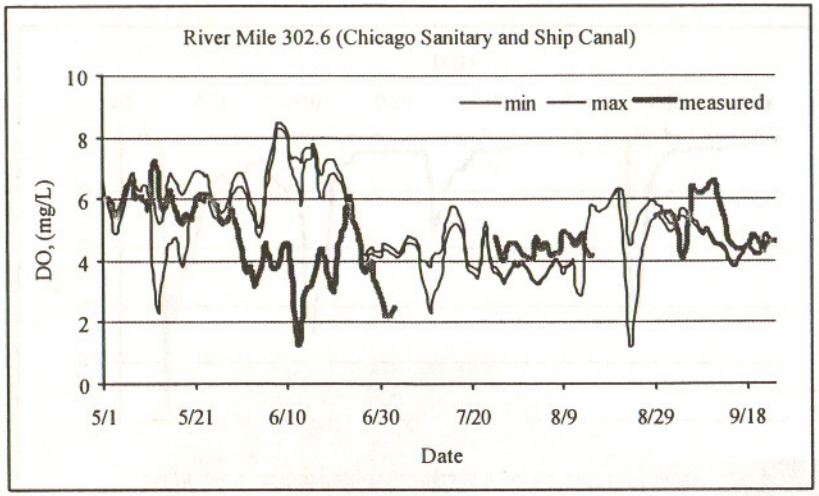
River Mile 302.6 (Chicago Sanitary and Ship Canal)
min
max
measured
DO, (mg/L)
10
8
6
4
2
0
5/1
5/21
6/10
6/30
7/20
8/9
8/29
9/18
Date

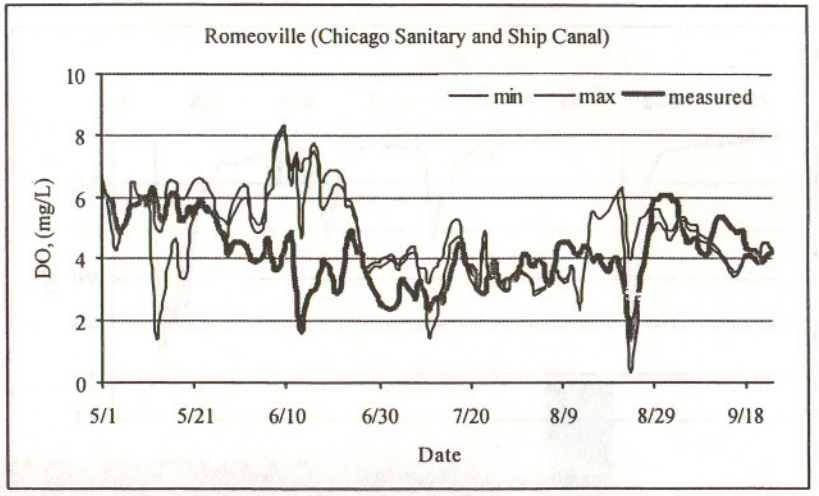
Romeoville (Chicago Sanitary and Ship Canal)
min
max
measured
DO, (mg/L)
10
8
6
4
2
0
5/1
5/21
6/10
6/30
7/20
8/9
8/29
9/18
Date

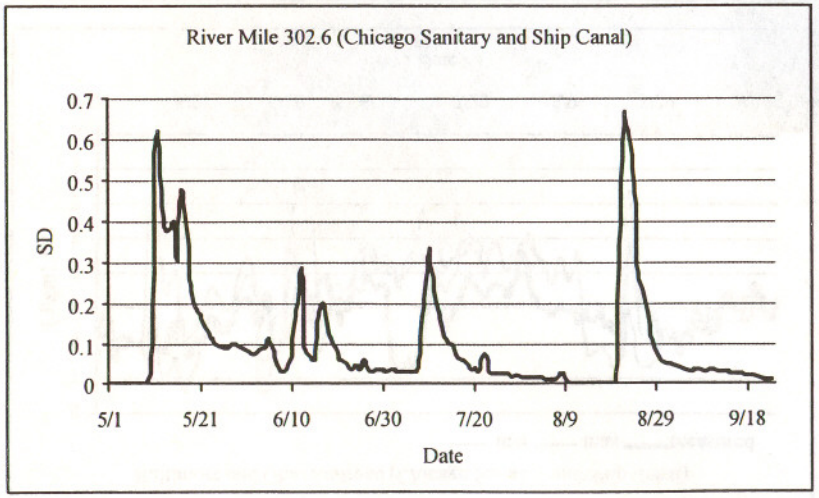
River Mile 302.6 (Chicago Sanitary and Ship Canal)
SD
0.7
0.6
0.5
0.4
0.3
0.2
0.1
0
5/1
5/21
6/10
6/30
7/20
8/9
8/29
9/18
Date

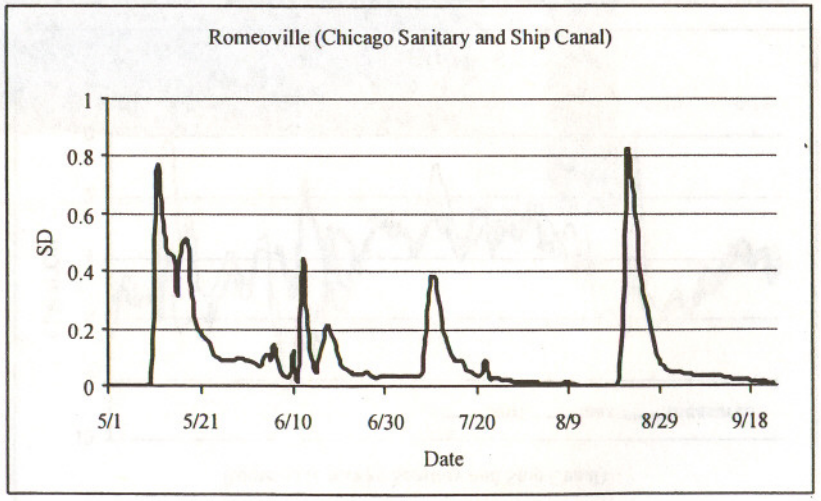
Romeoville (Chicago Sanitary and Ship Canal)
SD
1
0.8
0.6
0.4
0.2
0
5/1
5/21
6/10
6/30
7/20
8/9
8/29
9/18
Date

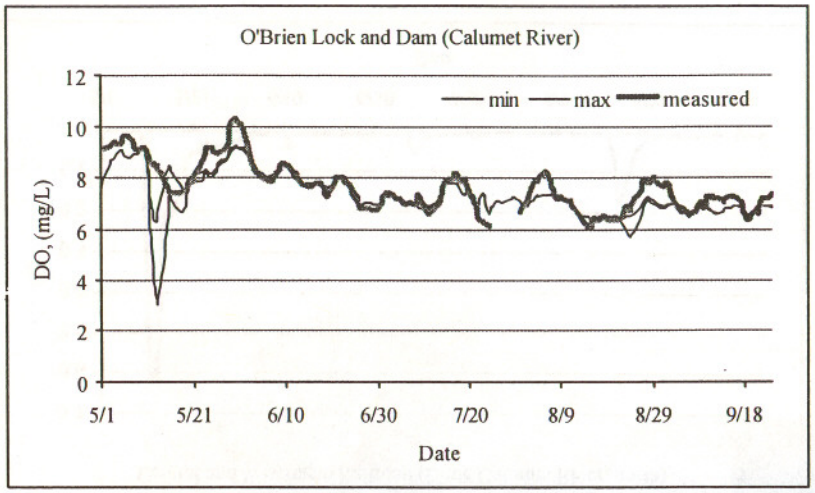
O'Brien Lock and Dam (Calumet River)
min
max
measured
DO, (mg/L)
12
10
8
6
4
2
0
5/1
5/21
6/10
6/30
7/20
8/9
8/29
9/18
Date

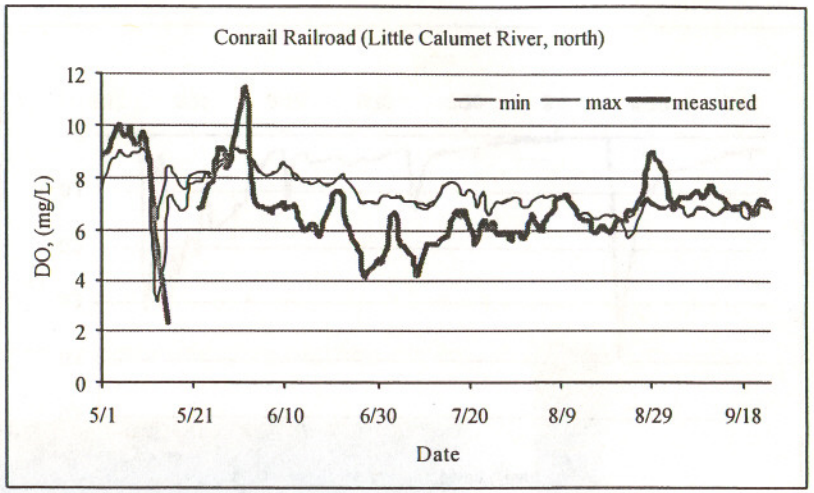
Conrail Railroad (Little Calumet River, north)
min
max
measured
DO, (mg/L)
12
10
8
6
4
2
0
5/1
5/21
6/10
6/30
7/20
8/9
8/29
9/18
Date

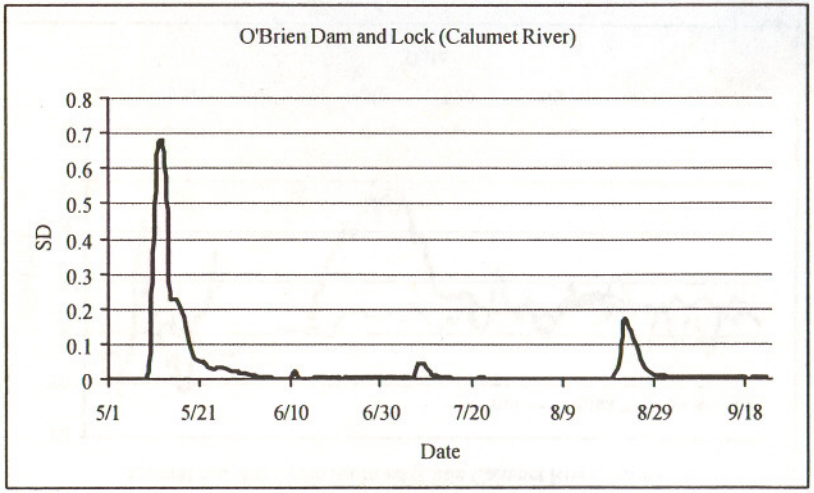
O'Brien Dam and Lock (Calumet River)
SD
0.8
0.7
0.6
0.5
0.4
0.3
0.2
0.1
0
5/1
5/21
6/10
6/30
7/20
8/9
8/29
9/18
Date

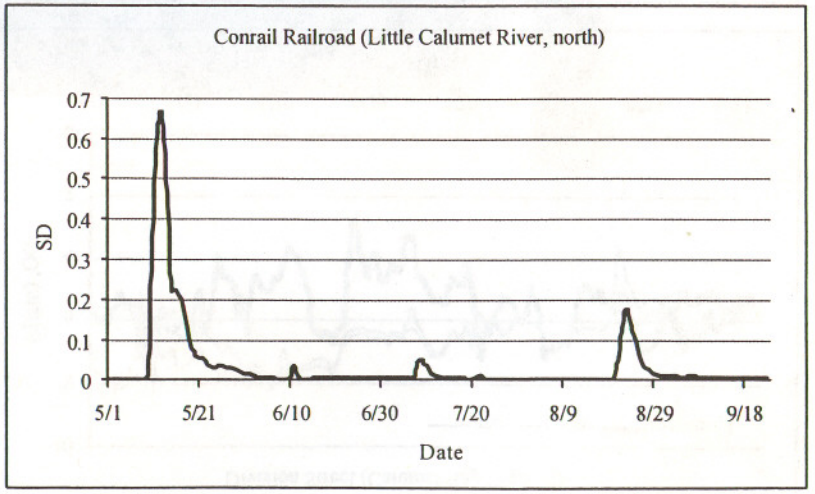
Conrail Railroad (Little Calumet River, north)
SD
0.7
0.6
0.5
0.4
0.3
0.2
0.1
0
5/1
5/21
6/10
6/30
7/20
8/9
8/29
9/18
Date

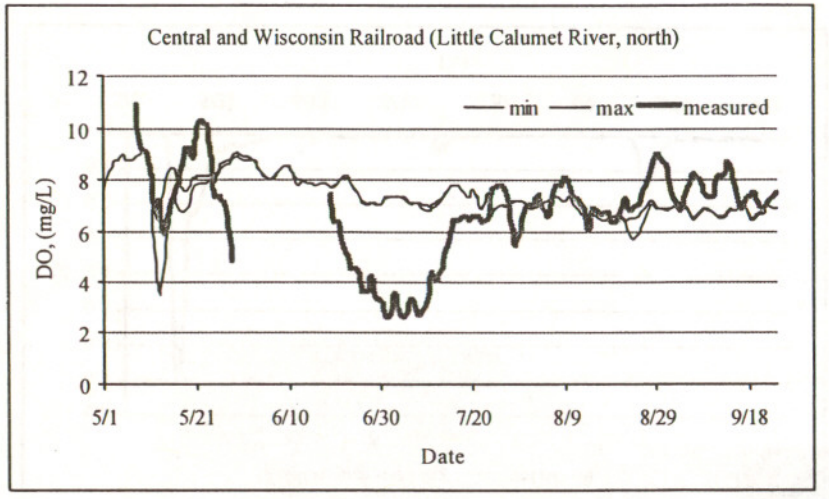
Central and Wisconsin Railroad (Little Calumet River, north)
min
max
measured
DO, (mg/L)
12
10
8
6
4
2
0
5/1
5/21
6/10
6/30
7/20
8/9
8/29
9/18
Date

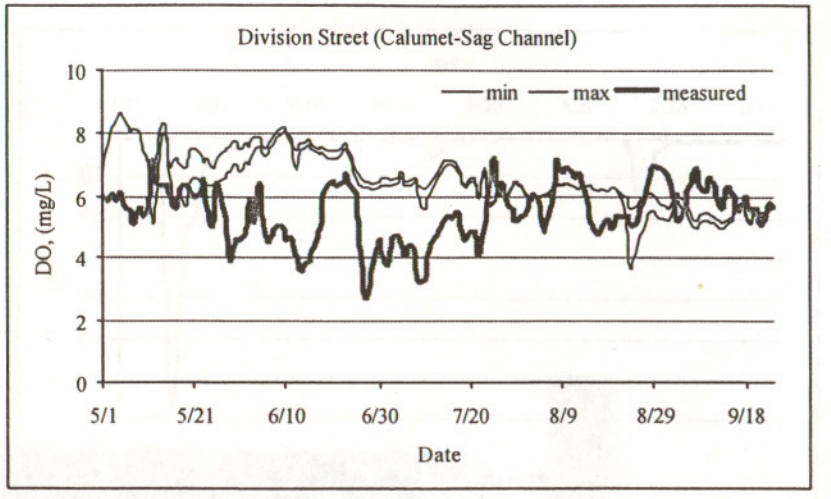
Division Street (Calumet-Sag Channel)
min
max
measured
DO, (mg/L)
10
8
6
4
2
0
5/1
5/21
6/10
6/30
7/20
8/9
8/29
9/18
Date

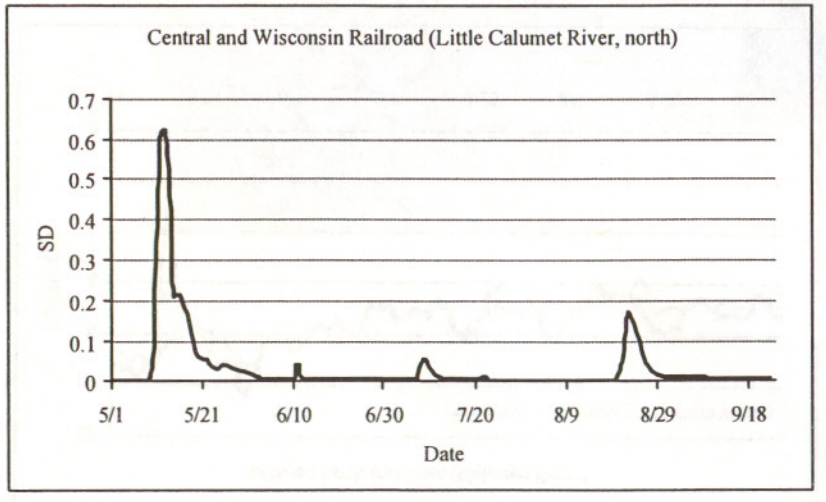
Central and Wisconsin Railroad (Little Calumet River, north)
SD
0.7
0.6
0.5
0.4
0.3
0.2
0.1
0
5/1
5/21
6/10
6/30
7/20
8/9
8/29
9/18
Date

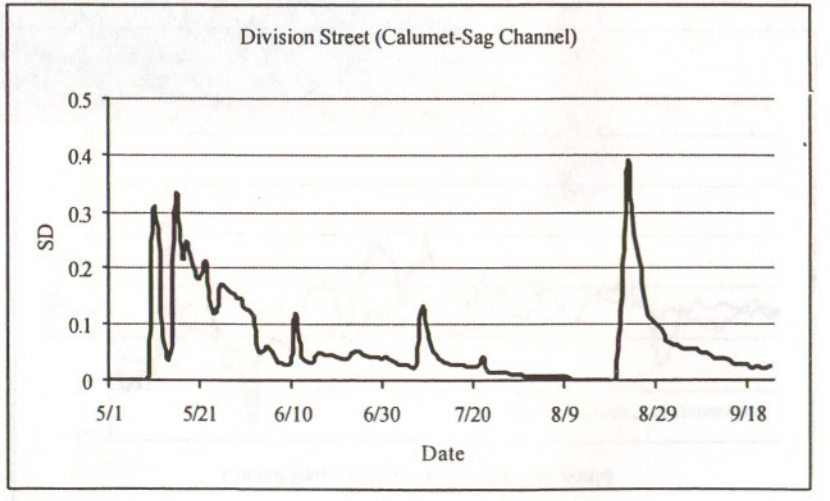
Division Street (Calumet-Sag Channel)
SD
0.5
0.4
0.3
0.2
0.1
0
5/1
5/21
6/10
6/30
7/20
8/9
8/29
9/18
Date

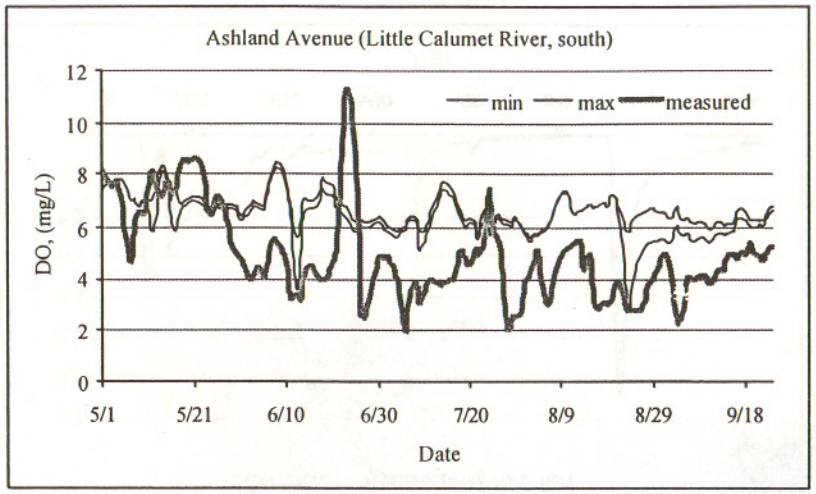
Ashland Avenue (Little Calumet River, south)
min
max
measured
DO, (mg/L)
12
10
8
6
4
2
0
5/1
5/21
6/10
6/30
7/20
8/9
8/29
9/18
Date

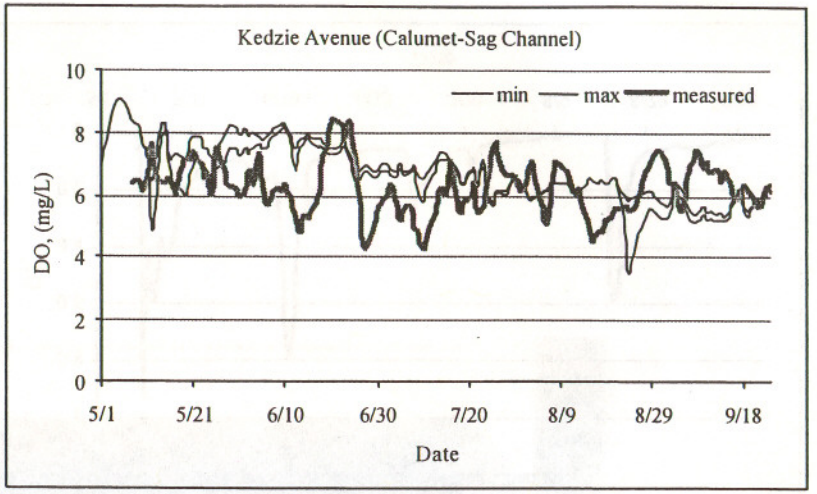
Kedzie Avenue (Calumet-Sag Channel)
min
max
measured
DO, (mg/L)
10
8
6
4
2
0
5/1
5/21
6/10
6/30
7/20
8/9
8/29
9/18
Date

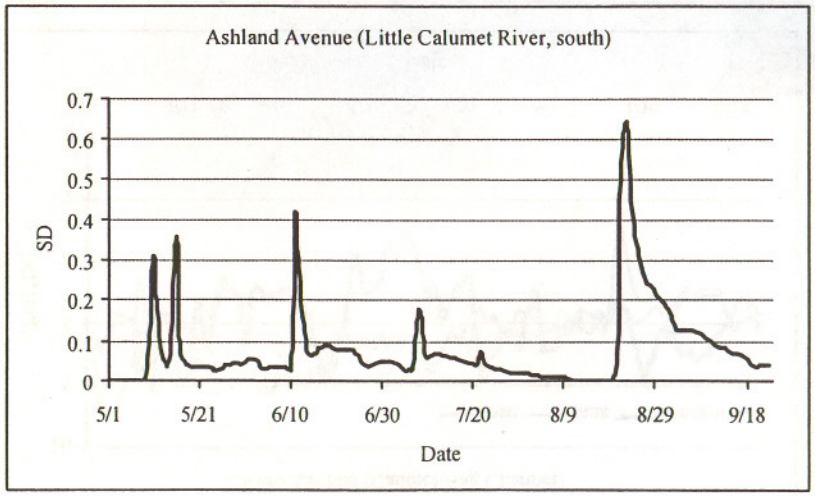
Ashland Avenue (Little Calumet River, south)
SD
0.7
0.6
0.5
0.4
0.3
0.2
0.1
0
5/1
5/21
6/10
6/30
7/20
8/9
8/29
9/18
Date

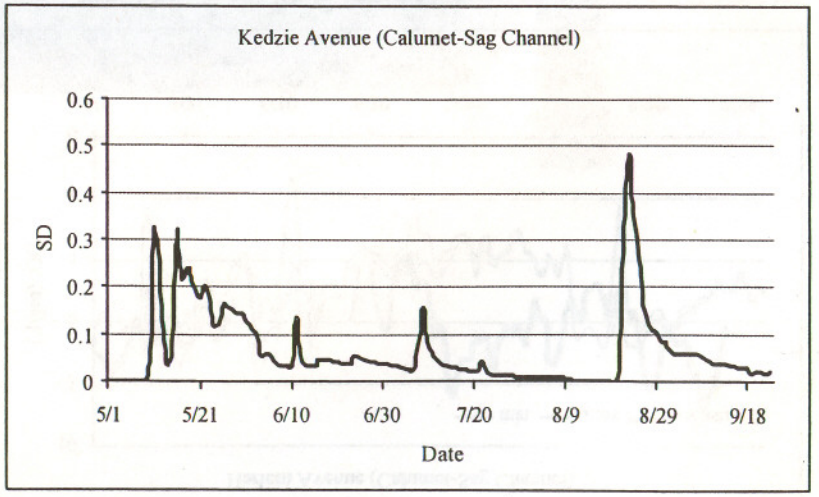
Kedzie Avenue (Calumet-Sag Channel)
SD
0.6
0.5
0.4
0.3
0.2
0.1
0
5/1
5/21
6/10
6/30
7/20
8/9
8/29
9/18
Date

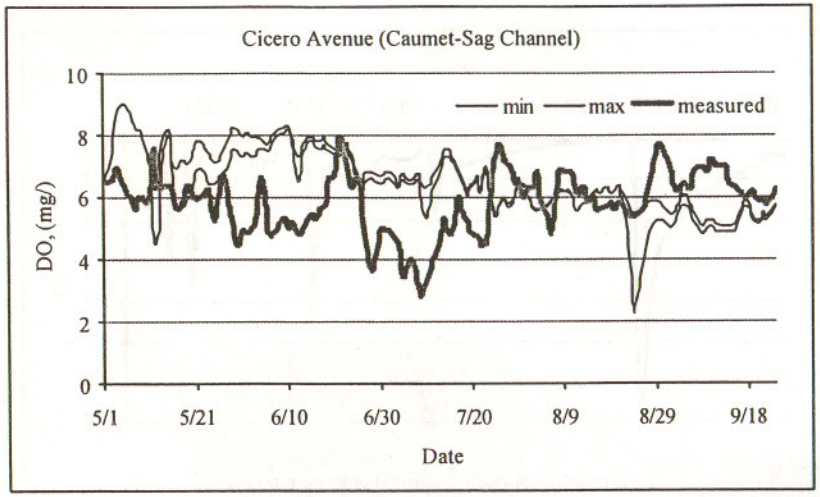
Cicero Avenue (Caumet-Sag Channel)
min
max
measured
DO, (mg/)
10
8
6
4
2
0
5/1
5/21
6/10
6/30
7/20
8/9
8/29
9/18
Date

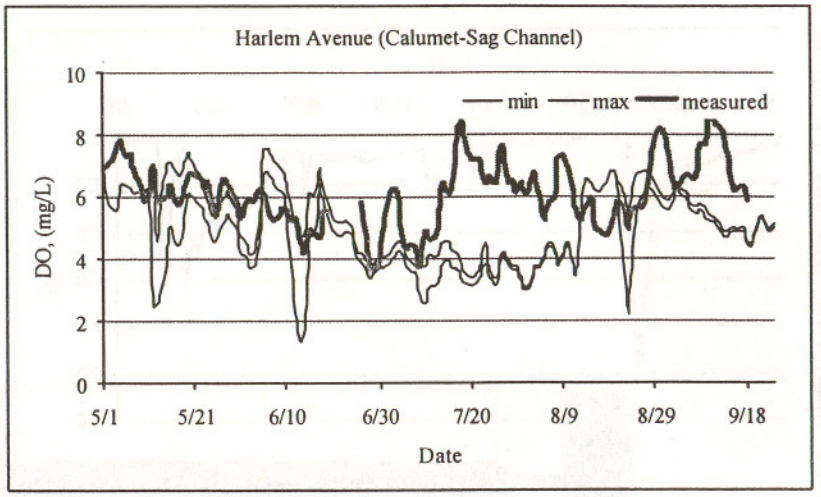
Harlem Avenue (Calumet-Sag Channel)
min
max
measured
DO, (mg/L)
10
8
6
4
2
0
5/1
5/21
6/10
6/30
7/20
8/9
8/29
9/18
Date

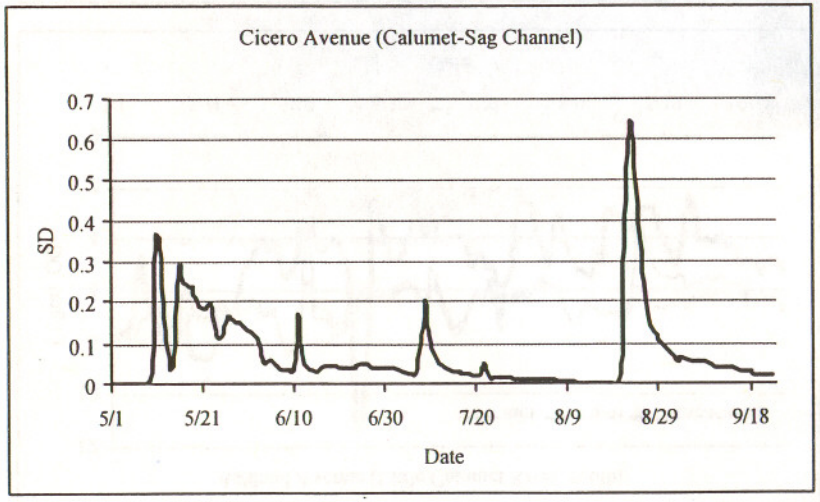
Cicero Avenue (Calumet-Sag Channel)
SD
0.7
0.6
0.5
0.4
0.3
0.2
0.1
0
5/1
5/21
6/10
6/30
7/20
8/9
8/29
9/18
Date

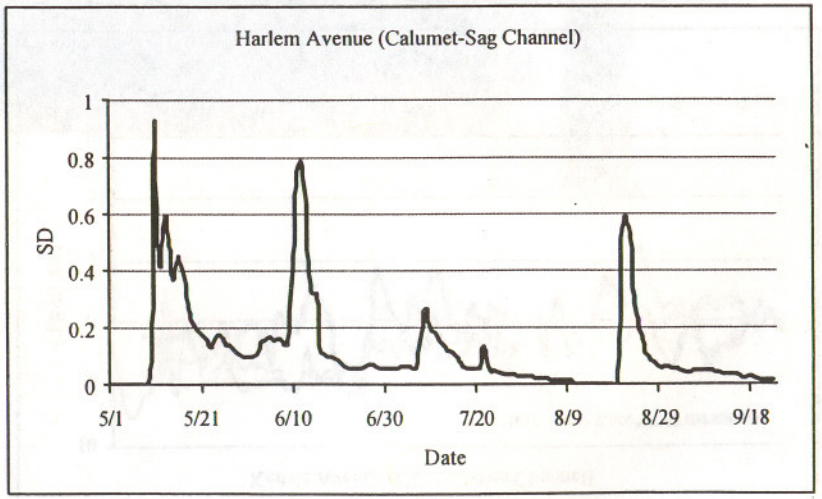
Harlem Avenue (Calumet-Sag Channel)
SD
1
0.8
0.6
0.4
0.2
0
5/1
5/21
6/10
6/30
7/20
8/9
8/29
9/18
Date

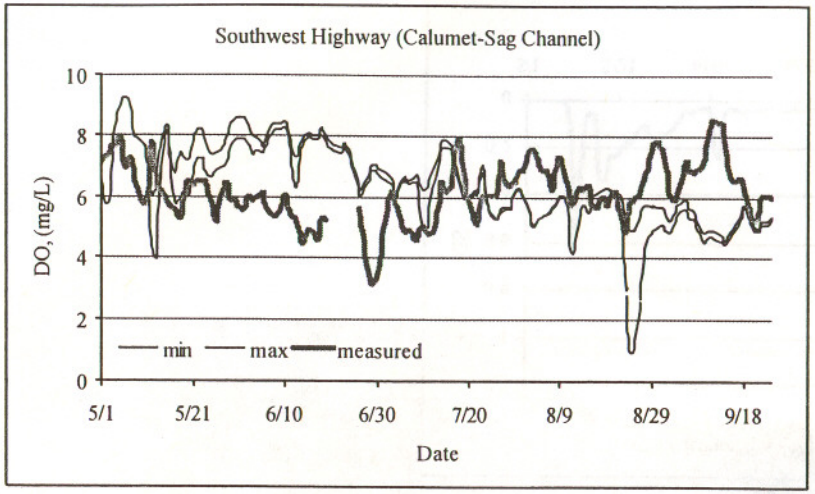
Southwest Highway (Calumet-Sag Channel)
DO, (mg/L)
10
8
6
4
2
0
min
max
measured
5/1
5/21
6/10
6/30
7/20
8/9
8/29
9/18
Date

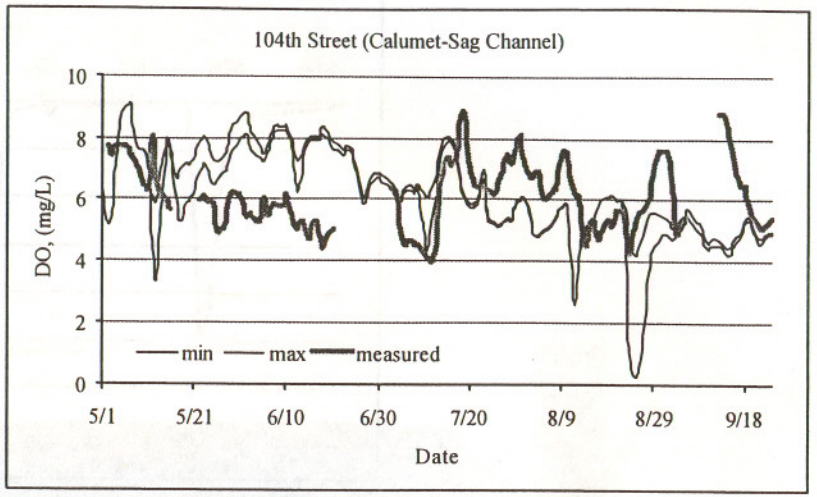
104th Street (Calumet-Sag Channel)
DO, (mg/L)
10
8
6
4
2
0
min
max
measured
5/1
5/21
6/10
6/30
7/20
8/9
8/29
9/18
Date

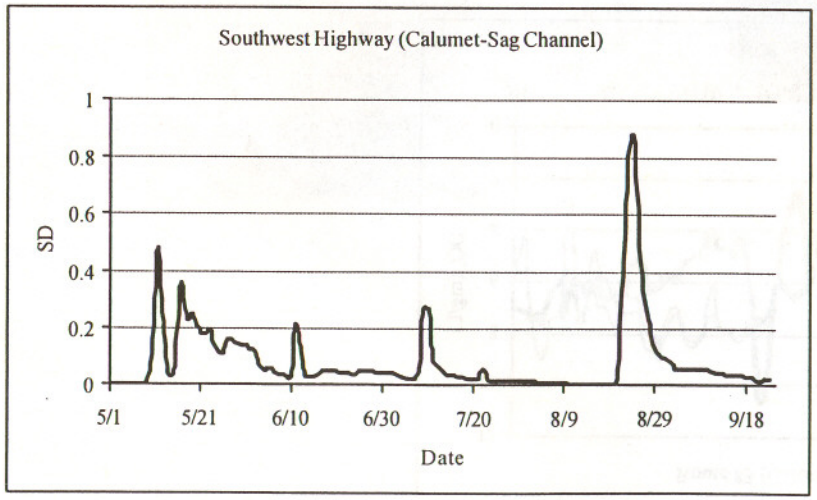
Southwest Highway (Calumet-Sag Channel)
SD
1
0.8
0.6
0.4
0.2
0
5/1
5/21
6/10
6/30
7/20
8/9
8/29
9/18
Date

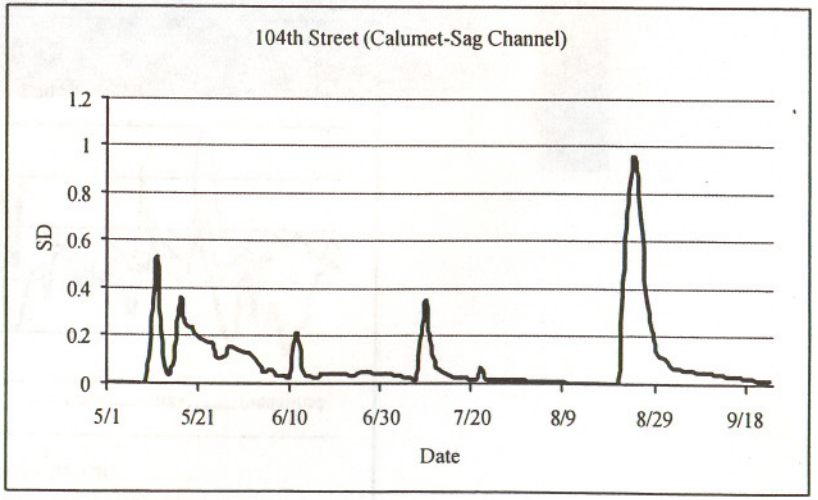
104th Street (Calumet-Sag Channel)
SD
1.2
1
0.8
0.6
0.4
0.2
0
5/1
5/21
6/10
6/30
7/20
8/9
8/29
9/18
Date

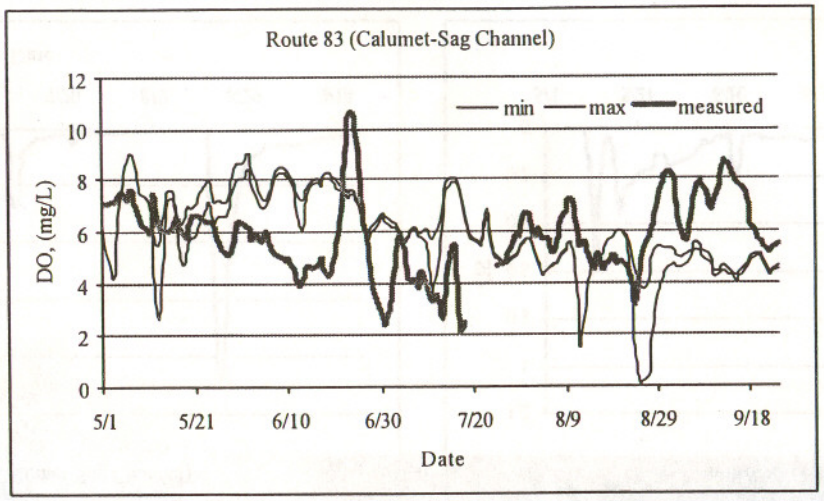
Route 83 (Calumet-Sag Channel)
min
max
measured
DO, (mg/L)
12
10
8
6
4
2
0
5/1
5/21
6/10
6/30
7/20
8/9
8/29
9/18
Date

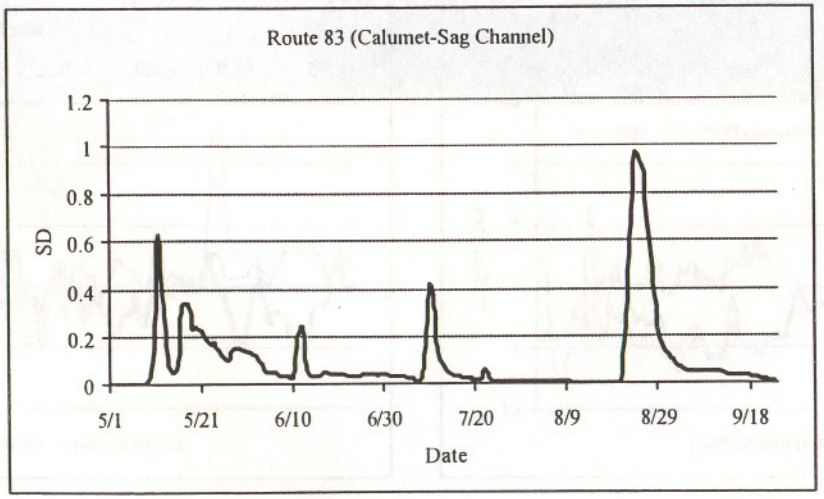
Route 83 (Calumet-Sag Channel)
SD
1.2
1
0.8
0.6
0.4
0.2
0
5/1
5/21
6/10
6/30
7/20
8/9
8/29
9/18
Date